UNIVERSITÉ DE SHERBROOKE
Faculté de génie
Département de génie chimique et de génie biotechnologique

Cinétique de cristallisation, structure et applications des stéréocomplexes de PLA

Crystallization kinetics, structure and applications of PLA stereocomplexes

Thèse de doctorat
Spécialité: génie chimique

Sajjad SAEIDLOU

Jury: Prof. Michel A. HUNEAULT (directeur de recherche)
Dr. Hongbo Li
Prof. Basil Favis
Prof. Mathieu Robert
Prof. Nathalie Faucheux

Sherbrooke (Québec) Canada Avril 2014

À ma chère Sahar

Résumé

Le poly(acide lactique) ou PLA est une famille de polyester thermoplastique linéaire qui a connu un essor commercial important durant la dernière décennie. L'enthousiasme pour le PLA vient de sa nature biosourcée, de ses bonnes propriétés mécaniques comme un module élastique élevé et de la possibilité de le biodégrader. Toutefois, certaines carences comme une faible résistance thermique et une faible élasticité à l'état fondu limitent son champ d'application. Fait à noter, le monomère d'acide lactique possède deux stéréo-isomères (*L* et *D*). Il est possible de polymériser les isomères *L* ou *D* pour former respectivement le PLLA ou le PDLA mais de façon surprenante, le mélange de PLLA et de PDLA permet la formation d'une structure cristalline distincte appelée le stéréocomplexe. Cette forme cristalline a un point de fusion 50 ^{o}C plus élevé par rapport aux formes cristallines du PLLA ou de PDLA d'où un premier intérêt pour augmenter la résistance thermique du matériau. Dans ce travail, l'usage de petites quantités (0-5 % massique) de PDLA comme additif dans une phase majeure de PLLA sera analysé. L'effet du stéréocomplexe formé à haute température sur la nucléation du PLLA et sur les propriétés rhéologiques du mélange sera plus particulièrement étudié.

La présente thèse comprend une revue de littérature sur la cristallisation des PLA suivie de quatre parties expérimentales, conclusions et recommandations. La revue de littérature a pour objectif de réinterpréter l'ensemble des données disponibles sur la cristallisation du PLA afin d'en tirer des conclusions claires. La première partie expérimentale porte sur la cinétique de formation du stéréocomplexe à l'état fondu. Il a été constaté que la formation du stéréocomplexe est lente aux températures usuelles de mise en forme du PLLA ($\sim$180 ^{o}C). De plus, la coexistence d'une morphologie baptisée dans ce travail « structure en réseau » et d'une morphologie sphérulitique a été révélée pour la première fois. Il a été démontré que la structure de réseau a une température de fusion moins élevée que la structure sphérulitique. Dans la seconde partie du travail, la cinétique de stéréocomplexation a été améliorée significativement pour adapter celle-ci aux cycles de refroidissement courts typiques des méthodes de mise en forme à l'état fondu. Ceci a été réalisé en ajoutant des agents nucléants qui initient la cristallisation à plus haute température et des agents plastifiants qui viennent augmenter la mobilité des polymères. Cette stratégie a permis de réduire le temps de cristallisation d'un ordre de grandeur. Dans un troisième temps, l'effet du stéréocomplexe sur les propriétés rhéologiques d'un mélange PDLA/PLLA a été investigué. En raison de son point de fusion élevé, le stéréocomplexe peut être préservé dans une matrice PLLA fondue et ainsi changer significativement les propriétés rhéologiques. La présence du stéréocomplexe a mené à une augmentation significative de la viscosité et de l'élasticité du PLA expliqué par la formation de points de « réticulation physique » dans la matrice amorphe. Enfin, dans la dernière partie expérimentale, le stéréocomplexe a été utilisé pour améliorer le comportement en moussage du PLA. Des expériences de visualisation et de moussage en mode discontinu ont montré que la présence de stéréocomplexe augmente la densité de nucléation de bulles et améliore significativement la morphologie de la mousse finale grâce à un effet de nucléation et à l'augmentation de l'élasticité du fluide. La revue de littérature et les trois premières parties expérimentales sont présentées sous forme d'articles scientifiques. La dernière partie expérimentale est à titre prospectif pour la suite du projet et ne sera pas soumis pour publication.

Mots-clés : poly(acide lactique), stéréocomplexe, cristallisation

Abstract

Poly(lactic acid), or PLA, is a family of linear thermoplastic polyesters that has experienced strong market growth over the past decade. The enthusiasm for PLA originates from its bio-based nature, its good properties and its biodegradability. However, some of PLA deficiencies such as low thermal resistance and low melt elasticity have limited the development of this polymer. It is noteworthy that the lactic acid monomer has two stereo-isomers (*L* and *D*) that can be polymerized respectively into PLLA and PDLA but surprisingly, blending of PLLA and PDLA can lead to the formation of a "stereocomplex" which has a distinct crystalline structure from that of the homopolymers. This crystalline form has a melting point 50 ^{o}C greater than the crystalline PDLA or PLLA forms, thus it has by itself an interest in terms of heat resistance. In this work, the use of small amounts of PDLA (0-5%) in a matrix of PLLA will be explored. Particular emphasis will be on the nucleating ability of the stereocomplex (formed at high temperature) on PLLA crystallization and on its effect on the blends rheological properties.

The current thesis comprises a literature review on PLA crystallization followed by four experimental sections. The objective of the literature review was to reinterpret the large body of data available on PLA in order to draw clear conclusions on PLA crystallization. The first experimental part of the work focused on the kinetics and conditions of stereocomplex formation in the melt state. It was found that stereocomplex formation is slow in the melt processing temperature range of PLLA (~180 ^{o}C). Co-existence of a so-called "network structure" with a spherulitic structure was revealed for the first time. It was shown that the network structure has a lower melting point than the spherulitic one. In the second part of the work, stereocomplexation kinetics was improved significantly to match it with the fast cooling cycles typical of melt processing techniques. This was achieved by adding nucleating agents that initiated crystallization at higher temperatures and plasticizers that enabled more polymer fluidity. This strategy enabled an order of magnitude decrease in crystallization time. The third part of the work was the investigation of rheological properties upon formation of the stereocomplex structure in 0-5% PDLA in PLLA blends. Due to its higher melting point, the stereocomplex can be preserved in molten PLLA and alter significantly the blend melt rheology. Stereocomplex formation was monitored through rheological measurements and compared to classical calorimetry data. The presence of the stereocomplex lead to a significant increase in viscosity and in melt elasticity explained through the presence of physical crosslink points in the amorphous matrix. Finally, in the last experimental part of the work, the stereocomplex was employed to enhance PLA foaming behavior. Foaming visualization experiments as well as batch foaming tests showed that the presence of the stereocomplex can increase bubble nucleation density and led to a finer and more uniform foam morphology due to its nucleating effect and to the increased melt elasticity.

The literature review and the three first experimental sections are presented in Peer-reviewed journal format. The last experimental section is meant as an exploratory and prospective part for the project and will not be submitted for publication.

Key words: Poly(lactic acid), stereocomplex, crystallization

Acknowledgements

I would like to express my sincere gratitude to my supervisor, Professor Michel Huneault, for placing his trust in me, supporting me and most importantly, his friendship during my graduate studies at Universite de Sherbrooke. Indeed, without his immense knowledge, encouragement and patience I was not able to finish this project.

For experimental work, I had a great privilege to work at National Research Council of Canada in Boucherville with enormous support of Doctor Hongbo Li. His inspiration and valuable advises has meant more to me than I could ever express. Also my greatest appreciation goes to the technicians and staff of this research center. I could not complete my work without their invaluable friendly assistance.

I would like to acknowledge financial support from the NSERC Network for Innovative Plastic Materials and Manufacturing Processes (NIPMMP) under the leadership of Professor Chul B. Park. I also gratefully thank Professor Park for his insightful advises and providing the experimental setup for the foaming experiment in Toronto.

I would like to extend my gratitude to my parents, Manij and Ali, for their unconditional love and support. I hope I have made them proud with this work.

Last but foremost, all my deepest love and appreciation to my brilliant and outrageously loving and supportive wife, Sahar.

TABLE OF CONTENT

List of figures

List of tables

Chapter 1. Introduction

1.1 Context

Poly(lactic acid) is a linear thermoplastic polyester which has been the subject of a vast research in the past decade [1-6]. It is no wonder why it has been so popular these days as it possesses lots of advantages simultaneously. PLA is a bio-based polymer that can be produced from annually renewable resources such as starch and other polysaccharides [2]. On the other hand, it is a compostable polymer. Thus, it originates from and goes back to the nature. In terms of applications, PLA is even more interesting. Its biocompatibility and bioresorbability has made it suitable for specialty biomedical applications such as tissue engineering and drug delivery [7]. Moreover, good mechanical, optical and barrier properties in combination with compostability has positioned PLA as a cost-competitive biobased polymer substituting petroleum-based material in applications such as packaging, textiles and molded articles [1, 8, 9]. The other side of the coin is that this interesting polymer has some disadvantages which are obstacles for its further product development. The main weaknesses are low crystallinity and crystallization rate , a low heat resistance (originating from a low T_g about 55 ^oC and low crystallinity [6]), lack of reactive groups and brittleness (low impact resistance) [4]. The main challenges for melt processing of PLA are its low melt strength and elasticity which is problematic in processes such as extrusion foaming and film blowing requiring a certain degree of melt strength [8].

Lactic acid is available in two enantiomeric forms called L-lactic acid and D-lactic acid. Most commercial PLA resins are polymerized primarily from L-lactic acid with D-Lactic acid being a “contaminant” with a level between 0-15 wt.% . In this context, the D component acts as a non-crystallizing comonomer and leads to a lowering of PLA final crystallinity and crystallization rate [6]. If pure enantiomeric L or D forms are used, the corresponding polymers are known as PLLA or PDLA respectively. These polymers have very similar properties with a melting point about 175 ^oC. Surprisingly, the co-crystallization of PLLA and PDLA chains yields a crystalline form called stereocomplex with a melting point 50 ^oC higher than PLLA or PDLA homocrystals [10]. This higher melting point structure could be employed to improve PLA heat resistance. In this work however, the focus has been placed on blends where PDLA is used as an additive, in the 0-10 wt.% concentration range, to form a minor stereocomplex phase that in turn can play a

role on PLLA crystallization (as a nucleant for homocrystallization) or on its melt rheology. For melt rheology, the minor stereocomplex phase will tie together different PLLA chains leading conceptually to a physically cross-linked structure within an amorphous molten PLA.

1.2 Problem definition and objectives

As we will see in the literature review, most of the published work on stereocomplexation involved solvent mixing and solution casting and competition between homocrystallization and stereocomplex formation was an important challenge when the viscosity of the media is high. It appeared that stereocomplexation from the melt and at elevated temperatures was not fully investigated and deserved more attention since the vast majority of polymer processing operations involve solvent-free melt processing, short processing times and fast cooling rates. Based on the current state of understanding, it was decided to focus the project according to the following objectives:

- To study the structure and stereocomplex formation conditions in the molten state.
- To examine the heterogeneous nucleation and plasticization on stereocomplex formation rate and microstructure and to determine the effect of a stereocomplex minor phase on the homocrystallization rate of PLA
- To determine if the presence of the stereocomplex minor phase in amorphous (molten) PLA can increase PLA melt elasticity.
- To assess the potential of the stereocomplex for the polymer foaming process

1.3 Thesis organization

The thesis has been organized in the following manner. In chapter 2, a literature review on PLA crystallization has been presented in two sections. Homocrystallization is reflected in the first section which is published as a review paper. The second part of the literature review focuses on the general knowledge about PLA stereocomplex. Chapters 3 to 6 are the four distinct experimental parts responding to the four main objectives described above. Chapter 3 presents a study of stereocomplexation kinetics from the melt and elucidates a dual network/spherulitic crystalline morphology which is formed at isothermal stereocomplex formation in the melt state. In chapter 4, the effect of nucleation and plasticization on stereocomplex formation and their effect on crystalline morphology is determined. In chapter 5, stereocomplex formation from the

melt is investigated by rheological measurements and the effect of the developed structure on PLA rheological properties are demonstrated. Chapter 6 presents the application of stereocomplex structure in the improvement of the PLA foaming process. Finally, in chapter 7, the most important conclusions of this work are summarized and some recommendations are given regarding the future work in this area.

1.4 Original contributions

This work has several original contributions to the subject of PLA stereocomplex in relation to the stated objectives. In the first phase of the project which aimed at the determination of the structure and conditions of stereocomplex formation in the melt state, a dual network/spherulitic crystalline morphology was reported for the first time for blends crystallized isothermally from the melt. In addition, the observation of a transcrystalline layer at the surface of stereocomplex spherulites was another original aspect at this stage. In the second experimental part where the enhancement of the stereocomplex formation kinetics in the melt state was intended, plasticization and heterogeneous nucleation were employed simultaneously for the first time in the case of PLA stereocomplex in melt blended systems. An aromatic phosphonate which was never used before for PLA stereocomplex nucleation was proved to be very effective. Also different stereocomplex crystalline morphologies were developed by the incorporation of nucleating agent and plasticizer and the variation of crystallization temperature. The third phase of the project was original in the sense that stereocomplex formation was not probed by rheological means in prior works. Kinetic curves obtained from rheological measurements were compared to common calorimetric curves and their difference was attributed to the change in the chain microstructure as a result of stereocomplex formation. Furthermore, another original aspect of the rheological experiments was the detection of a yield stress for PLA melt containing stereocomplex structure. Finally, the last phase of the project which was aimed to assess the potential of the stereocomplex for the foaming process was essentially original since it was not explored prior to the attempts reported in this thesis. Stereocomplex was shown to enhance cell nucleation through heterogeneous nucleation and stabilized cell formation resulting in a more homogeneous and finer cell morphology.

Chapter 2. Literature review

Avant-propos

Auteurs et affiliation:

Sajjad Saeidlou: *Département de génie chimique et de génie biotechnologique, Faculté de genie, Université de Sherbrooke*

Michel A. Huneault: *Département de génie chimique et de génie biotechnologique, Faculté de genie, Université de Sherbrooke*

Hongbo Li: *National Research Council of Canada*

Chul B. Park: *Department of Mechanical and Industrial Engineering, University of Toronto*

Date d'acception: 16 juillet 2012

État de l'acceptation: version finale publiée

Revue: Progress in Polymer Science

Référence: *Progress in Polymer Science*, 2012.**37**: p. 1657-1677.

Titre français: Cristallisation du poly(acide lactique)

Contribution au document: revue de la littérature pertinente aux travaux expérimentaux

Résumé français: *Le poly(acide lactique) est un polyester thermoplastique biosourcé et compostable qui a rapidement évolué pour devenir un matériau de base compétitif durant la dernière décennie. Le principal obstacle à l'augmentation de l'utilisation du PLA est le contrôle de sa cristallinité. Comprendre le phénomène de cristallisation est particulièrement important pour contrôler le taux de dégradation du PLA, sa résistance thermique ainsi que ses propriétés optiques, mécaniques et barrières. La cristallisation du PLA a également été un sujet particulièrement riche d'un point de vue fondamental en raison de l'existence des deux formes énantiomères de l'acide lactique qui peuvent être utilisées pour contrôler le taux de cristallisation, mais aussi pour former des structures stéréocomplexes ayant un point de fusion élevé. Cet article présente un aperçu des connaissances actuelles sur les principes fondamentaux de la cristallisation du PLA dans des conditions de quiescence et sur les moyens pratiques d'améliorer son taux. Les données apportées par une littérature abondante sur la cristallisation*

de PLA ont été compilées et analysées pour fournir des relations globales entre la cinétique de cristallisation et les caractéristiques principales de la structure moléculaire du PLA. En outre, les efforts les plus prometteurs dans l'amélioration de la cinétique de cristallisation du PLA par plastification ou nucléation hétérogène ont été discutés.

2.1 Poly(lactic acid) Crystallization

Sajjad Saeidlou[a], Michel A. Huneault[a], Hongbo Li[b], Chul B. Park[c]

[a]*Department of Chemical and Biotechnological Engineering, Faculty of Engineering, Université de Sherbrooke, Sherbrooke, QC, Canada J1K 2R1*

[b]*National Research Council of Canada, 75, de Mortagne, Boucherville, QC, Canada J4B 6Y4*

[c]*Department of Mechanical and Industrial Engineering, University of Toronto, 5 King's College Road, Toronto, ON, Canada M5S 3G8*

Abstract: *Poly(lactic acid) is a biobased and compostable thermoplastic polyester that has rapidly evolved into a competitive commodity material over the last decade. One key bottleneck in extending the use of PLA is the control of its crystallinity. Understanding the crystallization behavior is particularly crucial to control PLA's degradation rate, thermal resistance as well as optical, mechanical and barrier properties. PLA crystallization has also been a particularly rich topic from a fundamental point of view because of the existence of the two enantiomeric forms of lactic acid that can be used to control the crystallization rate but also to form high melting point stereocomplex structures. This article presents an overview of the current understanding on the fundamentals of PLA crystallization in quiescent conditions and on the practical means to enhance its rate. Data from the abundant literature on PLA crystallization were compiled and analyzed to provide comprehensive relationships between crystallization kinetics and the main molecular structure characteristics of PLA. In addition, the most promising efforts in enhancing PLA crystallization kinetics through plasticization or heterogeneous nucleation were reviewed.*
Keywords: Poly(lactic acid), Polylactide, PLA, Crystallization, Kinetics, Review

2.1.1 Introduction

Poly(lactic acid) or PLA is a biodegradable polymer that can be produced from annually renewable resources [1]. It is an aliphatic thermoplastic polyester that boasts a high modulus, high strength and good clarity. Therefore, it has raised a lot of interest as a potential replacement for petroleum-based polymers. Before its introduction as a packaging and commodity material, specialty grades of PLA had been developed for biomedical uses. Its biocompatibility and

bioresorbability had made it a suitable choice for applications such as drug delivery systems, sutures, blood vessels, etc. [11]. The commercial introduction of bio-based PLA in 2003 has opened the way for more common applications. In particular, PLA has been finding an increasing number of applications in the packaging industry due to its good mechanical properties, transparency and compostability.

The term Poly(lactic acid) is slightly misleading. The PLA now commercialized for commodity applications is made from ring-opening polymerization of lactide, a dimer of lactic acid. Therefore, from a nomenclature point of view, we should refer to polylactide rather than to poly(lactic acid) but both terms are used indifferently in the scientific literature. Another precision that needs to be made is that PLA does not refer to a single material but rather to a family of materials with a range of properties due to the chiral nature of lactic acid as we will explain later. One general drawback of the PLA family of material is that they exhibit a lower glass transition temperature (T_g), up to about 60 ^oC, compared to competing polyesters. The ubiquitous polyethylene terephthalate (PET), for example, possesses a T_g around 80 ^oC. Therefore, unless PLA can be crystallized to a large extent, its thermal resistance will remain relatively poor. For example, heat deflection temperature (HDT) and Vicat penetration temperature were increased more than 30 and 100 ^oC respectively, after amorphous samples were fully crystallized. As well, an increase in flexural modulus and strength by 25% and increased impact resistance were reported following the full crystallization of amorphous PLA [12, 13]. On the other hand, if one is interested in maintaining the PLA clarity or maximizing the biodegradability of PLA, it might be useful to understand how to limit crystallization. Enzymatic degradation rate can be reduced by more than 7 times for highly crystalline PLA compared to the amorphous samples [14]. Furthermore, barrier properties are improved due to PLA crystallization. A study by Drieskens et al. [15] showed for crystallized PLA that oxygen and water vapor permeability coefficients were decreased by more than 4 and 3 times respectively, compared to amorphous references. This stresses the importance of PLA crystallization not only from a fundamental point of view but also for obvious market development considerations. Several authors have reviewed the synthesis, properties, processing and applications of PLA [1, 8, 9, 16-18]. The current review will focus specifically on the current understanding of PLA crystallization. In particular, we will examine the microstructure of PLA, the isothermal and non-

isothermal crystallization kinetics and will summarize the different strategies used to control or enhance crystallinity development during melt processing operations.

2.1.2 Chain structure

To understand the crystallization behavior of PLA, it is useful to first examine its chain structure. PLA can be synthesized by two polymerization routes, polycondensation of lactic acid or ring-opening polymerization of lactide [18]. In both cases, lactic acid is the feedstock for PLA production. Due to an asymmetric carbon atom, lactic acid has two optically active forms called L-lactic acid and D-lactic acid. When producing PLA from lactide, three forms are possible: the LL-lactide made from two L-lactates, the DD-lactide from two D-lactates, and the LD or meso-lactide made from a combination of one L- and one D-lactate. In Figure 2.1, schematics of the lactic acid and lactide molecules are illustrated.

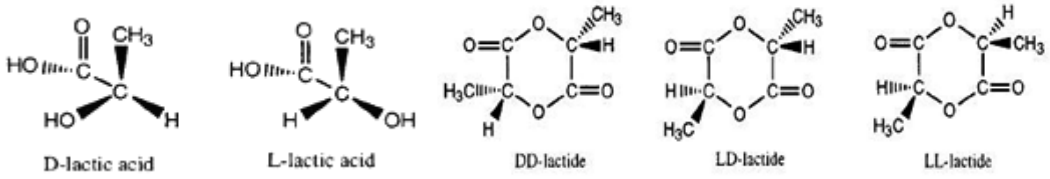

Figure 2.1 Stereochemistry of lactic acid and lactide molecules

The polymers coming from pure L- or pure D- feed are referred to as PLLA and PDLA respectively. Commercial PLA grades however are usually based on an L-rich mixture as the majority of lactic acid bacteria (LAB) used in fermentation processes such as Lactobacillus and Lactococcus produce L-lactic acid predominantly. Due to purification issues, they typically comprise a minimum of 1-2% D units. Since the two repeating units are optically active, they rotate polarized light in opposite directions. Specific optical rotation values in chloroform at 25 ^{o}C ($[\alpha]^{25}$) equal to -156^{o} and +156^{o} are commonly used in the literature for 100% pure PLLA and PDLA, respectively [19-23]. A higher content of one repeating unit in polymer chain results in a higher rotation angle in that direction. Thus, by employing the following equation [24], one can calculate the molar fraction of D units (X_D) in PLA:

$$X_D = \frac{[\alpha]^{25} + 156}{312} \qquad \textbf{Equation 2.1}$$

Based on the molar fraction and source of D units in PLA chains, i.e., DD-lactide or meso-lactide, another important parameter called the average isotactic sequence length ($\bar{\zeta}$) is defined for L-lactide rich PLA as:

$$\bar{\zeta} = \frac{a}{X_D} \qquad \textbf{Equation 2.2}$$

where *a* is a coefficient that depends on the source of D units in polymerization feed. It is equal to 1 if all D units are incorporated via meso-lactide, equal to 2 if they are all comprised of DD-lactide and between 1 and 2 depending on the ratio of meso and DD-lactide in the polymerization feed. Using the coefficient 2 for DD-lactide is due to the paring of D units in the random copolymerization of LL-lactide and DD-lactide. Another clarification about the latter equation is that it is correct for random copolymers. In some cases by employing specific initiators, it is possible to have a preferential monomer insertion into the growing chain resulting in a PLA with longer isotactic sequences compared to a statistical copolymer with the same X_D [21, 22].

A higher $\bar{\zeta}$ value means a higher level of chain order. Therefore, this parameter influences directly the crystallization behavior of PLA. It can be controlled by adjusting the ratio of LL, DD and meso-lactide in the monomer feed for PLA polymerization. However, in the course of polymerization, L or D units may convert into their counterpart form [25]. This undesirable reaction called racemization will influence $\bar{\zeta}$ and thus will disturb chain order. Another way that chain order may be disturbed is by inter or intramolecular trans-esterification reactions [19].

Chain architecture is another aspect of chain structure. PLA is typically linear in its structure, but it is possible to produce it in different branched architectures by employing multifunctional initiators [26-28] or co-monomers bearing initiation groups [29, 30] in polymerization reaction. Multifunctional chain extenders [31, 32] or peroxides [33, 34] sometimes used for PLA to counterbalance chain scission are other potential sources of branching. Accordingly, it is useful to understand the effect of branching parameters such as branch's length, amount and architecture on PLA crystallization behavior.

2.1.3 Crystal structure

Different crystal structures have been reported for PLA, the formation of which depends on the crystallization conditions. The most common α-form occurring in conventional melt and

solution crystallization conditions was first reported by De Santis and Kovacs [35] and investigated further in a number of studies [36-38]. Based on WAXD and IR data, Zhang et al. reported the slightly different α′-form for PLA crystallized below 120 °C [39]. The chain conformation and crystal system of the α′-form is similar to α structure, but with a looser and less ordered chain packing. More recent studies suggest that only the α′ crystal is formed at crystallization temperatures below 100 °C while crystallization between 100 and 120 °C gives rise to the coexistence of α′ and α crystal structures [40, 41]. As a consequence of its looser chain packing and disordered structure, the α′ crystal leads to a lower modulus and barrier properties and to higher elongation at break compared to α crystal [42]. A β-form, first observed by Eling et al. [43], is created by stretching the α-form at high draw-ratio and high temperature such as in hot-drawing of melt or solution spun fibers [37, 43]. Melting temperature of the β structure is about 10 ^{o}C lower compared to the α crystal, implying that β form is thermally less stable [37]. Later, Puiggali et al. [44] suggested that β-form crystal is a frustrated structure with a trigonal cell containing three chains which are randomly oriented up and down. A more ordered crystal modification called γ was also reported by the same group [45]. In the γ-form which was obtained by epitaxial crystallization of PLA on hexamethyl benzene, two chains are oriented antiparallel in the crystal cell. Besides the homocrystallization of PLLA and PDLA, these two enantiomeric chains can co-crystallize together and form a stereocomplex [10]. In contrast to PLLA or PDLA homocrystals, the stereocomplex crystal cell contains one PLLA and one PDLA chain. Interestingly, melting point of the stereocomplex is about 50 °C higher than that of PLA homocrystal. Thus, stereocomplexation may provide greater temperature resistance to the material. Properties of PLA crystal form are summarized in Table 2.1. The densities were calculated based on the reported cell parameters and the number of monomers in each unit cell.

Table 2.1: Properties of different PLA crystal types

Crystal type	Crystal system	Chain conformation	Cell parameters						$\rho_{theoretical}$ (g/cm^3)
			a (nm)	*b* (nm)	*c* (nm)	α (°)	β (°)	γ (°)	
α [35]	Pseudo-orthorombic	10_3 helical	1.07	0.645	2.78	90	90	90	1.247
α [38]	Orthorombic	10_3 helical	1.05	0.61	2.88	90	90	90	1.297
β [37]	Orthorombic	3_1 helical	1.031	1.821	0.90	90	90	90	1.275
β [44]	Trigonal	3_1 helical	1.052	1.052	0.88	90	90	120	1.277
γ [45]	Orthorombic	3_1 helical	0.995	0.625	0.88	90	90	90	1.312

SC [46]	Triclinic	3_1 helical	0.916	0.916	0.870	109.2	109.2	109.8	1.274
SC [47]	Trigonal	3_1 helical	1.498	1.498	0.87	90	90	120	1.274

2.1.4 Structure-properties relationship

2.1.4.1 Glass transition temperature

The glass transition temperature, T_g, plays an important role on the determination of PLA crystallization window since polymer chain mobility is related to T-T_g. Figure 2.2 presents T_g data as a function of molecular weight for different D-lactate contents. The T_g increases rapidly when the molecular weight is increased to 80-100 kg/mol but then reaches a constant value. At a given molecular weight, an increase in optical impurity, i.e. increase in minor unit concentration (defined as D-lactate in the case of an L-rich PLA and as L-lactate for a D-rich PLA), decreases the glass transition temperature to some extent but its effect on T_g is not as significant as on T_m.

The data points for different D-lactate contents presented in Figure 2.2 have been fitted with the predictions of the Flory-Fox equation given by

$$T_g = T_g^{\infty} - \frac{K}{M_n} \qquad \textbf{Equation 2.3}$$

where T_g^{∞} is the glass transition temperature for infinite molecular weight, K is a constant and M_n is the number-average molecular weight. Accordingly, we have found that K increases linearly with D-lactate concentration and that T_g^{∞} shows a decreasing trend that can be predicted quite well with a rational function.

$$T_g^{\infty} = \frac{13.36 + 1371.68 X_D}{0.22 + 24.3 X_D + 0.42 X_D^2} \qquad \textbf{Equation 2.4}$$

$$K = 52.23 + 791 X_D \qquad \textbf{Equation 2.5}$$

where T_g^{∞} and K are respectively expressed in ^{o}C and in ^{o}C.kg/mol.

The solid curves in Figure 2.2 are the relationships obtained using Equation 2.3 and the equation parameters T_g^{∞} and K described above, showing that T_g of PLA can be correctly estimated from these equations.

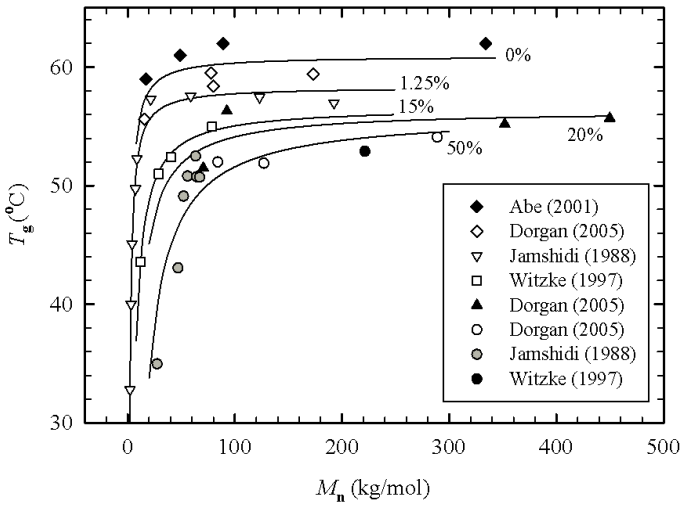

Figure 2.2 T_g vs. M_n for different D-lactate concentrations, data adapted from [48-51]

PLA chain architecture is another influential parameter for T_g. Compared to the linear structure, a branched PLA has a lower T_g value. This is due to the existence of a higher free volume caused by the higher number of chain ends. Pitet et al. [29] reported a 10 °C decrease in T_g for hyper branched PLA produced by copolymerization of lactide and glycidol while Zhao et al. [52] reported a 5 °C decrease in T_g for a 32-arms star shaped PLA produced by a poly(amido amine) dendrimer initiator. For lower branching contents such as star or comb like architectures with 4-9 arms [28] or by adding chain extender [53], no significant difference in T_g was reported.

2.1.4.2 Melting temperature and equilibrium melting point

Figure 2.3 compares the melting point data from several authors as a function of D-unit content in the polymer structure. Pure PLLA (0% data) exhibits the maximum melting temperature, between 175 and 180 °C depending on authors. The melting point decreases linearly with the D-lactate content. The best linear fit for each data set is presented as well. The slope of these lines varies between -5.5 to -5.0, meaning that 1% D-unit content results in approximately 5 °C reduction in melting temperature. The difference between data presented in Figure 2.3 is due to the different molecular weight. For example, Kolstad reported T_m for PLA with M_n between 50 to 130 kg/mol [54] while data reported by Witzke [51] and Bigg [55] concern PLA with M_w higher than 100 kg/mol. Furthermore, the thermal history applied by the authors differed slightly.

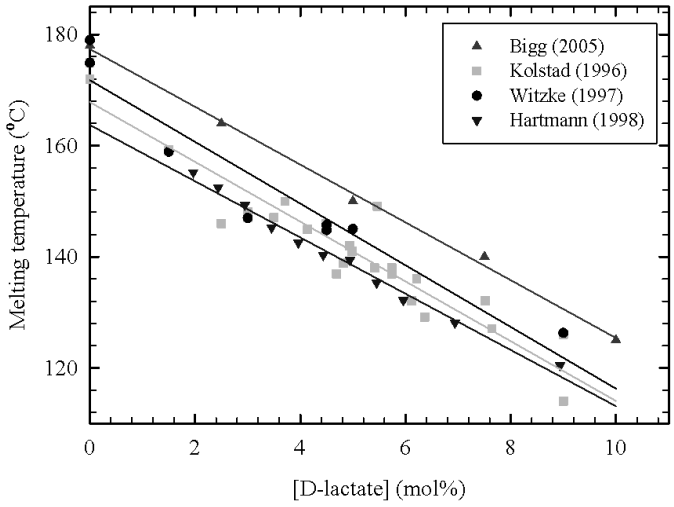

Figure 2.3 Melting temperature as a function of D-lactate content, data adapted from [51, 54-56]

The melting temperature of a polymer is expected to increase with the temperature at which it was crystallized (T_c). Due to the kinetic barrier for crystallization when approaching the melting temperature, polymer crystallization is typically carried out at high undercoolings which limits the crystal thickness. However, in the limiting case when crystallization is in equilibrium with melting of crystals, the crystal grows large enough in all directions so that the melting point reaches its maximum value, the so-called equilibrium melting point (T_m^0). The effect of the D-content on the T_m^0 of PLA can be calculated based on Hoffman-Weeks procedure [57]. Figure 2.4 addresses the effect of crystallization temperature and of minor unit concentration on melting point and presents the T_m^0 values obtained for each minor unit concentration (i.e. the T_c=T_m line). As expected, T_m decreases with minor unit concentration for all crystallization temperature. The melting point for any given minor unit content clearly increases as a function of the crystallization temperature. The data at $T_c = T_m$ is compared to the Baur Model prediction. This model is used to calculate melting point depression due to random copolymerization with a non-crystallizable co-monomer. The Baur model [58] is a modification based on earlier development proposed by Flory [59] and is given by

$$\frac{1}{T_m^0(\text{copolymer})} - \frac{1}{T_m^0(\text{homopolymer})} = -R\frac{(\ln X - \frac{1}{\zeta})}{\Delta H_m^0} \qquad \textbf{Equation 2.6}$$

where X is the molar fraction of crystallizable units, ΔH_m^0 is the equilibrium enthalpy of fusion, R is the gas constant and $\bar{\zeta}$ is the average sequence length of crystallizable units (see Equation 2.2). The model is identical to the one proposed by Flory except for the $1/\bar{\zeta}$ term. The equilibrium melting point depression is well described by the Baur Model. The validity of the Baur equation was also reported by Huang et al. [60] as well as Baratian et al. [61] for PLA systems.

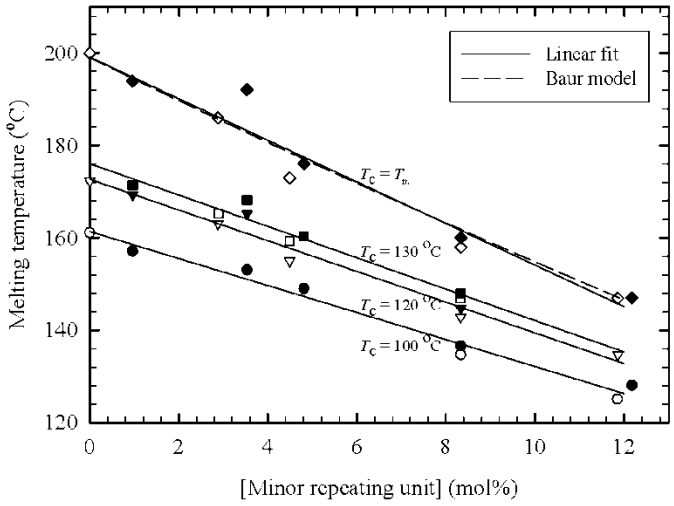

Figure 2.4 T_m and T_m^0 as a function of minor repeating unit concentration, filled symbols for PDLA and open symbols for PLLA, data adapted from [24]

The reported equilibrium melting temperature and equilibrium enthalpy of fusion of PLA are summarized in Table 2.2 with their calculation methods. Most authors report equilibrium melting temperatures between 200 and 215 ^oC. Variations may be due to variations in molecular weights and purity of the investigated polymers. In terms of equilibrium melting enthalpies, estimations vary between 80 and 135 J/g.

Table 2.2 Reported equilibrium melting temperature and melting enthalpy for PLA

T_m^0 (°C)			ΔH_m^0 (J/g)		
Method	**Value**	**Ref.**	**Method**	**Value**	**Ref.**
Hoffman-Weeks Baur	200 199	[24]	Baur	82	[24]
Gibbs-Thomson Data fitting	214 215	[60]	-	100	[60]
Hoffman-Weeks	207	[62]	Extrapolation to infinite crystal thickness Flory model for solution grown crystals	81 93	[63]
Hoffman-Weeks	205	[64]			
Hoffman-Weeks	206	[65]			
Hoffman-Weeks	211, 212	[66]			
Hoffman-Weeks	215	[67]			
Hoffman-Weeks	215 ± 10	[36]	Extrapolation to crystal	135	[68]

Marand Hoffman-Weeks	227 199	[48]	density (Density-Enthalpy relation)
Hoffman-Weeks (pseudo-equilibrium lamellar crystals)	215	[69]	

Molecular weight is another factor that significantly influences the melting temperature. Figure 2.5 illustrates the melting point variation with the number averaged molecular weight M_n. The data has been compiled from seven papers where the PLA had less than 1.25% minor units [24, 48, 50, 51, 61, 70, 71]. The melting temperature increases dramatically with molecular weight for low M_n but reaches an asymptotical value at M_n>100 kg/mol. It can be as low as 90°C for PLA oligomers and increases up to 185 °C for PLA in the 100 kg/mol range. It is noteworthy that commercial PLA grades with a molecular weight in the 50-150 kg/mol range are in the high-molecular weight plateau region and therefore are not highly sensitive to molecular weight changes. In order to express the relationship between melting point and molecular weight in a simple way, the data from Figure 2.5 was fitted using the following equation:

$$T_m = T_m^{\infty} - \frac{A}{M_n} \qquad \textbf{Equation 2.7}$$

with T_m^{∞} = 181.3 °C and $A = 1.02\times10^5$ °Cg/mol. This is a common molecular weight dependency used for expressing changes in polymer properties such as glass transition temperature, tensile strength, etc. The property is expressed as a function of the number-averaged molecular weight M_n, and of a theoretical property value obtained at infinite molecular weight. As can be seen on the figure, Equation 2.7 gives a fair account of the effect of molecular weight on the melting temperature.

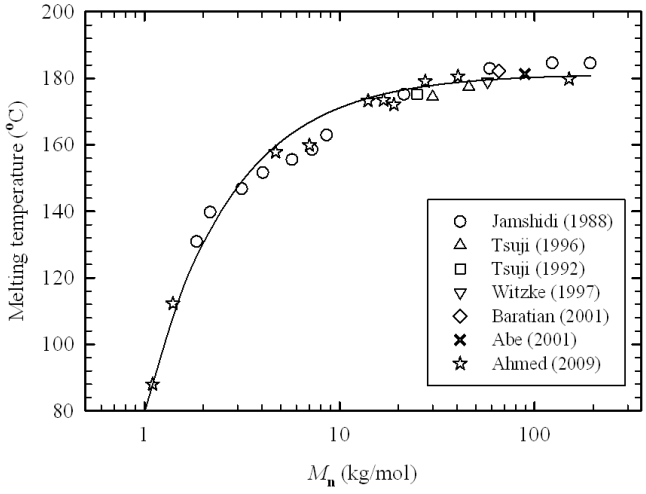

Figure 2.5 PLA Melting point as a function of molecular weight, data adapted from [24, 48, 50, 51, 61, 70, 71]

In some circumstances, two peculiarities are observed in the DSC heating scans of semi-crystalline PLA. One is the emergence of a small exothermic peak just before the melting peak and the other one is the occurrence of a double melting peak. These two phenomena can be well explained by taking into consideration the crystallization conditions in parallel with the α' and α crystal formation requirements [40, 41, 72, 73]. When PLA is crystallized at temperatures corresponding to α' crystal formation, the small exotherm appearing just before the single melting peak is due to the transformation of disordered α' crystals to the ordered α-form. On the other hand, a double melting behavior appears when the crystallization temperature is situated in the region of simultaneous α' and α type formation. For high crystallization temperatures, only α crystals are produced leading to a single melting peak.

Effect of branched structure on the melting point was also reported in a number of studies [28, 31, 52, 53, 74]. T_m was insensitive to branching when different contents of reactive copolymers (chain extenders) were employed to produce long chain branched PLA [31, 53]. However, in the case of star-shaped PLAs synthesized by multifunctional initiators, the magnitude of T_m reduction was in direct relation with the number of arms. T_m reduction between 5 and 40 ^oC were observed for branched PLAs with 4-9 arms [28, 74] and 32 arms [52], respectively. This behavior was attributed to the poor folding property of branched architecture due to steric hindrance as well as crystal imperfections caused by chain ends and branching points.

2.1.4.3 Maximum achievable crystallinity

Both the molecular weight and D-Lactate content determine the maximum achievable crystallinity. The enthalpy of fusion data obtained from various data sets are summarized in Figure 2.6. The maximum enthalpy of fusion decreases generally with molecular weight and minor unit concentration. The molecular weight effect can be explained by the higher restrictions of chain motion at higher molecular weights, while the reduction in maximum achievable crystallinity by increasing D-lactate content is expected from crystal disruption. At about 10 to 12 mol.% (in the case of random distribution) of non-crystallizable unit, crystallinity is extremely low and so lengthy that PLA can be considered completely amorphous. Furthermore, crystallinity is diminished if branching is imparted to PLA structure as a consequence of more

difficult chain segment transportation to crystallization sites. Compared to linear PLA, 7-15% less crystallinity was achieved for star-shaped and long chain branched PLA [28, 31, 52, 74].

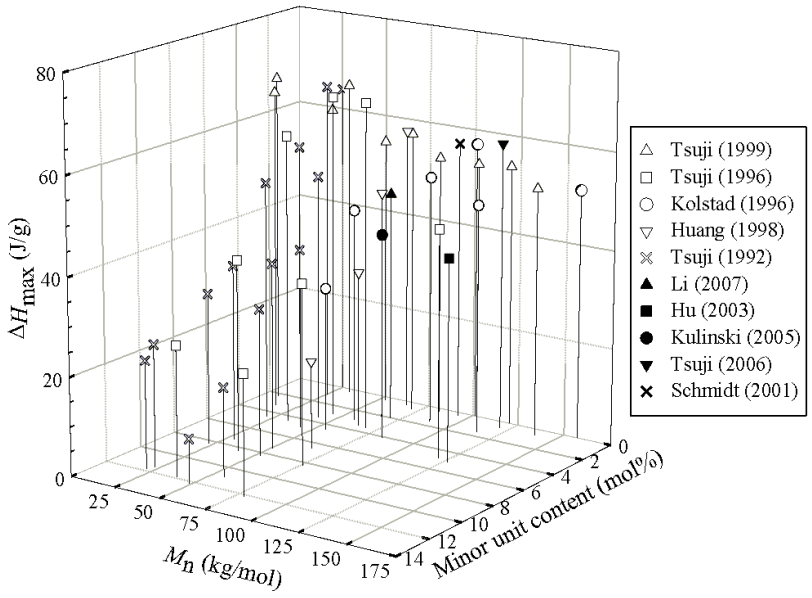

Figure 2.6 Effect of molecular weight and minor unit concentration on maximum enthalpy of fusion, data adapted from [24, 54, 60, 70, 75-80]

2.1.5 Crystallization kinetics

2.1.5.1 Kinetics through visual observation

The overall crystallization kinetics is typically examined in terms of two independent phenomena: initial crystal nucleation and of subsequent crystal growth. In practice, optical microscopy on thin polymer films is used to determine the nucleation density and spherulite growth rates in isothermal conditions. The polymer film is usually first melted and rapidly cooled to the desired temperature. The size and number of spherulites can then be monitored over time. High-quality images and more accurate measurements are also reported by observation via an Atomic Force Microscopy technique [81, 82]. The relation between the number of crystallization sites (spherulite density) with crystallization temperature for PLA is illustrated in Figure 2.7. The spherulite density was shown to decrease with temperature and the decreasing rate gradually accelerates with temperature.

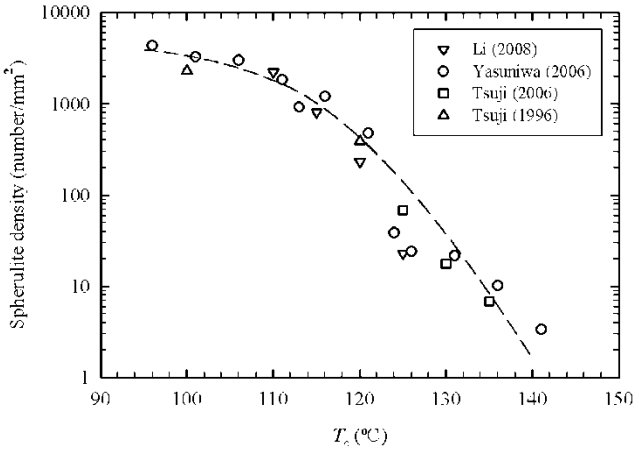

Figure 2.7 Spherulite density as a function of crystallization temperature, data adapted from [24, 79, 83, 84]

The growth phenomenon is evaluated by measuring spherulite radius with time. The crystal growth rate (G) is equal to the slope of the spherulite radius vs. time curve, while extrapolation of this data to zero-radius can be used to determine the induction time (related to nucleation kinetics). Usually G is constant for a specific T_c, implying a constant concentration of impurities like non-crystallizable segments at the growth front because of their rejection to inter-lamellar regions. One of the most important theories on polymer crystallization is the Hoffman-Lauritzen theory that deals with the crystal growth kinetics [85, 86]. It defines three crystallization regimes based on the ratio between the rate of surface nucleation and the rate of chain deposition on the crystal surface. It is noteworthy that this theory concerns the secondary nucleation occurring on preformed lamellae. It is different from the primary nucleation defined as the initiation of a new lamella from a polymer melt. In regime I which covers low undercoolings, surface nucleation is slow and is the limiting factor while chain mobility is high. By decreasing temperature and moving to regime II, surface nucleation becomes more effective while chain movement is reduced. However the combination of the two factors gives higher growth rates. Finally, upon further cooling, we move to regime III. Contrary to regime I and due to high undercoolings, surface nucleation is maximum and chain motion is the limiting factor, resulting in lower growth rates compared to regime II. According to this theory, the crystal growth rate (G) of a homopolymer is given by:

$$G = G_0 e^{-\frac{U^*}{R(T_c - T_\infty)}} e^{-\frac{K_g}{T_c \Delta T f}}$$ **Equation 2.8**

where G_0 is a pre-exponent constant known as front factor, U^* is the activation energy for local motion, R is the gas constant, T_c is the crystallization temperature, T_∞ is the temperature at which flow ceases, ΔT is the undercooling (T_m^0-T_c), and f is a factor to account the change in heat of fusion with temperature. K_g known as the nucleation constant is a parameter given by:

$$K_g = \frac{ab\sigma\sigma_e T_m^0}{k\Delta H_f} \qquad \textbf{Equation 2.9}$$

where a is a constant that depends on the crystallization regime (2 for regime II crystallization and 4 for regime I and III), b is the surface nucleus thickness, σ is the lateral surface free energy, σ_e is the fold surface free energy, T_m^0 is the equilibrium melting temperature, ΔH_f is the heat of fusion for 100% crystallinity and k is the Boltzmann constant. Typical values of Hoffman-Lauritzen equation parameters reported for PLLA are summarized in Table 2.3.

Table 2.3 Hoffman-Lauritzen Eq. parameters for PLLA

Parameter	Description	Value
U^*	Activation energy for local motion	6.27×10^3 J/mol [62]
R	Gas constant	8.314 $JK^{-1}mol^{-1}$
T_∞	Temperature at which flow ceases	T_g-30 K
ΔT	Undercooling	T_m^0 - T_c
f	Factor to account the change in heat of fusion with temperature	$2T_c/(T_m^0+T_c)$
T_m^0	Equilibrium melting temperature	(SeeTable 2.2)
b	Surface nucleus thickness	5.17×10^{-10} m [36]
σ	Lateral surface free energy	12.03×10^{-3} Jm^{-2}[62]
σ_e	Fold surface free energy	60.89×10^{-3} Jm^{-2}[62]
ΔH_f	Heat of fusion	(SeeTable 2.2)
k	Boltzmann constant	1.38×10^{-23} JK^{-1}

When the growth rate measurement is done for different crystallization temperatures, plotting $\ln(G) + \frac{U^*}{R(T_c - T_\infty)}$ versus $\frac{1}{T_c \Delta T f}$ will lead to a linear plot where the slope is -K_g and the intercept is ln(G_0). In addition, the regime change temperature can be obtained from the points of slope variation. Regime I-II transition for PLA was reported to occur at 163 [62] or 147 ^oC [48] while regime II-III transition occurs at 120 ^oC [40, 48, 87, 88]. Furthermore, G is maximum at

about 130 ^{o}C [40, 60, 62, 87, 89]. In some cases, however, an unusual behavior is reported for the variation of G with T_c for PLA where two local maxima are observed at temperatures around 105-115 ^{o}C and 125-135 ^{o}C instead of a bell-shaped curve [48, 69, 82, 83, 88, 90-93]. The origin of this double peak behavior is not known exactly. Transition from regime II to III [48, 88, 94] or growth of α' and α crystal structures [91] are assumed to be the main causes for such behavior. Interestingly, the temperatures for regime II-III transition and transition from pure α to a mixture of α' and α crystal formation coincide (120 ^{o}C). Besides, there are arguments on whether the crystal structure or spherulite morphology remains the same [48, 90, 91] or varies for these two growth rate peaks [83].

In Table 2.4, some of the reported values for K_g and G_0 are summarized. Reported G_0 data are varying widely, however K_g values are more consistent. Additionally, ratios of K_g(III)/K_g(II) and K_g(I)/K_g(II) are close to the theoretical value of 2.

Table 2.4 Reported front factor and nucleation constant for different crystallization regimes

M_w (kg/mol)	D (%)	G_0 (μm/min) × 10^{-7}			K_g × 10^{-5} (K^2)			Ref.
		I	II	III	I	II	III	
150-690 (M_v)	-	2.13×10^6	1.56-3.38	-	4.87	2.29-2.44	-	[62]
50-200	-	-	-	-	-	1.21-2.08	-	[68]
127.4	0.4	-	-	-	-	2.4	-	[60]
22-701	0	-	1530-2700	-	8.11-11.27	4.64-5.01	6.33-9.7	[48]
101	-	-	-	-	-	1.85	4.38	[87]
26-1218	0.3-0.96	-	1.79-3.98	1780-53200	-	2.27-2.55	4.73-5.51	[88]
124.8-151.3	0-1	-	1700-2080	-	4.52-6.32	2.41-3.46	4.78-7.01	[69]
101	-	-	-	-	-	1.85	4.38-5.97	[90]
136	0.96	-	510	-	-	3.03	-	[89]
206	0.8	-	-	-	-	3.22	6.02	[40]
27.18-28.08	-	-	3.98-8.86	7200-10700	-	2.2-2.5	4.48-4.7	[92]

For high melting point polyesters, like PLA, Hoffman et al. [95] related the lateral surface free energy to chain flexibility through the following equation:

$$\sigma \cong \Delta H_f \left(\frac{a_0}{2}\right) \frac{1}{C_\infty} \qquad \textbf{Equation 2.10}$$

where a_0 is the surface nucleus height and equals to 5.97 Å for PLA according to Kalb and Pennings [36]. C_∞ is the characteristic ratio defined as the mean-square end-to-end distance of an

unperturbed linear polymer chain over that of an equivalent random-flight chain. This ratio is a representation of chain flexibility and assumes higher values for stiffer polymer chains and more extended conformations. There is a discrepancy in the literature about PLA chain flexibility. Different values of C_∞ are reported for PLA ranging from 2 up to 12 [49, 96-102]. Dorgan et al. [49, 102] identified a number of reasons for this inconsistency and with a series of careful experiments in melt and solution state, they suggested that PLA has a flexible polymer chain with a characteristic ratio of about 6.5, in agreement with the simulation study by Blomqvist [101]. Presence of an oxygen atom in the backbone gives flexibility to the chain, having a nearly free-rotation around O-C bond. In terms of crystallization, this implies less extended chains that should pass a higher entropy barrier to crystallize [95]. Replacing the lateral surface free energy in Hoffman-Lauritzen model by Equation 2.10 likewise confirms that for a more flexible chain (smaller C_∞), the exponential term associated to secondary nucleation becomes smaller and its contribution to growth rate is reduced.

An additional factor affecting growth rate is the D-lactate concentration. This is illustrated in Figure 2.8 where the growth rate is plotted versus crystallization temperature for PLA of similar molecular weight but with different D-lactate concentration. Open symbols represent data for which D-unit is incorporated through copolymerization of LL-lactide with meso-lactide, while filled symbols are for LL-lactide copolymerized with DD-lactide. It should be noted that the nominal concentration of meso or DD-lactide for the samples with lowest D-unit concentration were 0%. The optimum T_c (at which G is maximum) is in the 115-130 °C range. Increasing the optical impurity decreases dramatically the maximum spherulite growth rate. It is around 4.5 μm/min for a PLA with 0.4% D impurity and is decreased by a factor of 40 (less than 0.1 μm/min) with the addition of only 6.6% D-lactate. The way that D-unit is introduced into the PLA structure also influences the growth rate significantly. Comparison of the data sets with similar D-lactate concentration suggests that when DD-lactide is the source of impurity, the growth rate is higher compared to the situation where meso-lactide is the impurity source. This is logical since for DD-lactide, each two D-units are connected to each other. Thus, the average isotactic sequence length of L-units is doubled compared to the PLA having meso-lactide as the feed component (see Equation 2.2). Finally, from Figure 2.8 it is clear that the optimal crystallization temperature shifts to lower values when the D-lactate concentration increases.

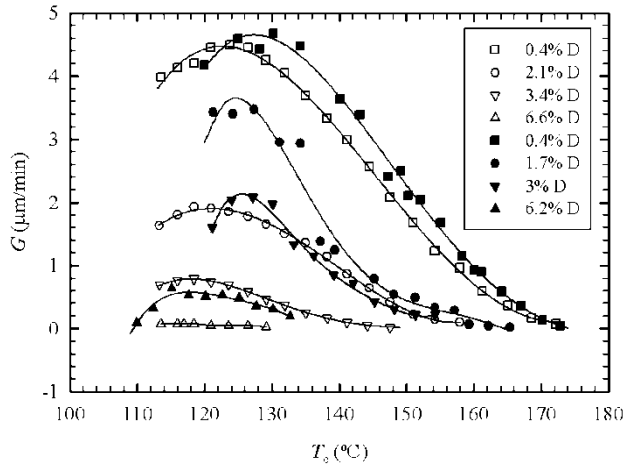

Figure 2.8 Effect of D unit concentration on the spherulite growth rate of Poly(LL-co-meso-lactide) (open symbols, Mn ≈ 65 kg/mol) and Poly(LL-co-DD-lactide) (filled symbols, Mn ≈ 74 kg/mol), data adapted from [60, 61]

The molecular weight's effect on the maximum growth rate is shown in Figure 2.9. The molecular weight is a number average, except for the viscosity average molecular weight data of Vasanthakumari and Pennings [62]. The data is for PLA having low D-unit concentration (0-1%). However, for some data points this parameter is not specified by the authors. Once more, we chose the general form of Flory-Fox equation for regression of the maximum growth rate data. Thereby, the following parameters were used to draw the solid-line curve in Figure 2.9:

$$G_{\max} = G_{\max}^{\infty} - \frac{A}{M_n} \qquad \textbf{Equation 2.11}$$

where $G_{\max}^{\infty}$ = 1.4 μm/min and A = -3.8×10^5 (μm.g)/(min.mol).

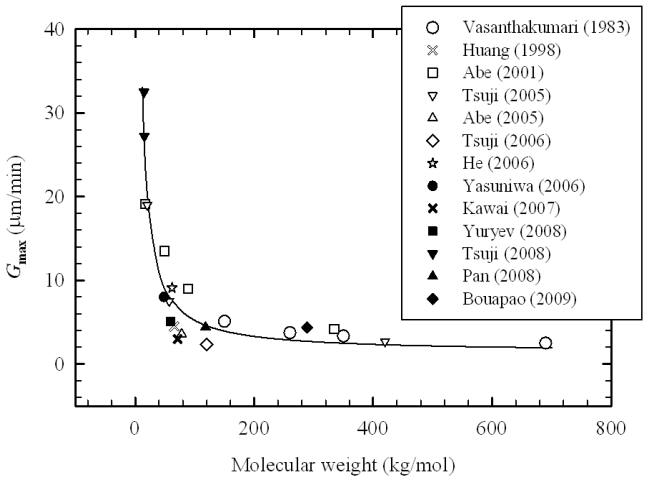

Figure 2.9 Maximum spherulite growth rate as a function of molecular weight, data adapted from [40, 48, 60, 62, 69, 79, 82, 83, 88, 89, 91-93]

Obviously, the growth rate decreases with molecular weight as expected from more restricted chain mobility. The decrease is sharp at lower molecular weights, while in the range of molecular weights typical of commercially available PLA, the effect is not as dramatic as that of the optical impurity.

2.1.5.2 Kinetics through calorimetry

Calorimetry is another technique used to study the crystallization kinetics. In particular, calorimetry enables quantification of transition temperatures and enthalpies in isothermal and non-isothermal modes. For isothermal characterizations, after initial quenching below the glass transition temperature or directly from the melt state, the amorphous polymer is rapidly brought to the selected crystallization temperature T_c. Heat flow is then measured as a function of time until crystallization is completed. The heat flow data is converted into an absolute crystallinity level or more commonly, to a fraction relative to the final crystallinity level. Such crystallinity growth curves are illustrated in Figure 2.10 for a PLLA crystallized at temperatures between 90 and 130˚C. Once this data is obtained, it can be curve-fitted with the Avrami model:

$$X_t = 1 - \exp[-(kt)^n] \qquad \textbf{Equation 2.12}$$

where k is a kinetic rate constant and n is the Avrami exponent. The Avrami exponent is typically between 2 and 4 for polymer crystallization and is associated to the nucleation mechanism (homogeneous vs. heterogeneous and simultaneous vs. sporadic), dimensionality of crystal growth and growth mechanism, i.e., linear or diffusion controlled due to the high impurity concentration. The solid lines in Figure 2.10 are data regression obtained using the Avrami model. The Avrami exponents for this specific example were in the range of 2.5-2.8 for the temperature range of 90 to 130 ^{o}C, suggesting a change in crystal growth from two to three dimensional with simultaneous nucleation [103]. Likewise, there are other reports of the Avrami exponent around 2 [104-106], between 2.5 and 3.5 [54, 65, 79, 107-111] and between 3.5 and 4.3 [68, 112, 113]. The higher n values are attributed to three dimensional spherulitic growth with a sporadic or a combination of sporadic and simultaneous nucleation type, while the lower values are associated to two dimensional growth with instantaneous and some sporadic nucleation.

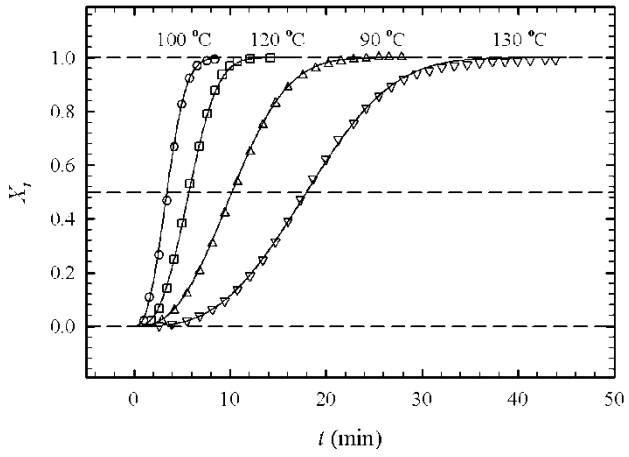

Figure 2.10 Degree of crystallization of PLLA (Mn = 1.23×10^5 g/mol, PDI = 1.8) vs. time for different crystallization temperatures, data adapted from [103]

To rapidly compare the crystallization rates of materials, it is convenient to report the crystallization half-time ($t_{1/2}$) defined as the time required to attain half of the final crystallinity (X_t = 0.5). The half-time is typically reported as a function of temperature enabling the determination of the optimal temperature window. In Figure 2.11, $t_{1/2}$ is plotted versus crystallization temperature for PLA having different molecular weights (M_n in kg/mol) and D-lactate concentration. Even though the materials varied widely in terms of molecular weight and optical purity, all curves go through the typical minimum. This minimum is associated to the competition between the increased mobility and the reduced nucleation rate as a function of temperature. The lowest reported half-time was in the 2-3 minutes range. This is relatively high compared to other semi-crystalline commodity polymers. The half-time increases clearly with the D-lactate content and the typical U-shaped curves are shifted up. A useful general rule reported by Kolstad [54] is that the crystallization half-time increases by about 45% for each 1% increase in meso-lactide content. The data in Figure 2.11 does not enable a systematic evaluation of molecular weight effects but one-to-one comparison of data with similar D-contents show that the half-time was increased with molecular weight as expected from the reduced chain mobility.

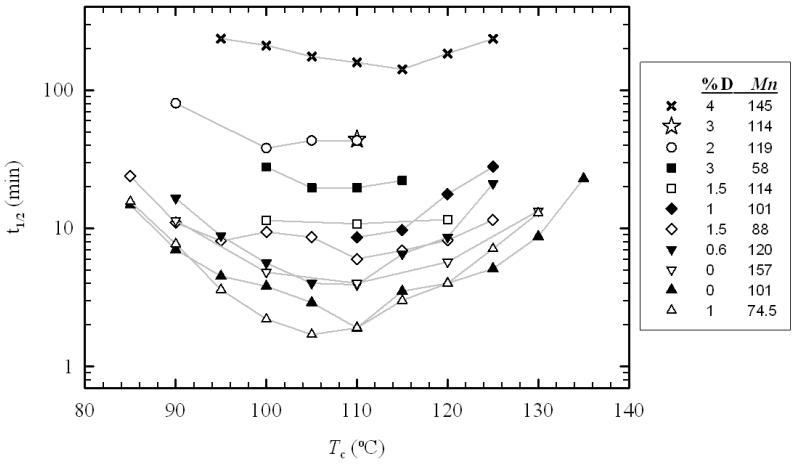

Figure 2.11 Crystallization half-time as a function of crystallization temperature for different D-lactate concentrations and molecular weights, Data adapted from [54, 76, 79, 110, 114]

The maximum crystallization rate, or the minimum half-time, was reached in the 105-110 ^{o}C range. It is noteworthy that the optimal crystallization temperature observed by isothermal calorimetry is 15-20 °C lower than the one determined from *in situ* spherulite growth rate measurement reviewed earlier. Also, the dual peaks sometimes reported for the growth rate are not observed in half-time curves. This illustrates the fact that the overall crystallization rate measured by calorimetry takes into account the increased number of crystallization sites emerging by reducing the temperature. It is also in agreement with the trend observed in Figure 2.7 where spherulite density sharply decreases above 110 ^{o}C. Therefore, at temperatures lower than the optimal growth rate temperature, the crystal growth rate decrease was compensated by a larger number of crystallization sites (higher nuclei density) due to increased driving force for nucleation.

Although it has a negative effect on total crystallinity and melting point, higher crystallization rates have been observed for branched PLA compared to linear one [31, 53]. The cold crystallization temperature was decreased and the crystallization peak was shifted to higher temperatures for branched PLA compared to the linear structure as a consequence of the nucleating effect of branching points. In addition, the magnitude of both the cold crystallization peak and crystallization peak upon cooling was increased due to the faster overall crystallization rate. It was also observed that increasing the branching level intensified the shifts of T_c and T_{cc} as well as peak amplitude.

2.1.6 PLA heterogeneous nucleation and plasticization

2.1.6.1 Nucleation

As discussed above, the overall nucleation and crystallization rates of PLA in homogeneous conditions are relatively low. This has prompted tremendous efforts in the scientific community toward the improvement of PLA crystallization kinetics by adding nucleants to increase its nucleation density and by adding plasticizers to increase chain mobility. Nucleating agents will reduce the nucleation induction period and increase the number of primary nucleation sites. In a general classification, nucleation can be either physical or chemical. The physical agents can be categorized as mineral, organic and mineral-organic hybrids. The different classes of nucleating agents are explained hereafter. It is noteworthy that the additional processing step required to blend additives into PLA may lead to molecular weight reduction by hydrolytic or thermal degradation. Therefore care must be taken in distinguishing between nucleation, plasticization and molecular weight reduction effects.

2.1.6.1.1 Chemical nucleating agents

Chemical nucleating agents are those for which nucleation proceeds through a chemical reaction mechanism. For example, Legras and co-workers [115-117] studied the nucleating effect of organic salts of sodium on the crystallization of polyesters such as PET and polycarbonate (PC). They showed that when sodium 2-chlorobenzoate is added to PET, it dissolves in the polymer melt and reacts with ester linkages through a chain scission mechanism to produce sodium-terminated ionomers. Acceleration in crystallization kinetics was associated to the decrease in molecular weight and to the association of ionic end-groups into clusters, the latter being more important. Garcia [118] and Zhang [119] did similar studies on the chemical nucleation of organic sodium salts on PET and PTT respectively. In the case of PLA, sodium salts such as sodium stearate have been explored for nucleating PLA crystallization but failed to provide significant improvement of the crystallization rate while severely decreasing the PLA viscosity due to extensive chain scission [76]. Another sodium salt investigated for this purpose was sodium benzoate [120]. At a concentration of 0.2%, it reduced the M_w of PLA from 163.3 to 127.5kg/mol, yet no enhancement in crystallization kinetics was observed.

2.1.6.1.2 Mineral nucleating agents

Talc is an effective physical nucleating agent for PLA and is commonly used as a reference to compare the nucleation ability of other additives [12, 54, 76, 80, 121-126]. For example, Kolstad [54] found that 6% talc increased the nucleation density by 500 times. This led to a 7 folds reduction in crystallization half-time, $t_{1/2}$, at the optimum crystallization temperature. In another study, a 35-fold reduction in $t_{1/2}$ with 1% talc was reported [76]. In addition, the optimum crystallization temperature was shifted from 100 to 120 ^{o}C in presence of talc [124]. In non-isothermal condition, the crystallization peak upon cooling ($T_{c.}$) is also shifted to higher temperatures. For example, it was reported that for the investigated cooling rates up to 80 ^{o}C/min, T_c was increased by 2-3 ^{o}C with increasing talc concentration from 1 to 2%. Further addition provided only an additional T_c increase of 0.5 ^{o}C/% talc indicating that relatively low talc amounts are sufficient for nucleation [76]. In another report using a low cooling rate of 1 ^{o}C/min, it was shown that the peak crystallization temperature was shifted from 107 to 123 ^{o}C when 3% talc was incorporated via solution blending [125].

Clay has been employed to improve thermal, mechanical and barrier properties of polymers. It is therefore interesting to examine its effect on the crystallization of PLA. In a qualitative study, narrowing of cold crystallization peaks were observed for PLA in presence of clay [127]. In another study, a crystallization rate increase around 50% was reported in presence of 4% organically modified montmorillonite [128]. The effect of clay exfoliation on crystallization was investigated by employing four different organo-modified clays. It was shown that the crystallinity and nucleation density of intercalated and flocculated samples were greater than those of nearly exfoliated clay. On the other hand, exfoliation of the silicate layers resulted in a lowering by about 10 ^{o}C of the cold crystallization temperature compared to intercalated morphology [129]. Kirkorian and Pochan confirmed that the exfoliated morphology had a lower nucleation effect but showed that the spherulite growth rate was increased in presence of exfoliated morphology [130]. They later used FTIR spectroscopy to identify the origin of these phenomena and concluded that in pure PLLA the inter-chain interactions precede helix formation, while for intercalated morphology inter and intra-chain interactions are simultaneous leading to faster crystallization. On the other hand, in exfoliated morphology, the helix formation started earlier and the silicate layers hindered the inter-chain interactions necessary for crystal nucleation [131]. The Avrami exponent was also used to demonstrate the effect of clay

exfoliation on PLA crystallization. In the optimum crystallization temperature range, natural clay with poor dispersion increased the exponent by about one unit implying a nucleation effect while the exponent was reduced relative to the neat PLA reference for organoclays due to the restriction of crystal growth [132]. Compared to talc, clay is a less efficient nucleating agent for PLA as the reduction in $t_{1/2}$ is moderate in isothermal mode and it is not effective for high cooling rates in non-isothermal crystallization.

2.1.6.1.3 Organic nucleants

Organic materials can also physically nucleate the crystallization of PLA. This is typically achieved by adding a low molecular weight substance that will crystallize more rapidly and at a higher temperature than the polymer, providing organic nucleation sites. It was reported that calcium lactate could increase the crystallization rate of an L-lactide/meso-lactide copolymer containing 10% meso-lactide [133]. This was not corroborated however by later work from Li and Huneault where calcium lactate was compared with talc and sodium stearate [76]. Stronger nucleation effects were reported by Nam et al. using N,N-ethylenebis(12-hydroxystearamide), (EBHSA) on a PLLA with 0.8% D content [134]. Upon heating at 5 ^{o}C/min, the cold crystallization temperature (T_{cc}) was reduced from 100.7 to 79.7 ^{o}C, showing that EBHSA can play a nucleating role. Cold crystallization is an experiment where the sample is heated from the solid amorphous state rather than cooled from the melt state. Optical micrographs at the interface of PLA and EBHSA showed a well-developed layer of trans-crystallites grown from EBHSA surface, an evidence for epitaxial crystallization of PLA. Since EBHSA crystallizes rapidly, it acted as nucleating agent given the condition that the isothermal crystallization was carried out below the melting point of EBHSA (144.5 ^{o}C). At high crystallization temperatures (130 ^{o}C), the nucleation density in presence of EBHSA was increased 40 times and the overall crystallization rate was increased 4 times. One advantage of organic nucleating agents is that they can be very finely dispersed in molten PLA. Nakajima et al. took advantage of this point to prepare haze-free crystalline PLA [135]. Different derivatives of 1,3,5-benzene tricarboxyamide (BTA) were solution blended with PLA and screened based on the solubility parameter and melting point characteristics in a cold crystallization experiment. PLA sheets with 1% of selected derivatives crystallized at 100 ^{o}C for 5 min exhibited 44% crystallinity while the neat PLA reference showed a crystallinity of 17% in the same conditions. More interestingly, the derivative with a lower melting point (206 ^{o}C) than processing temperature (235 ^{o}C) and similar solubility parameter to

PLA preserved PLA's transparency regardless of the high degree of crystallinity. Kawamoto et al. [123] compared the nucleating ability of hydrazide compounds with talc and EBHSA using a PLLA with 99.4% optical purity. Samples containing 1% nucleating agent were completely melted and their nucleation behavior was compared at a rate of 20 ^{o}C/min. Selected hydrazide compounds enabled complete PLA crystallization upon cooling with enthalpy of crystallization, ΔH_c, reaching 46 J/g. Talc and EBHSA showed ΔH_c of 26 and 35 J/g in the same conditions. The crystallization peak, T_c, was also higher for the hydrazide, 131 ^{o}C compared to 102 and 110 ^{o}C for talc and EBHSA. Finally, *p-tert*-butylcalix[8]arene is another organic material that has revealed interesting nucleating effect for PLA [111]. PLA with 1% of this material revealed a sharp crystallization peak at 134.3 ^{o}C upon cooling at a rate of 5 ^{o}C/min, 15 ^{o}C higher than that of 1% talc and nearly 26 ^{o}C higher than neat PLA. Furthermore, the Avrami exponent was increased from about 3 for neat PLA to nearly 5 for nucleated PLA as a result of change in crystal growth from spherulite to sheaf-like morphology.

2.1.6.1.4 Bio-based nucleants

Among organic nucleating agents, biobased nucleants are a particular subset of interest for PLA. Harris and Lee reported a reduction in the crystallization half-time of a 1.4% D PLA from 38 to 1.8 min when adding 2% of a vegetable-based ethylene bis-stearamide (EBS). Talc in the same conditions led to a lower half-time of 0.6 min. Upon cooling at 10 ^{o}C/min, addition of EBS enabled some crystallization with a broad and weak exotherm centered around 97 ^{o}C but again talc was more effective revealing a sharp peak at 107 ^{o}C [12].

Starch is a biopolymer that has raised a lot of interest in recent years and its blends with other polymers are under extensive investigation. The effect of starch on PLA crystallization was found to be relatively modest with a crystallization half-time reduction from 14 min to 1.8-3.2 for samples containing 1-40 % starch. Again, 1 % talc was found to be more efficient and decreased $t_{1/2}$ to about 0.4 min. It also shifted the optimum crystallization temperature up by about 15 ^{o}C compared to only 5 ^{o}C for starch [124].

Stronger effects were found by Li and Huneault when using starch in a thermoplastic state [136]. In this form, starch is an amorphous and highly plasticized polymer. It was found that the dispersed phase size reduction, obtained through interfacial modification, had a significant influence on PLA crystallinity. In fact, the unmodified blend comprising 20% of very coarsely

dispersed thermoplastic starch did not reveal any crystallization peaks at a cooling rate of 10 ^{o}C/min. However, in the same condition, the interface modified and finely dispersed blends crystallized to their maximum level (ΔH_c = 50 J/g). In isothermal crystallization, the minimum crystallization half-time was reduced to 75 s when using an interfacial modifier.

Cellulose nanocrystal (CNC) is another emerging material that has prompted high interest due to its high tensile properties and biobased origin. It was found that unmodified CNC, with a 15 nm diameter and 200-300 nm length, did not significantly affect PLA crystallinity [110]. However, when its surface was partially silylated (SCNC), it had a modest positive effect on crystallinity. Used at 1%, the modified CNC increased PLLA X_c from 14% to 30% upon slow cooling at 10˚C/min. In isothermal experiments, the crystallization half-time was decreased 2-fold to around 4 min when 1% SCNC was incorporated.

Orotic acid is another bio-based chemical that was recently investigated [137]. As little as 0.3% orotic acid had a significant effect on crystallinity development in non-isothermal and isothermal mode. At a cooling rate of 10 ^{o}C/min, a sharp crystallization peak at 124 ^{o}C with a high crystallization enthalpy 34 J/g was found. Besides, the $t_{1/2}$ in the 120-140 ^{o}C temperature range exhibited 10-20 fold decreases down to as low as 0.64 min. Authors believed that the good match between *b*-spacing of PLA and *a*-spacing of orotic acid crystals may explain this strong nucleating effect.

2.1.6.1.5 Carbon nanotubes (CNT)

Recently, carbon nanotubes have attracted attention because of their high aspect ratio and outstanding mechanical, thermal and electrical properties. Unmodified and modified CNT were investigated in a number of studies as nucleating agents for PLA [104, 138-143]. Xu et al. [141] reported modest nucleating effects for multi-wall carbon nanotubes (MWCNT) solvent-mixed at very low loading (up to 0.08 wt.%) in PLLA. Upon cooling, the crystallization peak temperature, T_c, was shifted to higher temperatures but did not enable significant crystallinity development at cooling rates of 10 ^{o}C/min and higher. PLA-grafted carbon nanotubes (PLA-*g*-CNT) were also investigated in a PLA with 2% D [104, 139]. At the moderate cooling rate of 5 ^{o}C/min, crystallinity of 12-14% were attained with 5-10% PLA-*g*-CNT [139]. Moreover, in isothermal experiments on similar material, the minimum $t_{1/2}$ was decreased from 4.2 min to 1.9 min with 5% PLA-*g*-CNT [104]. Li et al. [142] investigated the nucleating effect of maleic anhydride

functionalized multi-wall carbon nanotubes on a PLA containing 4.3% D unit. Since the PLA had a large optical impurity, slow cooling and annealing were required to develop full crystallinity. Samples comprising the CNT exhibited sharper diffraction peaks in WAXD analysis but DSC analysis revealed that the CNT were not effective nucleating agents in moderate (i.e., 10 ^{o}C/min) or rapid cooling conditions. According to the above mentioned examples, it seems that carbon nanotubes cannot play a significant nucleating role for PLA melt processing.

2.1.6.1.6 PLA stereocomplex

As mentioned above, mixture of PDLA and PLLA can crystallize in the form of a stereocomplex that has a melting point about 50 ^{o}C higher than the PLLA or PDLA homocrystals. Because the stereocomplex will form at higher temperature upon cooling than the homocrystals, small concentrations of PLA stereocomplex may be suitable for nucleating PLA homo-crystallization.

Brochu et al. [144] reported that in presence of the PLA stereocomplex, the spherulite density was higher and the homopolymer crystalline fraction was larger than that in the pure polymer, implying the nucleating effect of stereocomplex crystals. They concluded that PLLA crystals can form epitaxially on stereocomplex lamellae that were previously formed at higher temperatures. Schmidt and Hillmyer [80] studied the nucleation effect of the stereocomplex for PLLA crystallization in solvent mixed blends. They used the following nucleation efficiency (*NE*) scale based on the self-nucleation of polymers [145] in order to quantify the nucleation performance:

$$NE = \left(\frac{T_C - T_C^{\min}}{T_C^{\max} - T_C^{\min}}\right) \times 100 \qquad \textbf{Equation 2.13}$$

$T_c^{\min}$ is the crystallization temperature observed when the neat polymer is cooled from the amorphous state. $T_c^{\max}$ is the crystallization temperature when the crystallized polymer is partially melted and self-nucleated with the remaining crystals. In this case, *NE* is assumed to be 100% since there is a high concentration of well distributed nucleating crystals which have a high affinity to the melt. For the investigated systems, $T_c^{\max}$ and $T_c^{\min}$ were 157 ^{o}C and 106 ^{o}C, respectively. It was shown by measuring the crystallization temperature, T_c, for various

compositions that addition of small PDLA contents (forming the stereocomplex *in situ* in the PLLA major phase) had a higher nucleation efficiency than talc. For example, the nucleating efficiency of 6 % talc was 32% whereas that of 6 wt.% PDLA was 56%. In addition, the nucleation density with as little as 0.25 wt.% PDLA was more than 170 times that of pure PLLA. The use of 1% talc only doubled the nucleation density in the same conditions. Unfortunately, the nucleation density increase was not accompanied by an overall increase in the extent of crystallization of the PLLA. This behavior was related to the tethering effect of stereocomplex crystallites, reducing PLLA chain mobility.

In another study on PLLA crystallization, Anderson and Hillmyer used the scaling concept but this time for stereocomplex formed in the melt state [122]. They quantified the effect of PDLA molecular weight (M_n equal to 5.8, 14 and 48 kg/mol) and concentration (0.5-3 wt.%) on the nucleating efficiency of the stereocomplex. The highest efficiency was observed using the 14 kg/mol PDLA. Nucleating efficiency values up to 94% were achieved when 3% of this PDLA was used, suggesting an almost ideal nucleation behavior and implying that an optimum molecular weight exists. In addition, the final crystallinity of PLLA upon cooling at 5 ^{o}C/min was increased from 41% to 60% with the addition of 0.5% of 14 kg/mol PDLA. By contrast, the addition of 6% talc led to 54% crystallinity and a nucleating efficiency of 50%. The effect of the stereocomplex on the crystallization rate of PLA at 140 ^{o}C is depicted in Figure 2.12. For the lower molecular weight PLLA, the crystallization half-time, $t_{1/2}$ was reduced from 17 min to less than 1 min when 3% of a 14 kg/mol PDLA was melt blended. The same trend is observed for a higher molecular weight PLLA for which blends are prepared via solution mixing, but curves are shifted to higher half-times as a consequence of lower chain mobility. In both cases, the half-time for PDLA nucleated samples was one order of magnitude smaller than the corresponding PLA nucleated with 6% talc.

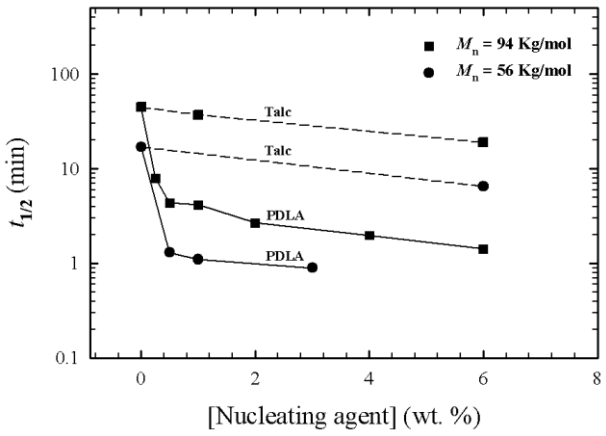

Figure 2.12 $t_{1/2}$ as a function of PDLA ($M_n \approx 14$ kg/mol) and talc concentration for two PLLAs of M_n = 56 and 94 kg/mol, data adapted from [80, 122]

Yamane and Sasai examined the role of higher molecular weight PDLA on the nucleation and crystallization of PLLA [146]. The PLLA with M_w =180 kg/mol was solution blended with PDLAs of 45, 120 and 260 kg/mol. Like Anderson and Hillmyer [122] and in contrast to the results obtained by Brochu et al. [144] and Schmidt and Hillmyer [80], they found that crystallinity increased with PDLA concentration when the PDLA content was very low, but tended to level off at higher PDLA concentrations. It is noteworthy that the nucleation efficiency for samples rapidly cooled from 200 ^oC was greater for the higher molecular weight PDLA and that this trend was reversed when the material was cooled from 240 ^oC. The authors explained that when cooling from temperatures below the stereocomplex melting point, the stereocomplex crystals are already present and those formed from higher molecular weight PDLA provide a larger surface area for PLLA crystallization. On the other hand, when samples are cooled from temperatures above the stereocomplex melting point, the stereocomplex has to be created within the limited timeframe of the cooling process, thus lower molecular weight PDLA is preferable because the stereocomplex is produced at a greater rate. Rahman et al. [147] also confirmed that PDLA with a lower molecular weight resulted in a higher stereocomplex crystallinity than a PDLA with higher molecular weight.

In Figure 2.13, the peak crystallization temperature upon cooling as a function of PDLA concentration is compared for different cooling rates (Φ in ^oC/min) and PDLA molecular weights (M_w in kg/mol). Two distinct trends arise from the stereocomplex formation route. For samples in which the stereocomplex exists from the beginning of the cooling cycle, the crystallization

temperature, T_c, increased with PDLA concentration up to a plateau. On the other hand, when the blends were cooled directly from the melt state without pre-existence of the stereocomplex, the nucleation effects were not observed until the PDLA concentration reached about 5%. This is due to the insufficient time to form the stereocomplex nucleation sites. Furthermore, when the cooling rate or molecular weight of PDLA was increased, T_c shifted to lower values.

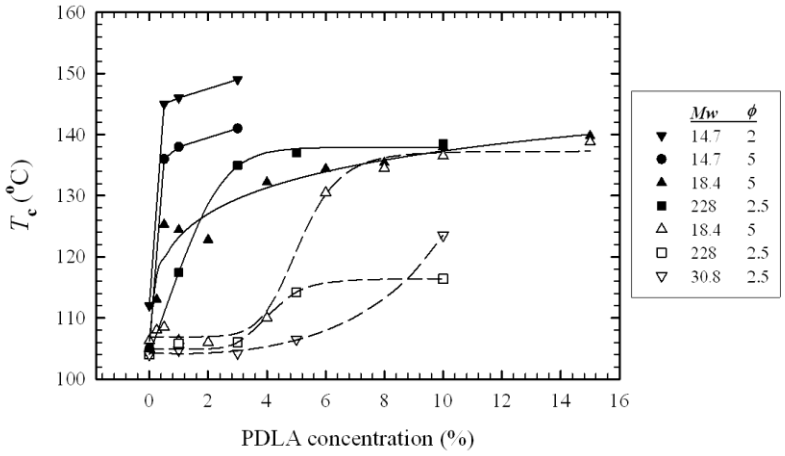

Figure 2.13 Effect of PDLA concentration on peak crystallization temperature for various molecular weight and cooling rate. Solid trend lines and filled symbols: pre-crystallized stereocomplex, dashed lines and open symbols: direct stereocomplex formation from the melt, data adapted from [80, 122, 147]

Tsuji et al. [79] compared the spherulite growth rates of stereocomplex-nucleated PLA with the stereocomplex growth rate observed in their previous study [148]. They concluded that the spherulites contained only PLLA crystallites because the growth rate was independent of the PDLA content. If the spherulites had contained stereocomplex crystallites other than nucleating sites, the growth rate should have increased due to the high stereocomplex growth rate. In addition, increasing the PDLA content did not have a significant influence on the induction time. Similarly, the nucleation constant (K_g) and front constant (G_0) did not show an explicit dependence on PDLA concentration indicating no growth mechanism variation related to the presence of the stereocomplex. Tsuji et al. also compared PLA stereocomplex to other nucleants such as talc, fullerene C_{60}, clay and polysaccharides [125]. The nucleating effect was ranked in the following order: PDLA > talc > C_{60} > montmorillonite > polysaccharides.

2.1.6.1.7 Nucleation based on inorganic-organic hybrids

Inorganic-organic hybrids are a new class of materials that include polyhedral oligomeric silsesquioxane (POSS) and layered metal phosphonates. Unlike organoclays, the organic and

inorganic components of these hybrid materials are connected through covalent rather than ionic bonds. In the case of POSS, the material core is constituted of a silicon and oxygen "nanocage" grafted with organic arms that can be modified depending on requirements. In a series of studies, Qiu et al. investigated the effect of POSS with isobutyl, methyl and vinyl arms on the PLA properties [149-152]. In cold crystallization experiments at a heating rate of 20 ^{o}C/min, POSS decreased the cold crystallization peak temperature, T_{cc}, between 10 and 22 ^{o}C depending on the organic arm and POSS concentration [149, 151, 152]. The developed crystallinity was also increased from 8 to 44%. In isothermal experiments, 1% POSS with vinyl arms decreased $t_{1/2}$ from 8 to 1.2 min [152]. Upon cooling at 5 ^{o}C/min, the crystallization temperature was increased by 10-15 ^{o}C compared to neat PLA and the samples were fully crystallized within the cooling cycle. At a cooling rate of 15 ^{o}C/min however, only a small crystallization exotherm appeared around 92 ^{o}C for 2% POSS. This was shifted slightly to 95 and 97 ^{o}C when POSS concentration was increased to 5 and 8%, respectively [151].

Layered metal phosphonates have also exhibited a nucleating effect on PLA. Pan et al. compared the nucleation effect of zinc phenylphosphonate (PPZn) to that of talc and PDLA at 1% nucleating agent content [126]. For crystallization upon cooling at 10 ^{o}C/min, the highest crystallization temperature, around 128^{o}C, and the sharpest crystallization peaks were achieved for PPZn. At the same cooling rate, a very high crystallinity of 47 to 56% was achieved when using PPZn in the range of 0.02 to 15% in PLA. The cold crystallization temperature of quenched samples was also shown to be reduced by up to 30 ^{o}C when adding PPZn. In isothermal tests, PPZn was also more effective than talc and PDLA in reducing the crystallization half-time, $t_{1/2}$, of PLA. Values as low as 0.63 min were found compared to over 6 min for talc and PDLA respectively. It was suggested that the match of the lattice parameters of PPZn and PLA α crystal explains such a great enhancement of the crystallization behavior. In another study, Wang et al. investigated the effect of metal type on PLA/layered metal phosphonate composites by comparing zinc, calcium and baryum phosphonates (PPZn, PPCa and PPBa) [153]. It was found that the nucleating ability decreased in the following order PPZn > PPCa > PPBa due to the different dispersion and interfacial interaction of nucleating agents with PLA matrix.

2.1.6.2 Plasticization

Since PLA is a brittle material, plasticization has been employed extensively for toughening and extending its applications [5]. Plasticization may have contrasting effects on the crystallization behavior. On one hand, the T_g depression, a measure of plasticization efficiency, will shift the crystallization temperature window to lower temperatures. The increased chain mobility will facilitate the movement of chains from the amorphous phase unto the existing crystal surface, especially at lower temperatures. Consequently, parameters that are directly associated with chain mobility will be affected. For example in isothermal crystallization mode, spherulite growth rate should increase and the optimum growth temperature should be lowered. For cold crystallization, the crystallization peak should be sharper and shifted to lower temperatures. On the other hand, plasticization may also cause melting point and equilibrium melting point depression, adversely influencing the growth rate and overall crystallization rate at a given crystallization temperature due to the reduced degree of undercooling ($T_m^0 - T_c$) driving the crystallization and primary nucleation processes. Therefore, the enhancement in chain mobility may be partially compensated for by reduced primary and secondary nucleation.

In Table 2.5, average T_g and T_m depression as a function of plasticizer concentration is compared for some of the plasticizers explored for PLA.

Table 2.5 Average T_g and T_m depression of PLA as a function of plasticizer type and concentration

Plasticizer	Abbr.	M_w (g/mol)	ΔT_g/[Plasticizer] (°C/%)	ΔT_m/[Plasticizer] (°C/%)	Ref.
Polyethylene glycol	PEG	200	2.34	0.6	[154]
		400	2.33	0.46	[154, 155]
		578	2.51		[156]
		1000	1.91	0.16	[154, 157]
		1500	1.55	0.1	[155]
		8000	1.87	0	[77, 158, 159]
Polypropylene glycol	PPG	530	2.25		[156]
		1123	2.17		[156]
Poly(ethylene glycol-co-propylene glycol)	PEPG	12000	1.78	0.13	[160]
Triphenyl phosphate	TPP	326.3	1.34	0.37	[161]
Dioctyl phthalate	DOP	390.56	1.75	0.46	[162]
Di(2-ethylhexyl) adipate	DOA	371	1.48	0.4	[163-165]
Polymeric adipate	G206/2	1532	1.76	0.23	[163]
	G206/3	2000	1.96	0.4	[164, 165]
	G206/5	2700	1.48		[164]

	G206/7	2565-3400	1.75	0.26	[163-165]
Poly(1,3-butylene adipate)	PBA	1500-3000	1.03		[166]
Triethyl citrate	TEC	276	1.45	0.81	[167, 168]
Tributyl citrate	TBC	360	1.85	0.43	[167-170]
TBC- oligoester	TBC-3	980-4450	1.27	0.3	[169, 170]
	TBC-7	2200-63600	0.6	0.2	[169, 170]
Acetyl triethyl citrate	ATEC	318	1.28	0.39	[167, 168]
Acetyl tributyl citrate	ATBC	402	2	0.46	[166-168]
Glycerol			0.33	0.78	[155]
Oligomeric lactic acid	OLA	-	2.05	0.9	[155]
Poly(1,3-butanediol)	PBOH	2100	1.2	0.12	[154]
Acetyl glycerol monolaurate	AGM	358	1.54	0.36	[154]
Dibutyl sebacate	DBS	314	1.53	0.45	[154]
Diethyl bishydroxymethyl malonate	DBM	220	1.67	0.57	[169, 171]
DBM-oligoester	DBM-A-8	4200	0.87	0.2	[169]
	DBM-A-18	8900	0.67	0.2	[169]
	DBM-S-4	1800	1.07	0.4	[169]
	DBM-S-7	3500	0.8	0.27	[169]
	DBMAT	2300	0.87	0.2	[169]
DBM-oligoesteramide	DBMATA	3200	1.13	0.4	[169]
Glyceryl triacetate	GTA	218.2	1.85	0.59	[165, 168]

Polyethylene glycol (PEG) is the most investigated plasticizer for PLA. It is available in a wide range of molecular weights. Copolymers of ethylene glycol or ethylene oxide with lactic acid and the possibility to have different chain termination groups are also of great interest to manipulate its properties. The addition of PEG reduces the T_g by approximately 2˚C per % plasticizer while it does not affect melting point significantly. Combination of these two characteristics makes PEG a suitable crystallization promoter for PLA. In different studies on PLA plasticization, PEG was compared to glucose monoester and partial fatty acid ester [172], to citrate ester, glycerol and oligomeric lactic acid [155] and to poly(1,3-butanediol), dibutyl sebacate and acetyl glycerol monolaurate [154]. Among these plasticizers, PEG was found to be the most efficient in decreasing the glass transition temperature and the cold crystallization temperature. Even a PLA with 5% D units which does not readily cold crystallize was found to cold crystallize between 88 and 90 ^{o}C with 10% PEG and up when heated at a rate of 10 ^{o}C/min [77]. The crystallinity of PLA and PEG was also found to be proportional indicating that PEG in the intra-spherulitic region crystallized much faster than that in the inter-spherulitic amorphous region. The effect of PEG end-group on plasticization and crystallization was also investigated

[78, 173, 174]. For PEG in the lower range of M_w (400-750 g/mol) and concentrations up to 10%, the end-groups did not exhibit any significant influence on crystallization parameters such as transition temperatures, crystallinity and growth rate [78]. However, when comparing methyl-methyl, hydroxyl-hydroxyl, methyl-hydroxyl and amine-amine terminated 2000 g/mol PEG [173, 174], it was found that the miscibility decreased in the following order: $2NH_2$> $2CH_3$> 1OH-1CH_3> 2OH. Furthermore, the melting point depression was found to increase according to the miscibility ranking. Hydroxyl-terminated PEG showed the smallest depression (3 and 7 ^oC for 10 and 30%) while the amine-terminated PEG showed the highest effect (14 and 26 ^oC for 10 and 30%). High miscibility of amine-terminated PEG with PLA and highest melting point reduction were associated to the ionic interaction of amine groups with the carboxylic acid groups at PLA chain ends. Due to the competition between chain mobility and nucleation, it was found that the crystallization half-time, $t_{1/2}$, went through a minimum when increasing the PEG content. This concentration was lower for amine-terminated PEG than other types of PEG, i.e., 10% vs. 30% plasticizer. Regarding the crystallization kinetics, contrary to the prediction based on the melting point reduction, amine-terminated PEG enabled fastest crystallization, a behavior that was attributed to the lowest fold-surface free energy when PEG has two amine end-groups compared to other end-group types.

Polypropylene glycol (PPG) is another oligomeric plasticizer investigated for PLA [156, 175]. As the data in Table 2.5 suggests, PEG and PPG have similar effects on T_g. However, PPG may be less miscible with PLA and blends with only 12.5% PPG were shown to exhibit a second T_g around -77 ^oC related to a phase-separated PPG phase [156]. PPG was found to be less efficient in cold crystallization enhancement than PEG. Finally, based on the spherulite size measurements with a Small Angle Light Scattering (SALS) technique, it was shown that the growth rate and nucleation density were greater with PEG than with PPG [175].

Among the low molecular weight plasticizers for PLA, citrate esters are the most investigated ones. These materials are as effective as PEG for reducing the glass transition temperature but induce a higher melting point reduction. Among common citrates, tributyl citrate and acetyl triethyl citrate were found to be more efficient than triethyl citrate and acetyl tributyl citrate [167]. In another study, glycerin triacetate also known as triacetine was compared with the aforementioned citrate esters. It was found that tributyl citrate and triacetine led to the strongest

cold crystallization temperature decrease, from 95 to around 67-70 ^{o}C by incorporation of 20-25% plasticizer. However, no significant effect on crystallization upon cooling was observed [168]. In addition to citrate esters, other low molecular weight plasticizers such as triphenyl phosphate and dioctyl phthalate were found to enhance PLA crystallization [161, 162]. In the case of triphenyl phosphate, the plasticizer used at 10, 20 and 30 % reduced significantly the T_g of PLA by 14, 26 and 39 ^{o}C, respectively, and increased the spherulite growth rate. The maximum growth rate for PLA was 16.8 μm/min, appearing at 132 ^{o}C. For 10, 20 and 30% triphenyl phosphate, the growth rate was increased to 30.6, 53.4 and 52.8 μm/min and the optimum temperature was reduced to 123, 110 and 102 ^{o}C, respectively [161].

Adipates are another family of PLA plasticizers. For this group of plasticizers, the T_g decreases with plasticizer concentration only up to concentration of 10% probably due to limited miscibility with PLA. Accordingly, only modest crystallization enhancements were found when using adipate plasticization [163, 165].

Even though it cannot be used as a conventional plasticizer because of its high volatility, it is interesting to note that carbon dioxide is highly soluble in PLA and has shown outstanding plasticization and crystallization enhancement effects in PLA [176-181]. This is of practical importance mainly in the extrusion foaming process where CO_2 can be used as a physical blowing agent for PLA. On a weight-basis, CO_2 is much more effective in reducing T_g than the plasticizers mentioned in Table 2.5. For example, Reignier et al. [178] showed that the T_g was decreased by 24 ^{o}C, 46 ^{o}C and 58 ^{o}C for 5, 10 and 15 wt.% CO_2 respectively. On a pressure basis, Takada et al.[176] found that T_g and T_m decreased linearly with increasing CO_2 pressure at a rate of 3.66 and 2.18 ^{o}C/MPa respectively. Reignier et al. showed as well that crystallization accelerates in the chain mobility controlled region in the presence of CO_2 [178]. Similar effect of CO_2 on isothermal crystallization kinetics was reported by Yu et al. [177] where $t_{1/2}$ for cold crystallization at 70 ^{o}C was reduced sharply from about 360 min for atmospheric pressure to about 10 min by increasing CO_2 pressure to 2 MPa. In actual extrusion foaming trials, Mihai et al. have shown that a very rapid PLA crystallinity development was triggered by the presence of 6-7% CO_2. Above this concentration, highly crystalline PLA foams could be formed within the few seconds of foam formation even though the neat PLA had a crystallization half-time in excess of 40 minutes in quiescent conditions. This rapid crystallinity formation could not be

explained solely in terms of a plasticization effect and this pointed out that additional nucleation effects, possibly from supercritical carbon dioxide clusters, were necessary to explain the dramatic rise in crystallization rate [180, 181].

2.1.6.3 Combination of nucleation and plasticization

The heterogeneous nucleation provided by nucleants has its greatest impact on the overall crystallization rate at elevated temperature when the driving force for homogeneous nucleation is weak. Plasticization, on the other hand, will have its highest impact at a lower temperature when crystallization is hindered by a lack of chain mobility. Therefore combination of nucleation and plasticization is expected to widen the crystallization temperature window and increase the crystallization rate of PLA. Among the first promising reports on this topic were those of Pluta [182] followed by Ozkoc et al. [183, 184] focusing on blends of a PLA containing 4% D units with combinations of up to 20% PEG and 5% clay that was either pristine or organically modified. The cold crystallization peak, T_{cc}, for samples having both modifiers appeared at approximately 80 ^{o}C which was 20 ^{o}C less than the neat PLA. Upon cooling, neat PLA and its composites with 3 or 5% clay did not reveal any crystallization peaks even at a low cooling rate of 2 ^{o}C/min. At the same rate, plasticized formulations showed some crystallization peaks, with crystallization enthalpy up to 22 J/g but this value rapidly decreased to 13 J/g when the cooling rate was increased to 15 ^{o}C/min. The peak crystallization temperature T_c was 8-9 ^{o}C lower for plasticized composites compared to plasticized PLA [184]. This is in contrast with Pluta's work showing a drop in ΔH_c and a slight increase in T_c when clay was introduced [182]. Later, Li and Huneault [76] examined combinations of talc with ATEC or PEG as plasticizers for a PLA containing 2% D units. Much faster crystallization kinetics was achieved at 1% talc and 10% plasticizer levels than with the clay/PEG combination. Upon cooling at 10 and 20 ^{o}C/min, the materials exhibited a sharp crystallization peak around 105 ^{o}C and crystallized to their maximum level (over 40 J/g) within the cooling cycle. In comparison, sample with only 1% talc had a crystallization peak at 94 ^{o}C and reached only half of the full crystallinity. A similar study later confirmed these findings with 1% talc and up to 20% PEG [185]. Based on polarized optical micrographs obtained after non-isothermal crystallization at 2.5 ^{o}C/min from the melt, spherulite density decreased in the following order: PLA/talc > neat PLA > PLA/talc/20% PEG. Therefore, reduced nucleation due to plasticizer addition is compensated for by an increased growth rate, resulting in a higher overall crystallization rate. The effect of the plasticizer is highlighted at high

cooling rates in Figure 2.14. In this figure, the developed crystallinity upon cooling is depicted as a function of the cooling rate for nucleated and nucleated/plasticized samples. The crystallization enthalpy of the neat PLA control dropped sharply from 35 to nearly 0 J/g as the cooling rate was increased from 1.5 to 10 ^{o}C/min leading to essentially amorphous material. The talc filled PLA suffered a similar drop at higher cooling rates. The nucleated/plasticized formulations, however, were much less sensitive to the cooling rate. Even at a cooling rate of 80^{o}C/min, the formulation with talc/PEG still crystallized to a high level.

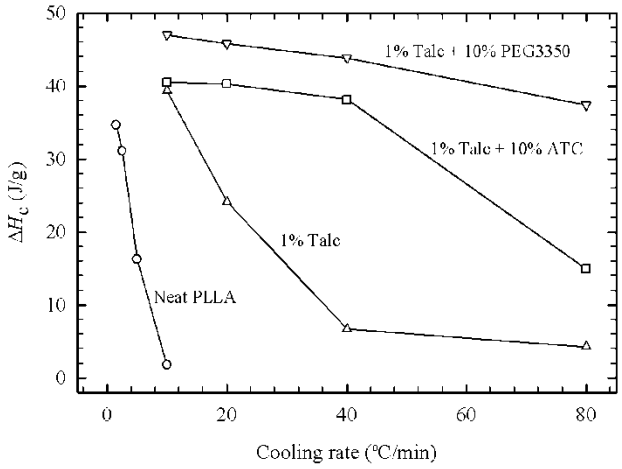

Figure 2.14 Crystallization enthalpy as a function of cooling rate for different formulations, data adapted from [76, 185]

Other plasticizer/nucleant combinations lead to more moderate improvements. Instead of PEG, Xiao et al. combined talc with triphenyl phosphate plasticizer (TPP) to enhance the crystallization of a PLA containing 2% D units [106, 186]. PLA containing talc and talc+TPP showed the fastest crystallization kinetics with the development of a crystallization enthalpy around 30 J/g at a cooling rate of 10 ^{o}C/min. In isothermal conditions, the crystallization half-time, $t_{1/2}$, was reduced from 3.6 min for the neat PLA to 0.7 and 0.9 min for the nucleated and nucleated/plasticized samples, respectively. Another investigated combination was CNT and PEG. As pointed out earlier, CNTs do not seem to provide a strong nucleating effect for PLA. Addition of up to 10% PEG to 0.5% CNT/PLA blends failed to show any significant crystallinity at cooling rates greater than 2 ^{o}C/min [187]. In addition, based on optical microscopy monitoring, it was shown that the presence of the CNT decreased the spherulite growth rate probably by restricting the PLA chain mobility.

The cooling rates investigated in differential calorimetry studies are typically far below the ones prevailing in polymer processing operations such as injection molding. In processing operations, crystallization is also preceded by rapid polymer flow that can lead to strain-induced crystallization. Therefore, it is interesting to see how crystallinity can develop in typical industrial processing conditions. Figure 2.15 reproduces crystallinity data as a function of the mold temperature of an injection molding process. The data from Li and Huneault [76] is for PLA with 1% talc / 5% ATC molded using a 1 minute cycle. The data from Harris and Lee [12] is for pure PLA and for a PLA nucleated with 2% talc but for a molding cycle of 3 minutes. Typically, low mold temperature will enable faster solidification of the molten material and thus will enable shorter cycle time. In the case of slow crystallizing materials, part solidification may occur through cooling below the glass transition temperature or through a significant increase in the material crystalline content. In the reported studies, quality parts were obtained at low mold temperatures, around 20-40 ^{o}C but these were essentially amorphous. At mold temperatures in the 50-60 ^{o}C range, close to PLA's T_g, the molded parts could not be ejected out of the mold because they were too soft. Finally, when maintaining the mold at 70-100 ^{o}C, highly crystallized quality parts were produced. It is noteworthy that in quiescent DSC conditions, getting fully crystallized samples in isothermal conditions below 100^{o}C would require a much longer time. The shearing and local orientation, inherent to the molding process, therefore had a positive effect on the final crystallinity.

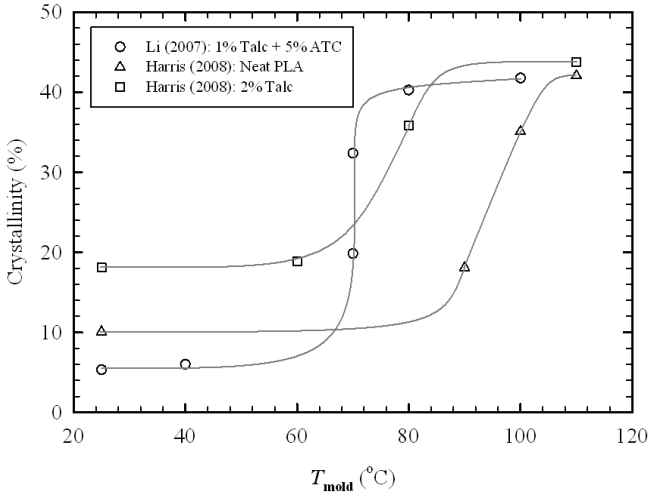

Figure 2.15 Crystallinity versus mold temperature for injection molded PLA, data adapted from [12, 76]

The significance of shear-induced crystallinity in PLA was supported by optical microscopy observations of Li et al. on sheared PLA in isothermal [84] and non-isothermal [188] conditions. They reported that in samples pre-sheared at 1 s^{-1} and then crystallized isothermally above 120 ^{o}C, thread-like precursors first appeared and then turned into cylindrite crystals before additional spherulites started to grow. By contrast, under quiescent conditions, only spherulites were formed. Compared to the crystallization in quiescent conditions, sheared samples had lower induction time and a higher nucleation density. This morphology change was not observed however at temperatures below 120 ^{o}C probably due to the greater supercooling and thus greater homogeneous nucleation rate. In a non-isothermal test procedure, pre-sheared samples were cooled at controlled rates between 0.5 and 5 ^{o}C/min. It was found that the formation of cylindrite crystals occurred only if the shear rate used for the pre-shearing was above a certain critical value. For example, at 2 ^{o}C/min cooling, cylindrites were formed only for shear rates above 5 s^{-1}. Furthermore, the onset crystallization temperature was shifted up by as much as 30 ^{o}C by the pre-shearing. The final crystalline content was increased from 9% in quiescent conditions up to more than 30% for pre-sheared samples. Similar observations were later reported by Huang et al. [189]. Considering that the deformation rates in actual polymer processing machinery are much higher than in these model experiments, it is likely that at elevated temperature, strain-induced nucleation of PLA has a positive effect on the overall crystallization of foamed, molded or extruded PLA.

2.2 Poly(lactic acid) Stereocomplex

In section 2.1, the subject of PLA stereocomplex was introduced briefly and its application as a nucleating agent was reviewed. In this section, more details about PLA stereocomplex formation are provided.

2.2.1 Structure of PLA stereocomplex

Upon discovery of the PLA stereocomplex, Ikada et al. reported that its X-ray diffraction pattern is different from homopolymer crystals; however, the crystal structure was not determined. Only by assuming a right-handed helical conformation for PDLA chain, based on the left-handed helical chain conformation of PLLA proposed by De Santis and Kovacs [35], they suggested the origin of this stereocomplex formation to be van der Waals forces such as dipole-dipole interactions. The crystalline structure of the PLA stereocomplex was studied in

detail by Okihara et al. [46] based on X-ray measurements and energy calculations. Crystal system was found to be triclinic with cell dimensions of a = 0.916 nm, b = 0.916 nm and c = 0.870 nm and angles of $\alpha = 109.2^{o}$, $\beta = 109.2^{o}$ and $\gamma = 109.8^{o}$. They suggested that chains' conformation is 3_1 helix, each unit cell containing a PLLA and a PDLA chain with the same number of L and D units. It means that in stereocomplex crystals, chains are more extended compared to PLLA α crystal in which chains are 10_3 helices. Figure 2.16 is a schematic illustration of the stereocomplex crystal structure.

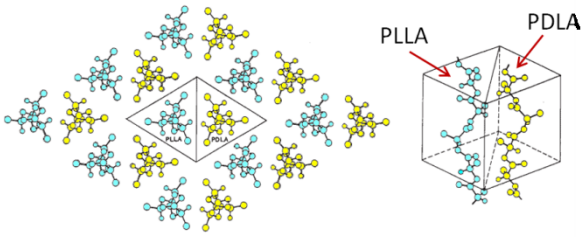

Figure 2.16 Crystal structure of PLA stereocomplex [190]

2.2.2 Stereocomplex detection and crystallinity measurement

DSC analysis: The most interesting characteristic of PLA stereocomplex is to have a melting point about 50 ^{o}C higher than that of each polymer homocrystals [10]. Difference between the melting point of the homocrystal and that of the stereocomplex gives the opportunity to evaluate the existence and amount of stereocomplex in blends of PLLA and PDLA or stereo-block copolymers, simply by DSC analysis.

XRD analysis: Ikada et al. [10] found that another feature of the PLA stereocomplex is its different XRD pattern compared to homocrystals. Therefore, the stereocomplex can be detected without altering the polymer's thermal history. They reported diffraction peaks for stereocomplex PLA appearing at 2θ around 12, 21 and 24 degree whereas PLA homocrystal diffraction peaks appear at 2θ equal to 15, 16, 18.5 and 22.5 degree. It is also possible to evaluate the amount of stereocomplex present in the system with this method [191].

Other methods have also been proposed that can detect the presence of stereocomplex. Microscopy techniques like SEM, TEM and AFM, spectroscopy techniques such as FTIR, Raman and NMR in which peaks' shapes, intensities and positions change as a consequence of

stereocomplexation can be named for such methods. However, these techniques are not useful for quantitative analysis of stereocomplex formation.

2.2.3 Thermodynamic aspect

In a study on the PLA stereocomplex formation at constant polymer concentrations [192], Tsuji et al. demonstrated that above a critical total concentration, a gel is formed in the solution after enough time is given. This concentration is higher for lower molecular weight polymers. Dried gel showed only a single endothermic peak at 216 ^{o}C in DSC experiment, showing that the crosslinking crystallites are only made by stereocomplex. As a result, one can reason that the critical concentration for stereocomplexation is lower than that for homocrystallization. In another study concerning the stereocomplex formation upon precipitation from solution by adding a non-solvent [193], only stereocomplex was formed over a wide range of molecular weights unless total concentration was increased.

Dominant formation of stereocomplex rather than homocrystal in the above examples suggests the energetically favorable co-crystallization compared to homocrystallization of PLA from a thermodynamic point of view. In addition, based on energy calculations by Okihara et al. [46], a 3_1 helix chain conformation in stereocomplex is more stable than a 10_3 helix in α-form crystal.

2.2.4 Parameters affecting co-crystallization

Despite that co-crystallization is more favorable thermodynamically; slow crystallization kinetics is the limiting factor to produce PLA stereocomplex efficiently. As a result, there is a competition between stereocomplex formation and homocrystallization. Different parameters influence the extent and kinetics of stereocomplex formation, which, in turn, influence the homocrystallization as well. Polymer structure, i.e. the enantiomeric purity and molecular weight of the constituents, blending method, crystallization conditions and procedure, and PLLA/PDLA blending ratio are the main parameters that determine the extent and kinetics of co-crystallization.

Blending ratio: DSC analysis by Ikada et al. revealed that the optimum blending ratio for PLLA and PDLA is 1:1. At this ratio, only stereocomplex was formed with the procedure they used for blending and by deviating from equimolar ratio, PLA homocrystallization occurred

simultaneously. Considering the proposed stereocomplex crystalline structure in which PLLA and PDLA chains are paired in each cell with the equilateral triangles structure, it is reasonable to say that equimolar blending ratio is the optimum ratio for efficient production of stereocomplex. Therefore, most of the research has been conducted at this blending ratio.

Tsuji et al. [193, 194] demonstrated that for PDLA fraction (X_D) between 0.1 to 0.3 and 0.7 to 0.9, melting peaks of both homocrystal and stereocomplex was observed, while only stereocomplex was detected for X_D between 0.4 to 0.6 with the maximum of ΔH_m at $X_D = 0.5$, and homocrystallization happened near $X_D = 0$ and 1.

Blending and crystallization route: Methods of producing stereocomplex PLA are divided to two main categories; stereocomplexation in solution and in bulk. Considering the efficiency, facility of production and required time for the stereocomplex formation, mostly solution methods, specifically solution casting and solution precipitation are employed. Although direct melt blending is the preferred route in polymer blending industry due to higher production capacity and the appeal for solvent-less processing. As will be seen in the reviewed literature below, only a small fraction of the literature in the field of stereocomplexation has dealt with melt processed blends. This is probably due to the high cost and limited availability of PDLA which made it unpractical for more material-consuming processes such as melt blending in industrial extruders.

Figure 2.17 compares solution precipitation and solution casting from the view point of stereocomplex formation efficiency and its competition with homocrystallization. The comparison is done for the 1:1 PLLA/PDLA blends.

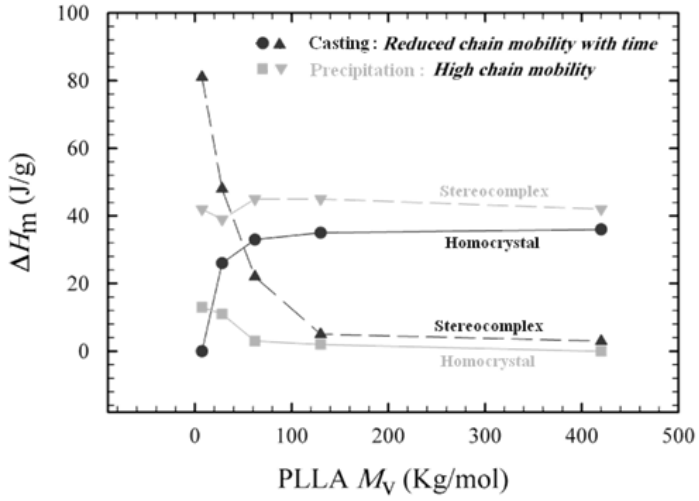

Figure 2.17 Competition between stereocomplex and homocrystal formation in solution casting and precipitation methods[193, 194]

As shown in this figure, when solution precipitation is employed, for a wide range of molecular weights only stereocomplex is formed. Only if concentrated solutions (5 g/dL) were precipitated or if precipitation was done without stirring, stereocomplexation was reduced for high molecular weight polymers and homocrystallization took place as well.

Contrarily, in the solution casting route, the amount of stereocomplex decreased rapidly and gave place to homocrystallization; the chains that could not participate in co-crystallization produced more homocrystals. Increasing polymer concentration and molecular weights, by decreasing chain mobility, prevented co-crystallization.

Another possible route is to blend polymers by solution casting method but perform crystallization studies from the melt [67]. In this case, the mixing level is similar to the previous studies but crystallization occurs in the melt state. It was found that stereocomplexation proceeded rapidly after cooling the melt while homocrystallization required much longer induction time. This may be the consequence of higher under-coolings as the equilibrium melting point of the stereocomplex is higher than that of the homocrystals. At the mixing ratio of 50:50, increasing the molecular weights of the components resulted in increased homocrystallization and reduced stereocomplex formation. Amount of melting enthalpy obtained in this way for stereocomplex and homocrystal is compared with solution casting in Figure 2.18.

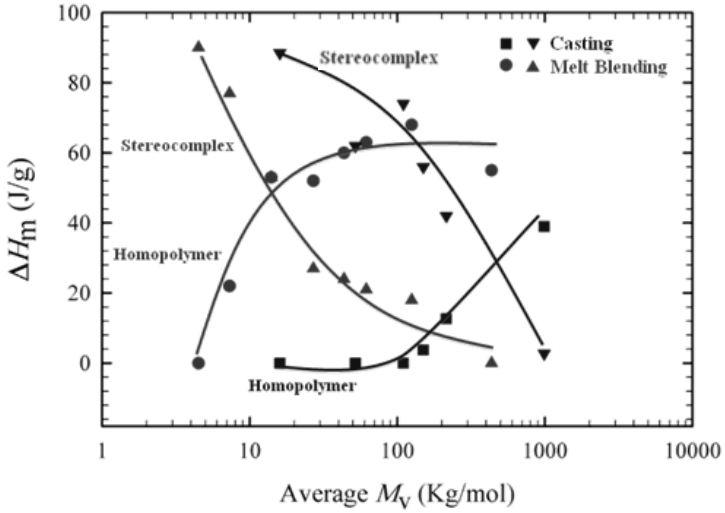

Figure 2.18 Competition between stereocomplex and homocrystal formation in solution casting and from the melt [67, 75]

Also by deviating from equimolar blending ratio, homocrystallization and stereocomplexation happened simultaneously. Overall stereocomplex crystallization was completed more rapidly compared to homocrystallization of PLLA or PDLA which was ascribed to higher spherulite density of stereocomplex.

Based on these behaviors, one can conclude that the melt blending conditions are less favorable to stereocomplex formation because the mixing level is not as high as solution blending. The crystallization from the melt also involves non-isothermal crystallization that must occur at high cooling rates. These are non-favorable conditions that must be faced in industrial scale polymer processing.

Molecular weight: Both Figure 2.17 and Figure 2.18 demonstrate molecular weight's effect on the extent of homo and co-crystallization. In Figure 2.17, PDLA has a viscosity average molecular weight of 360,000 g/mol and PLLAs with different molecular weights are used. When PLLA and PDLA are mixed by a solution blending method in a 50/50 ratio and that the mixture is concentrated slowly in a film casting process, the stereocomplex is preferentially produced only when either of the components had a low molecular weight. The stereocomplex is exclusively formed for polymers for viscosity-average molecular weights lower than 4×10^4 g/mol. However, homocrystallization is predominant when both polymers have high molecular weights, e.g. 1×10^5 g/mol [194]. In contrast, when the solution was precipitated directly, results

were different. At the moment of crystallization, chains are at high mobility in solution state and well mixed at the molecular scale. In that case, stereocomplexation was preferred to homocrystallization, irrespective of the molecular weight of components.

In Figure 2.18, PLLA and PDLA have almost similar molecular weights, with their average molecular weight as independent variable. The effect of molecular weight on stereocomplex formation was similar to solution casting except that the critical viscosity-average molecular weight below which only stereocomplex forms is lower, i.e. 6000 rather than 40000 g/mol. It is clear that in both cases, at low molecular weights, co-crystallization is dominant as it is thermodynamically more favorable and there are no kinetic limitations. In cast films, by increasing the molecular weight, from about 100,000 g/mol, homocrystallization starts to increase while enthalpy of fusion for co-crystallization falls as a consequence of chain mobility restriction. This is worse in the case of crystallization from melt since it starts from much lower molecular weights.

Chain's optical purity: Chain optical purity is decreased as the content of opposite enantiomeric monomer increases in the polymer. Similar to its effect on homocrystallization, optical purity of the polymers affects the extent of stereocomplexation. In a study by Tsuji and Ikada [24], 1:1 blends of similar optical purity PLLA and PDLA prepared by solution casting as well as non-blended polymers were subjected to DSC and POM analysis. Photomicrographs revealed that non-blended polymers with optical purity less than 76% had no spherulitic structure. Spherulite density was increased by decreasing isothermal crystallization temperature (T_{iso}), especially for lower optical purities. Furthermore, at a similar T_{iso}, spherulite density was higher for polymers with higher optical purity due to higher undercooling associated to higher equilibrium melting point (T_m^0). In addition, blended films had higher spherulite density than non-blended ones at any optical purity and crystallization temperature. When melt quenched PLLA and PDLA samples were heated in DSC tests, they showed T_g around 55 ^oC, a cold crystallization and subsequent melting peaks. Increasing optical purity reduced the cold crystallization temperature and increased the melting point. Optical purities less than 90% showed no homocrystallization and melting peaks. For blended samples, a melting peak associated to the stereocomplex was also observed around 230 ^oC. While homopolymers with 83% optical purity could not crystallize during heating in DSC, the blend of those polymers

could crystallize. At a fixed crystallization temperature, increasing optical purity increased the melting point. In this work, Tsuji and Ikada estimated the equilibrium melting temperature of stereocomplex crystallites (T_m^0) to be 279 ^oC.

Brochu et al. [144] examined the influence of composition and overall enantiomeric excess on the morphology of PLA stereocomplexes. They prepared the samples by solution blending PLLA and PDLA and slow solvent evaporation. For the PLLA they prepared a 100% pure sample, 100L. Two samples of PDLA was used, 100% pure PDLA, 100D, and a sample with 90% D-lactide, 80D (enantiomeric excess is 80%). For 100L/100D cast films and those isothermally crystallized at 140 ^oC for 1 h, enthalpy of fusion of the stereocomplex increased linearly by increasing PDLA content up to the maximum at 50:50 composition, similar to what was previously pointed out on the effect of blending ratio. Meanwhile ΔH_m of PLLA decreased linearly to the point that at 40% PDLA, no PLLA homocrystal was formed. This is an indication of prohibition of homocrystal formation in the presence of the stereocomplex. In 100L/80D cast films and isothermally crystallized samples at 115 ^oC for 1 h, the regular increase of the enthalpy was observed as well, but for cast film, the maximum was achieved at 65% of 80D component and PLLA homocrystals were formed up to 70% of 80D. By isothermal crystallization of these blends, maximum of ΔH_m for stereocomplex appeared at 56% of 80D and no PLLA homocrystal was formed above the 50% 80D. Also the amount of homocrystal was close to the calculated one based on the amount of 100L which is not incorporated in the stereocomplex, showing a greater freedom for crystallization compared to 100L/100D blends.

In addition it was observed that the amount of stereocomplex in cast films of 100L/80D blends was much less than that in 100L/100D ones. This was attributed to two factors. First of all, the rate of stereocomplexation is reduced, because the L units in 80D polymer should be excluded from the stereocomplex. The second reason was the higher molecular weight of 80D samples compared to 100L and 100D, resulting in slower chain diffusion for stereocomplex formation. Thus the isothermal crystallization helped to improve the amount of stereocomplex but no significant improvement was observed in 100L/100D blends.

Another aspect that was pointed in their work was the small variation of PLLA melting point as a function of composition which was concluded to be a sign of formation of separate domains which is not the case in copolymers showing large temperature dependence.

2.2.5 Stereocomplexation kinetics

Studying the spherulite growth of stereocomplex from the melt of 1:1 blends, with low molecular weight PLLA ($M_w = 1 \times 10^4$) and PDLA ($M_w = 2.2 \times 10^4$) showed that it can occur at higher temperatures (190 ^oC) compared to homocrystallites (140 ^oC) [148]. A blend was prepared by solution casting and solvent evaporation at 25 ^oC for 1 day. At the same temperature of 140 ^oC, induction period was shorter, radius growth rate was an order of magnitude higher and spherulite density was higher for stereocomplex compared to homopolymers. The combination of higher spherulite density, shorter induction time and faster growth rate results in more rapid completion of overall stereocomplex crystallization compared to homopolymers.

Bouapao and Tsuji [195] studied the effect of X_D in the wide range of 0-1 on the stereocomplex crystallization and spherulite growth of PLLA/PDLA blends during isothermal and non-isothermal crystallization from the melt. Low molecular weight PLAs (PLLA with M_w = 4000 g/mol and PDLA with M_w = 5400 g/mol) were solution blended and solvent was evaporated slowly at 25 ^oC for two days.

In isothermal tests, for T_c above 130 ^oC, only stereocomplex crystallites were formed and the stereocomplex spherulite growth happened in a higher temperature range (up to 180 ^oC) compared to homopolymers (below 120 or 130 ^oC). The growth rate (G) was maximum at X_D = 0.5 in the T_c range of 130-180 ^oC and it decreased by deviation from this blend ratio. This maximum G value at T_c 130 ^oC (154 μm/min) was 4.5 and 4.7 times higher than pure PLLA (34 μm/min) and PDLA (33 μm/min) at T_c = 105 and 110 ^oC respectively. Regime analysis showed the independency of crystallization mechanism to blending ratio. Also in non-isothermal tests, cold crystallization took place at lower temperatures and higher rates for the blends compared to pure polymers, as a result of faster stereocomplex crystallization and its nucleating effect.

Masaki et al. [196] studied stereocomplex formation by melt blending in a continuous process. They used two sets of high molecular weight PLLA and PDLA. In the first set, M_w of PLLA and PDLA were 2×10^5 and 1.8×10^5 g/mol respectively and some trace of active catalyst was detected in them. In the second set, PLLA and PDLA had M_w of 1.6×10^5 and the active catalyst was completely inactivated. 1:1 Blends of PLLA and PDLA were produced by feeding equal amounts of each polymer to the feeder. The extrudate was immediately quenched in ice-water at the exit of the mixer. Different temperatures were tried for blending. Between 170-200

^{o}C, solid granules were extruded while at temperatures between 210-240 ^{o}C, molten extrudate was produced. DSC curves obtained from heating with the rate of 10 ^{o}C/min from samples prepared at different temperatures showed that granular solids were highly crystalline with no crystallization exotherm and a large endotherm peak at 230 ^{o}C. On the other hand, samples prepared at temperature range of 210-240 ^{o}C showed and exotherm at 100 ^{o}C and two endotherm peaks at 175 and 220 ^{o}C, indicating the amorphous state of the samples and tendency to both homocrystallization and stereocomplex formation. WAXD analysis on samples prepared at temperatures between melting point of homopolymer and stereocomplex (170-200 ^{o}C) showed the presence of stereocomplex but no homocrystallization was detected. Samples prepared at 190 and 240 ^{o}C were again kneaded at 250 ^{o}C and the extrudate was quenched. DSC analysis on these samples revealed the following results. The sample prepared at 190 ^{o}C with a trace of catalyst, showed an exotherm at 100 ^{o}C and an endotherm at 220 ^{o}C at the first heating cycle with the rate of 10 ^{o}C/min. The following cooling cycle at the faster rate of 20 ^{o}C/min showed an exotherm peak at 120 ^{o}C. Finally the second heating cycle with the rate of 20 ^{o}C/min showed only a melting endotherm for the stereocomplex. However the sample prepared at 240 ^{o}C and the one prepared at 190 ^{o}C but with inactivated catalyst, showed both the melting peak of homopolymer crystals and stereocomplex. Based on these results, the authors concluded that PLLA and PDLA form the stereocomplex at their interface when they are melt-mixed at temperature between T_m of homopolymers and stereocomplex. Considering the high rate of stereocomplex crystallization, the system becomes a mixture of solid stereocomplex crystals and polymer melt. When the blend is kneaded at high temperatures, chains that are already connected to the stereocomplex cannot separate completely and form stereocomplex consistently. Presence of the active catalyst in the sample results enhanced trans-esterification reactions at elevated temperature between PLLA and PDLA and formation of block copolymers which may act as compatibilizer or nucleating agent for stereocomplex.

2.2.6 Conclusions

From a crystallization point of view, PLA is best viewed as a copolymer of L- and D-Lactic acid with PLLA and PDLA being the limiting case homopolymers. The minor unit plays the role of a non-crystallizable co-monomer with the consequence that crystallization rate decreases dramatically with the minor unit concentration leading to amorphous materials for

minor co-monomer concentration greater than 10%. The melting temperature of PLA also decreases with minor unit fraction but increases with molecular weight up to M_n values around 100 kg/mol. Conversely, its crystal growth rate is severely decreased by molecular weight in the same range. The fastest crystallization rates are observed in the 100-130 ^oC temperature range. A peculiar consequence of the stereoisomeric nature of lactic acid is that the PLLA and PDLA homopolymers can co-crystallize in the form of a stereocomplex that boasts a melting point that is 50^oC higher than the respective homopolymers. Numerous investigations have focused on the heterogeneous nucleation and plasticization as means to enhance the crystallization kinetics of PLA. Important nucleation rate improvements can be obtained with minerals such as talc, organics such as hydrazide compounds and organic-mineral hybrids such as layered metal phosphonates. The highest crystallization rates however were obtained when adding both nucleants and plasticizers to PLA. This widens the crystallization window and enables crystallization at high cooling rates. Further improvement in this direction will enable the development of fully crystallized extruded or injection molded applications and open the way to the production of PLA parts with greater thermal resistance.

In the specific case of the PLA stereocomplex, most of the research work has been done in the solution state. It is however important to explore the stereocomplex formation in melt blended systems for future applications in melt processing techniques. Thermodynamically, stereocomplex formation is favored over homocrystallization. On the other hand, the kinetic barrier originating from the mixing level and longer diffusion path of opposite chains results in a competition with homocrystallization. Increasing the crystallization temperature above the homocrystallization temperature prohibits homocrystallization at the expense of slower stereocomplex formation. Several parameters influence stereocomplex formation such as the molecular weight of the two components, their optical purity and ratio as well as the blend preparation and crystallization conditions and have been studied extensively. Nevertheless, very little literature exists on the kinetics of PLA stereocomplex formation in melt blended systems and contrary to homocrystallization, stereocomplex formation enhancement is neglected.

Chapter 3. Evidence of a dual network/spherulitic crystalline morphology in PLA stereocomplexes

Avant-propos

Auteurs et affiliation:

Sajjad Saeidlou: *Département de génie chimique et de génie biotechnologique, Faculté de genie, Université de Sherbrooke*

Michel A. Huneault: *Département de génie chimique et de génie biotechnologique, Faculté de genie, Université de Sherbrooke*

Hongbo Li: *National Research Council of Canada*

Pierre Sammut: *National Research Council of Canada*

Chul B. Park: *Department of Mechanical and Industrial Engineering, University of Toronto*

Date d'acception: 13 octobre 2012

État de l'acceptation: version finale publiée

Revue: Polymer

Référence: *Polymer*, 2012. **53**: p. 5816-5824.

Titre français: Preuve d'une morphologie cristalline double réseau / sphérulitique des stereocomplexes du PLA

Contribution au document: présenter l'étude de la cinétique de stéreocomplexation a partir de l'état fondu et élucider la structure cristalline double formée en condition isotherme.

Résumé français: *La formation d'un stéréocomplexe entre le poly(L-acide lactique) (PLLA) et le poly(D-acide lactique) (PDLA) à l'état fondu a été étudiée. Des mélanges contenant jusqu'à 5% de PDLA ont été préparés à l'état fondu et caractérisés en rhéologie, calorimétrie, diffraction des rayons X (XRD) et en microscopie optique. Les études cinétiques suggèrent que le demi-temps ($t_{1/2}$) de stéréocomplexation varie de 5 à 7 min. Le rôle de nucléant du stéréocomplexe pour l'homocristallisation du PLLA a été démontré par des observations en XRD et en microscopie optique. Ces dernières montrent une augmentation de la densité des*

sphérulites ainsi que le développement d'une couche trans-cristalline autour des sphérulites de stéréocomplexe. Plus intéressant encore, une double morphologie cristalline comprenant des sphérulites et une structure en réseau a été révélée par les observations de microscopie optique. Cette morphologie complexe est associée au double pic de fusion du stéréocomplexe observé après cristallisation isotherme en DSC. La morphologie en réseau est associée à une forte augmentation de la viscosité observée en présence d'une petite concentration de stéréocomplexe dans une masse fondue de PLLA.

Evidence of a dual network/spherulitic crystalline morphology in PLA stereocomplexes

Sajjad Saeidlou[a], Michel A. Huneault[a,]*, Hongbo Li [b], Pierre Sammut[b], Chul B. Park [c]

[a]Department of Chemical and Biotechnological Engineering, Université de Sherbrooke, Sherbrooke, QC J1K 2R1, Canada

[b]National Research Council of Canada, 75 de Mortagne, Boucherville, QCJ4B 6Y4, Canada

[c]Department of Mechanical and Industrial Engineering, University of Toronto, 5 King's College Road, Toronto, ON M5S 3G8, Canada

Abstract. *Stereocomplex formation between poly(L-lactic acid) (PLLA) and poly(D-lactic acid) (PDLA) in the melt state was investigated. Blends with up to 5% PDLA were prepared via melt-blending and characterized by rheological, calorimetric, X-ray diffraction (XRD) and optical microscopy techniques. Kinetic studies suggest that the stereocomplex formation half-time ($t_{1/2}$) is in the range of 5 to 7 min. The nucleating role of the stereocomplex for PLA homocrystallization was demonstrated in XRD experiment and in optical microscopy observations through an increase in the spherulite density as well as the growth of a trans-crystalline layer on stereocomplex spherulites. More interestingly, a dual crystalline morphology for PLA stereocomplex comprising a spherulitic and a network structure was revealed by optical microscopy observations. This complex morphology was associated to a double stereocomplex melting peak behavior observed after isothermal crystallization in DSC as well as to a huge viscosity increase observed in the presence of a small concentration of stereocomplex in a PLLA melt.*

Keywords: PLA, Stereocomplex, Crystallization

3.1 Introduction

PLA is a thermoplastic polyester that can be produced from annually renewable resources. It is also a compostable polymer with good mechanical, optical and barrier properties. These

advantages in parallel with the recent technological developments in PLA production have rapidly expanded its applications as a competitive commodity polymer in a variety of processes [1, 8]. On the other hand, PLA has a low temperature resistance and crystallization as a means to improve its thermal resistance has been a subject of considerable interest in recent years [12, 76]. The monomer, Lactic acid exists in two enantiomeric forms, *L*-lactic acid and *D*-lactic acid, resulting in a wide range of properties from completely amorphous to semicrystalline PLA, depending on the ratio and distribution of enantiomeric units along polymer chains [197]. An outcome of this stereochemical aspect is the possibility for *L*- and *D*-rich PLA chains called PLLA and PDLA, respectively, to co-crystallize and form a stereocomplex with a melting point about 50 ^{o}C higher than PLA homocrystals [10]. Many attempts have been made to identify the mechanism and effect of different parameters on PLA stereocomplex formation such as molecular weight of the two components, their optical purity, PLLA/PDLA blending ratio, preparation methods and crystallization conditions [24, 67, 75, 144, 192-194, 198-202]. Furthermore, research has been going on to apply this interesting phenomenon in the modification of different PLA properties. PLA stereocomplex is used as a nucleating agent for PLA itself to improve its crystallization kinetics [79, 80, 122, 125, 144, 146, 147]. Thermo-mechanical properties are improved significantly in the presence of stereocomplex compared to pure PLLA [75]. Moreover, higher melting point of the stereocomplex compared to PLA homocrystal makes it possible to preserve stereocomplex in the polymer melt, thus employing it as a rheological modifier [147, 203]. From the thermodynamic point of view, stereocomplex formation is favored over homocrystallization. Based on energy calculations by Okihara *et al.* the 3_1 helix chain conformation in the stereocomplex is more stable than the 10_3 helix in α-form crystal of PLLA [46]. Furthermore, Tsuji *et al.* showed that the critical concentration for crystallization in solution state is lower for stereocomplex formation compared to homocrystallization [192]. They showed as well that for dilute solutions, precipitation with a non-solvent resulted in the predominant stereocomplex formation over a wide range of molecular weights [193]. However, there is a kinetic barrier against stereocomplex formation originating from its competition with homocrystallization. This is due to a high level of mixing required between PLLA and PDLA chains to co-crystallize, while similar chains are already in the vicinity of each other for homocrystallization. Thus, in most of the studies on different aspects of PLA stereocomplex, PLLA/PDLA blends are prepared via solution blending followed by either evaporation of the solvent or precipitation of the polymer

mixture through the addition of a non-solvent. However, these methods require organic solvents in high proportions which is less favorable for mass-production than the conventional melt blending techniques used for preparing polymer blends. Nonetheless, there are a few reports on the PLA stereocomplex formation where PLLA/PDLA blends are prepared via melt-mixing [122, 196, 204, 205]. Another aspect where there is a lack of information is the kinetics of PLA stereocomplex formation, few studies addressing this issue [148, 195, 199, 206, 207]. Specifically, it is crucial to understand the stereocomplex formation at temperatures representing the PLA melt-processing in order to apply it in industrial applications. The objectives of this work are to investigate the stereocomplex formation of melt-blended enantiomeric PLAs at elevated temperatures, to elucidate the stereocomplex dual crystalline morphology and to clarify its relation with the thermal and rheological behavior of the PLLA/PDLA blends.

3.2 Experimental

3.2.1 Materials

A commercial PLA, grade 4032D was used as a PLLA source. It is a semi-crystalline grade supplied by NatureWorks LLC that comprises about 2% *D*- units. PDLA was also a semi-crystalline grade provided by Hycail, Finland that comprised 0.5% *L*- units. Table 3.1 summarizes the properties of polylactides used in this work. Molecular weights were measured via a ViscotekTDAmax GPC apparatus (Malvern Instruments Ltd) equipped with a triple detection system.

Table 3.1 Properties of polylactides

Polymer	M_w(kg/mol)	PDI	D-unit content (%)
PLLA	109	1.57	2
PDLA	61	2.1	99.5

3.2.2 Blending

Blends of PLLA and PDLA containing 1, 3 and 5 wt.% of PDLA were prepared using a HAAKE MiniLab conical twin-screw micro compounder (Thermo Scientific). In addition, PLLA without any PDLA was processed under the same conditions as a reference. Polymers were vacuum dried at 50 ^{o}C for 38 hr prior to melt mixing. Mixing was carried out at 180 ^{o}C for 5

minutes at a rotation speed of 60 rpm. The extruded blends were also dried in the same conditions prior to characterizations.

3.2.3 Rheological characterization

Compression molded specimens were prepared using a Carver laboratory press. The molding temperature was set to 240 °C and disk-shaped specimens were prepared to fit the rheometer geometry. The procedure was as follows: i) Pre-heat at 240 °C under ambient pressure for 1.5 min. ii) Press at 240 °C under 3.2 MPa for 30 sec. iii) Remove mold assembly from press and quench in 15 °C water bath to preserve the amorphous structure prior to tests. The amorphous structure was confirmed by X-ray diffraction technique.

A rotational rheometer (ARES LS model from TA Instruments) was used in parallel plate geometry (25mm diameter) for the rheological characterization. The average specimen thickness was around 0.9 mm. A thermal equilibration time of 30 s was used in the rheometer prior to the rheological measurement to insure that the samples had reached the specified test temperature of 180 °C. Small deformation (10%) oscillatory motion was then imposed on the samples at a frequency of 1 Hz (6.28 rad/s) over a time period of 30 min and the stress was monitored. The time sweeps were performed at 180 °C under a blanket of dry nitrogen to minimize hydrolytic degradation.

It is noteworthy that PLA can undergo rapid thermal degradation at 240 °C. This heating step is necessary to eliminate traces of stereocomplex. The duration of this step was limited to minimize degradation and rheological tests were carried out at 180 °C where the materials are relatively stable.

3.2.4 Wide-angle X-ray Diffraction analysis

Wide-angle X-ray Diffraction (WAXD) patterns of the blends were obtained with an X-ray diffractometer (D-8, Bruker) to make sure the samples were amorphous prior to rheological characterization and to determine the crystalline structure after the tests. The samples were exposed to an X-ray beam with the X-ray generators running at 40 kV and 40 mA. The scanning was carried out at a rate of 0.03^{o}/s in the angular region (2θ) of $2\text{-}40^{o}$.

3.2.5 Differential Scanning Calorimetry

Kinetics of the stereocomplex formation was studied in isothermal mode using a DSC Q2000 differential scanning calorimeter (TA instruments). Blends with 5% PDLA were first heated to 240 ^{o}C and kept at that temperature for 2 min to eliminate their thermal history, followed by rapid cooling to isothermal crystallization temperature. Specimens were kept for enough time to ensure completion of stereocomplex formation. Finally, they were heated with the rate of 10 ^{o}C/min to 240 ^{o}C to evaluate their melting behavior.

For deconvolution of overlapping peaks, a non-linear fitting software (PeakFit v4) was employed. An asymmetric logistic peak function with standard least-squares minimization was used to find the optimum fit.

3.2.6 Hot-stage Optical Microscopy

Optical microscopy (OPTIPHOT-2) was employed to observe the evolution of crystalline morphology through stereocomplex formation. Thin films were prepared by hot-pressing blend granules with 5% PDLA. A programmable hot stage (MettlerFP82HT) was used to perform the thermal procedures on the samples and observe the crystalline morphology evolution.

3.3 Results and discussion

3.3.1 Rheology

Figure 3.1 presents the evolution of PLLA/PDLA blend viscosity with time for samples at 180 ^{o}C containing 1, 3, and 5 wt.% PDLA as well as the reference. Note that according to the experimental procedure, samples were heated to test temperature within 30 s thus preserving their amorphous state. The initial viscosity was reduced by increasing the level of PDLA from 0 to 5 wt.%. This was expected since PDLA has a lower molecular weight, thus a lower melt viscosity. However, the melt viscosity increased gradually during the time-sweep characterization until a plateau was reached. The plateau viscosity level increased from 3 kPa.s for 0% PDLA gradually up to 6 kPa.s for 5% PDLA. This two-fold increase is particularly striking considering that the initial viscosity of the 5% PDLA blend was much lower, around 1 kPa.s.

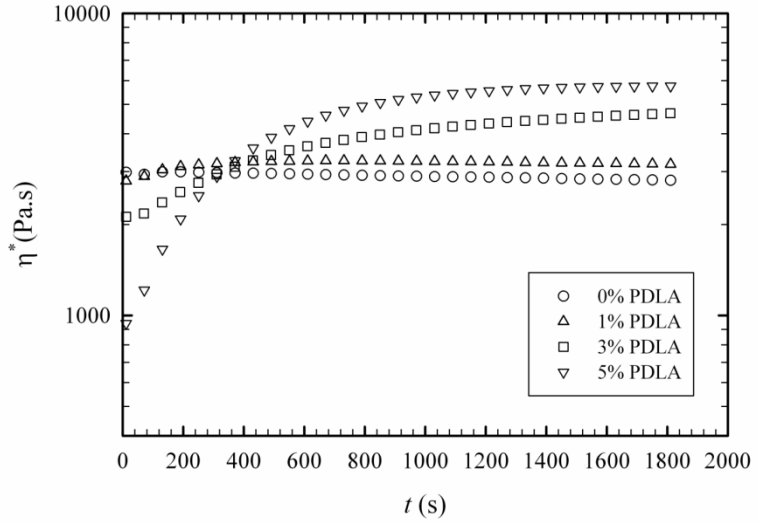

Figure 3.1 Variation of melt viscosity with time as a consequence of stereocomplex formation during time-sweep test at 180 °C

Similar tests performed at strains between 0.1 to 10% lead to very similar responses (data not shown). This confirmed that the observed effect was not induced by strain. It is useful to discuss how stereocomplex formation may influence the melt viscosity. First, stereocomplex crystals may act as dispersed solid particles in the melt and contribute to an increase in melt viscosity. In this case, the solid particulates may be stereocomplex lamellae or more complex spherulitic structures comprising some amorphous material as well. Secondly, PLLA and PDLA chains which are connected physically through stereocomplexation may be considered as macromolecules with higher apparent molecular weight [203]. Furthermore, the structure of physically connected chains are transformed from linear to branched since the pending segments of the chains that have not participated in stereocomplex formation will act as branches on the opposite chain [203]. Finally, another possible mechanism is the formation of a three dimensional network through physical cross-links by stereocomplex formation between multiple chains [75, 203].

In Figure 3.2, progress of stereocomplex formation is demonstrated by plotting the relative viscosity change $\frac{\eta-\eta_0}{\eta_{max}-\eta_0}$ vs. time where η is the dynamic viscosity at time *t*, η_0 is the initial blend viscosity at time zero and η_{max} is the maximum achieved viscosity. The selection of the initial blend viscosity as a reference (η_0) for each concentration minimizes the effect of sample degradation occurring before the rheological tests. For samples with 3 and 5 wt.% PDLA, maximum viscosity was obtained at the end of the test. However, for the 1% PDLA blend after

reaching a maximum at about 720 s, the viscosity started to decrease. Note however that this drop is very small in absolute terms because the viscosity change $\eta_{max} - \eta_0$ for the 1% PDLA blend is small.

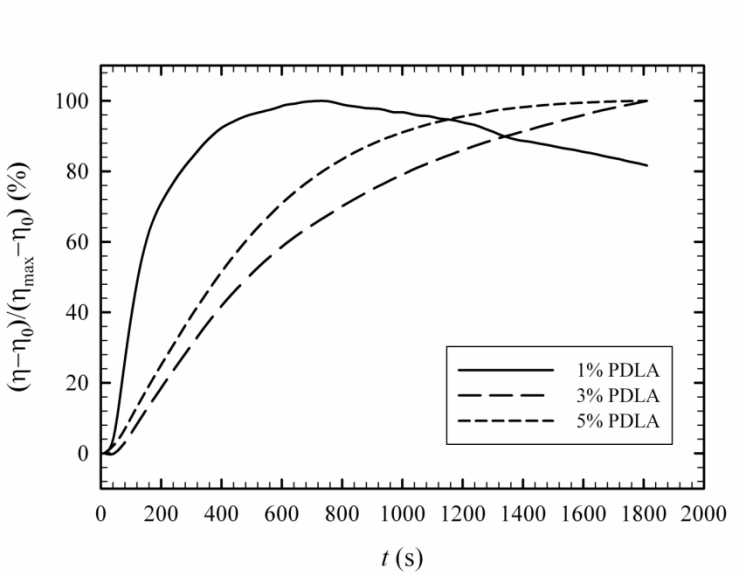

Figure 3.2 Degree of stereocomplex formation vs. time from time-sweep analysis at 180 °C for samples containing 1, 3 and 5% PDLA

It is noteworthy that PLLA was thermally stable throughout the rheological characterization window while PDLA showed a significant chain scission. The PDLA chains that do not participate in stereocomplex crystallites therefore lower the overall viscosity of the PLLA/PDLA blend. When comparing the dynamics of the viscosity evolution, it seems that the 1% PDLA blend reached its maximum stereocomplex level more rapidly, within around 700 s. The further decrease is possibly due to chain scission of PDLA chains that are not participating in a stereocomplex or to general hydrolytic degradation of the blend (noting once again that the denominator $\eta_{max} - \eta_0$ used to calculate the relative viscosity change is small). The kinetics related to 3% and 5% PDLA blends was slower with final maximum viscosities reached at around 1600 s for 5% PDLA and probably over 1800 s for the 3% blend.

Viscosity increase ratio (viscosity after complexation divided by viscosity before complexation) $\frac{\eta_{max}}{\eta_0}$ is plotted as a function of PDLA content in Figure 3.3 to compare the effect of PDLA concentration with theoretical viscosity variations that could be expected if the stereocomplex particles were considered as a solid filler in a matrix of amorphous PLLA. As previously mentioned, the maximum viscosity increased by a factor of 2 upon addition of 5%

PDLA. However, if we consider the ratio between the viscosity of the 5% PDLA blend after and before complexation, the viscosity increase is more than 6 times. This is particularly significant if we consider the blend viscosity increase ratio as more representative of the complexation effect. The data is compared with the predictions from Krieger-Dougherty model which is aimed at predicting the viscosity increase for concentrated suspensions. It is given by:

$$\frac{\eta}{\eta_0} = \left(1 - \frac{\varphi}{\varphi_{\max}}\right)^{-A\varphi_{\max}} \qquad \textbf{Equation 3.1}$$

where η is the viscosity of the mixture, η_0 is the matrix phase viscosity, φ is the volume fraction of solid particles, φ_{max} is the maximum packing equal to 0.61 and A is a constant equal to 3.28. The choice of matrix phase viscosity is not trivial since during the experiment, some PDLA will leave the melt phase to form the stereocomplex. Nonetheless, since the amount of PDLA involved is small, it was assumed more representative to select the initial blend viscosity as our matrix phase viscosity rather than use the initial PLLA viscosity.

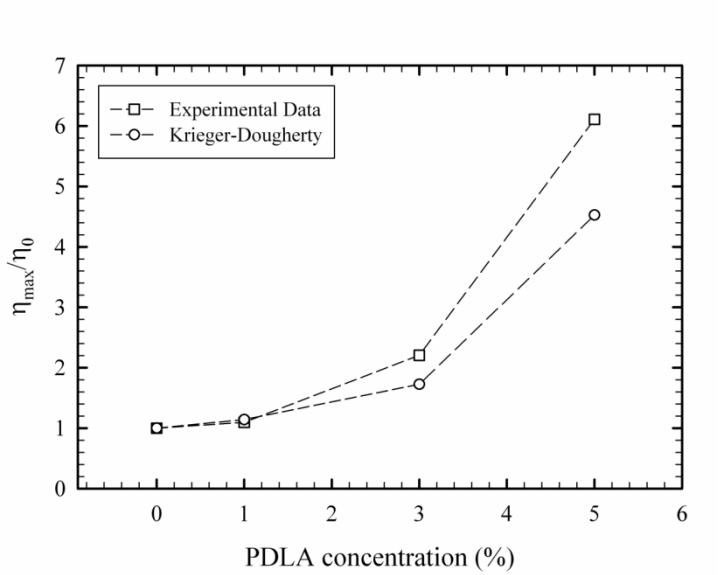

Figure 3.3 Effect of PDLA concentration on viscosity increase ratio and comparison with Krieger-Dougherty model prediction

Also, for the Krieger-Dougherty model, the density difference between the amorphous and crystalline phases was neglected and it was assumed that all the added PDLA took part in stereocomplex formation, thus volume fraction of the solid particle would be two times the PDLA concentration. Comparing the experimental data with Krieger-Dougherty model predictions shows

that the presence of stereocomplex in the polymer melt had a stronger effect than that expected from the simple addition of a solid crystalline phase. This is possibly due to some interaction between stereocomplex crystallites.

In Figure 3.4, complex viscosity as a function of oscillation frequency is compared for the neat PLLA and the 5% PDLA blend after stereocomplex formation. Neat PLLA demonstrates a Newtonian plateau at low frequencies, typical of polymer melts, while such behavior is not observed for 5% PDLA blend. In the presence of PDLA, significant deviation of complex viscosity at low frequencies relative to that of neat PLLA can be associated to the interaction between chains caused by stereocomplex formation. Such a rapid viscosity increase at low shear rates has been observed in highly filled polymeric systems where particles tend to aggregate and form structures like carbon black, as well as in some nanocomposites [208].

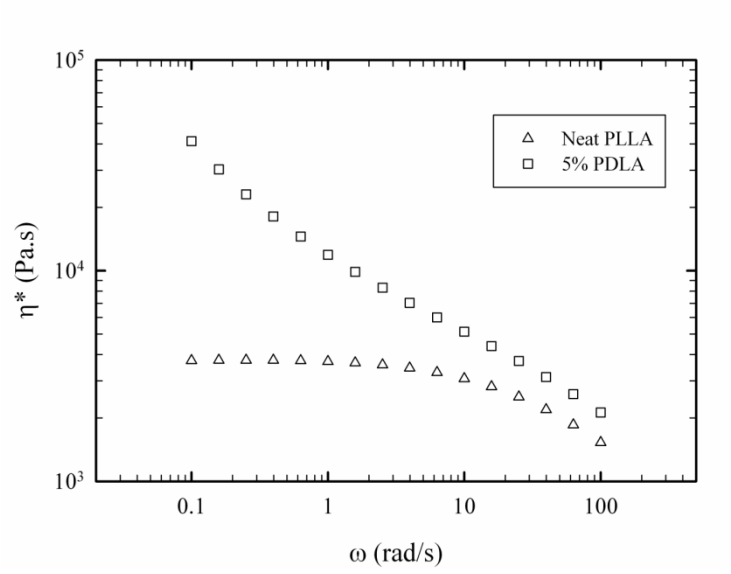

Figure 3.4 Frequency sweep behavior of PLA in the presence and absence of stereocomplex

3.3.2 XRD analysis

Figure 3.5 presents the XRD patterns before and after rheological characterization for samples containing 5% PDLA. Peaks at 2θ = 14.7, 16.4, 18.6 and 22 are associated to homopolymer crystals whereas those at 11.8, 20.5 and 23.6 are related to stereocomplex. Peak positions are in good agreement with the reported values [10]. The XRD patterns therefore confirm that the samples were completely amorphous prior to rheological characterization.

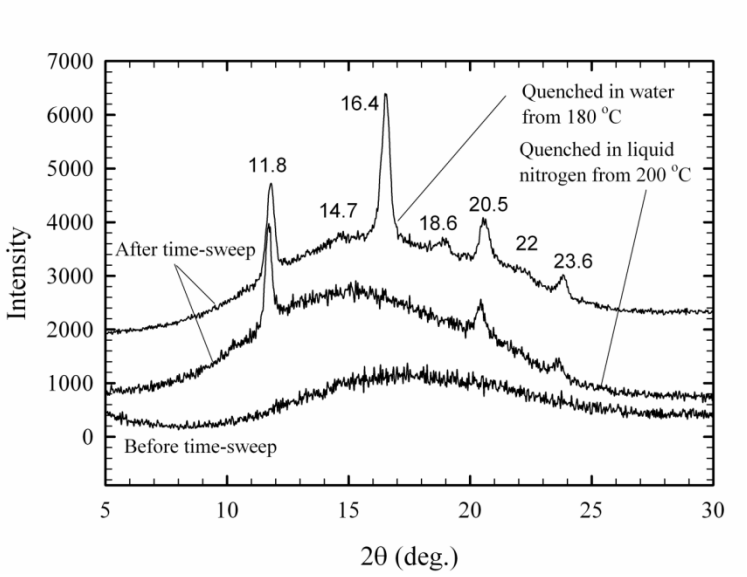

Figure 3.5 X-ray diffraction patterns of samples containing 5% PDLA before and after time-sweep test

After the time-sweep tests, depending on the quenching procedure, the crystalline structure was different. When the samples were directly quenched from 180 ^{o}C in cold water, they exhibited peaks related to both PLA homocrystals and stereocomplex simultaneously. The quenching procedure was modified to minimize homocrystallization. The samples were rapidly heated to 200 ^{o}C after the time-sweep test and were then quenched in liquid nitrogen. This resulted in samples where only the stereocomplex was formed as exhibited from the XRD results. At T = 200 ^{o}C, the temperature is greater than the homocrystallization temperature but lower than the melting point of the formed stereocomplex. Therefore, when rapidly quenching from T = 200 ^{o}C into liquid nitrogen, the time spent in the homocrystallization temperature window is minimized. Based on this observation, samples with 1, 3 and 5% PDLA were prepared using the procedure above after rheological characterization and then subjected to XRD analysis. Results are depicted in Figure 3.6. Only the three peaks related to stereocomplex crystals were detected and their intensity increased by incorporating more PDLA in blends. For blends with 3 and 5% PDLA it was possible to calculate the degree of crystallinity based on the XRD peak integration. By dividing the sum of stereocomplex peaks area to total peak area it was found that samples with 3 and 5% PDLA had a degree of crystallinity equal to 2.55 and 4.58%, respectively. In an ideal situation, 6 and 10% crystallinity were expected (2×[PDLA]). Therefore, stereocomplex formation efficiency was 42 and 45%, respectively. It is noteworthy that the calculated yields are based on the assumption that components are 100% pure in terms of enantiomeric isomers, while the PLLA and PDLA used in this study had some optical impurity. Especially, the PLLA contained about 2% *D* units that limit

the stereocomplex formation. In addition, the molecular weight of the components, blending route and crystallization method are other influential parameters for the achievable stereocomplex crystallinity. For example in samples prepared by solution casting, increasing the molecular weight of the components from about 27 to 360 kg/mol decreased the stereocomplex crystallinity from 50-55% to 1-10% for different PDLA concentrations [194]. However, the higher molecular weight combination had a stereocomplex yield of 32 to 51% when it was crystallized in a solution precipitation method where chains had a higher degree of mobility during crystallization [193]. Our results are in agreement with the literature, considering the important effect of molecular weight of the components. For low molecular weight oligomeric components (M_v 3.3-5.7 kg/mol) stereocomplex yields of 58 to 72% were reported [67]. The yield for slightly higher molecular weights (M_v 13.2-14.5 kg/mol) reached 50 to 60% [144] while for much higher molecular weights (M_w 215-228 kg/mol), only up to 13% stereocomplex yield were reported [147].

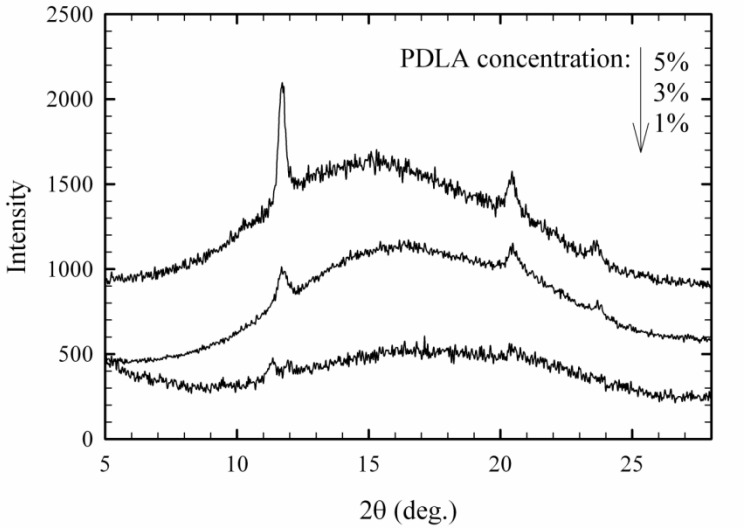

Figure 3.6 X-ray diffraction patterns of samples containing 1, 3 and 5% PDLA after time-sweep test

3.3.3 Differential Scanning Calorimetry

It is interesting to investigate the effect of crystallization temperature on the stereocomplex formation kinetics as well as the efficiency of our approach to form PLA stereocomplex in the melt state. For this purpose, samples containing 5% PDLA were characterized by DSC in isothermal mode. Reference samples (i.e. neat processed PLLA) were analyzed with the same procedure and data was subtracted from the 5% PDLA samples to eliminate the instabilities caused by rapid cooling to isothermal crystallization temperature. In Figure 3.7, crystallization

peaks obtained at different temperatures are showed. It can be seen that stereocomplexation initiates shortly after that temperature reaches the set point.

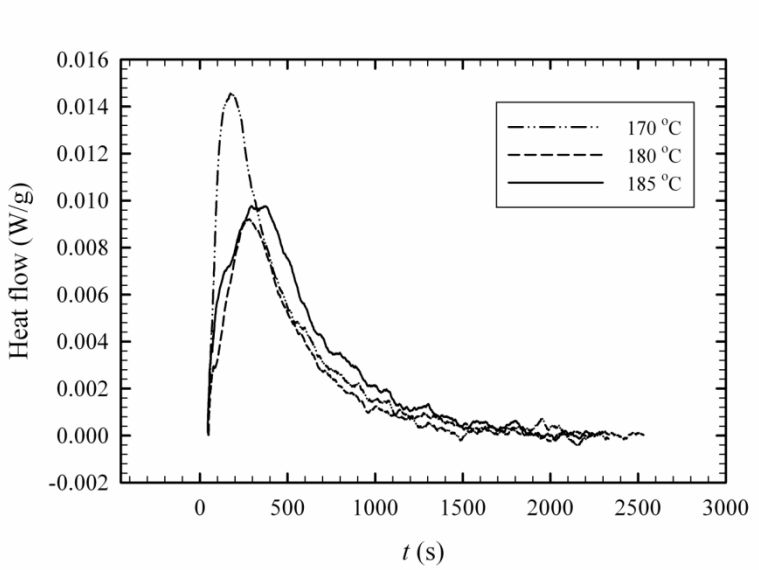

Figure 3.7 Isothermal crystallization peaks of the sample with 5% PDLA obtained at different temperatures

Stereocomplex crystallization enthalpy which is equal to the area under the crystallization peak was calculated for different crystallization times. The cumulative integrals normalized to the total peak area are plotted vs. crystallization time in Figure 3.8. In addition, in this figure, degree of stereocomplex formation obtained by rheological characterization at 180 °C is plotted to compare calorimetry and rheology as the stereocomplexation kinetics study methods.

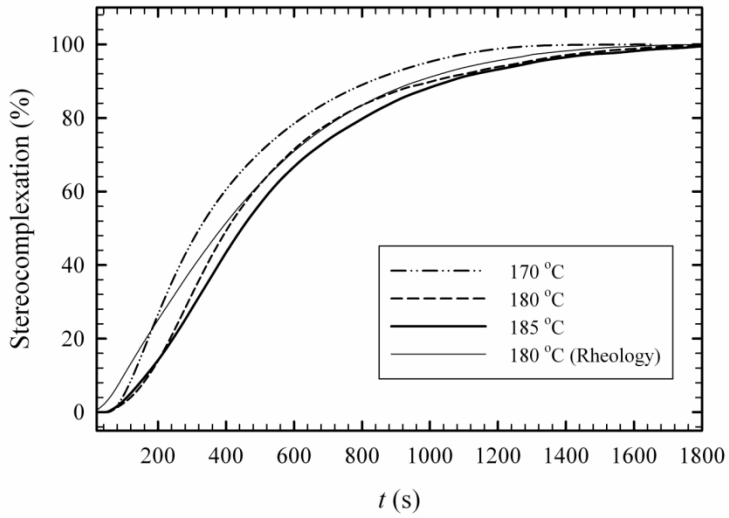

Figure 3.8 Degree of stereocomplexation expressed as a fraction of the maximum stereocomplex enthalpy obtained at different crystallization temperatures

Curves are shifted slightly to lower times as the temperature is reduced from 185 to 170 ^{o}C. The time required to reach 50% of stereocomplexation ($t_{1/2}$) at 185 ^{o}C is 7.45 min while this value is reduced to 6.75 min and 5.37 min for crystallization temperature of 180 and 170 ^{o}C, respectively. The DSC and rheological analysis at 180 ^{o}C match well with each other after 55% stereocomplex is formed. However, rheological studies show higher values at the first five minutes. This may have resulted from a greater sensitivity of viscosity to molecular weight changes which will be discussed later.

As explained in the experimental section, after the isothermal crystallization was completed, specimens were heated to 240 ^{o}C to measure the melting enthalpy and calculate the stereocomplex yield. Melting peaks obtained for the four different crystallization temperatures are depicted in Figure 3.9. A double melting peak behavior was observed above 200 ^{o}C which is much higher than the homocrystal melting temperature. Thus both peaks have a stereocomplex nature. The double peak behavior has been previously reported in different studies for PLA homocrystal melting in PLA fibers [43, 209-211] as well as for PLA crystallized in quiescent conditions [41, 72, 73, 212]. It was attributed to melt-recrystallization process or existence of two crystal forms such as α and β or α and α' structures. However, such behavior is not typical for melt crystallized PLA stereocomplex and is an indication of two different stereocomplex crystal size distributions. To examine the possibility of a reorganization and recrystallization mechanism responsible for the double melting peak behavior, isothermally crystallized samples were melted at various heating rates between 2 and 20 ^{o}C/min. However, the dual peak behavior was not dependent on the heating rate showing that the dual peak behavior is not the result of such a recrystallization.

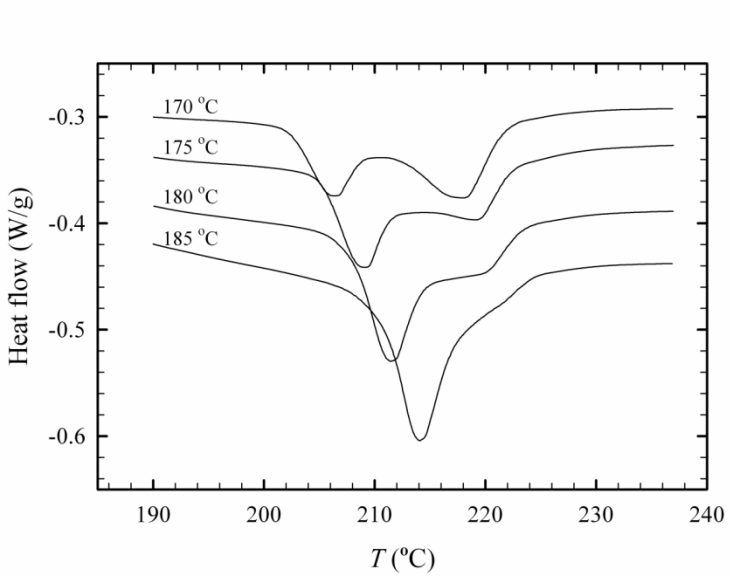

Figure 3.9 Melting behavior of stereocomplex formed isothermally at different temperatures

In order to better study these peaks, each curve was mathematically deconvoluted to two distinct peaks as illustrated in Figure 3.10. For the melting peak located at a lower temperature, a clear trend is observed with crystallization temperature. Increasing the crystallization temperature shifted this peak to higher temperatures while making it narrower. At the same time, its melting enthalpy increased slightly from 1.76 to 2.4J/g. On the other hand, for the melting peak located at a higher temperature, maximum occurs around 217 ^{o}C and does not depend on crystallization temperature. Melting enthalpy of this peak increased from 4.8 to about 6.6 J/g by increasing crystallization temperature and its shape became wider. The ratio between the enthalpy of the higher temperature to lower temperature peak remained almost constant at about 2.75, thus the share of higher melting point crystals in total stereocomplex crystallinity was about 75%. Assuming a value of 146 J/g for the melting enthalpy of 100% crystalline PLA in stereocomplex form [191], it is possible to calculate the crystallinity of blends after isothermal crystallization. For temperatures of 170, 175, 180 and 185 ^{o}C, degree of crystallinity was 4.5, 5, 5.8 and 6.2 % respectively. These values are in agreement with the degree of crystallinity obtained from XRD analysis.

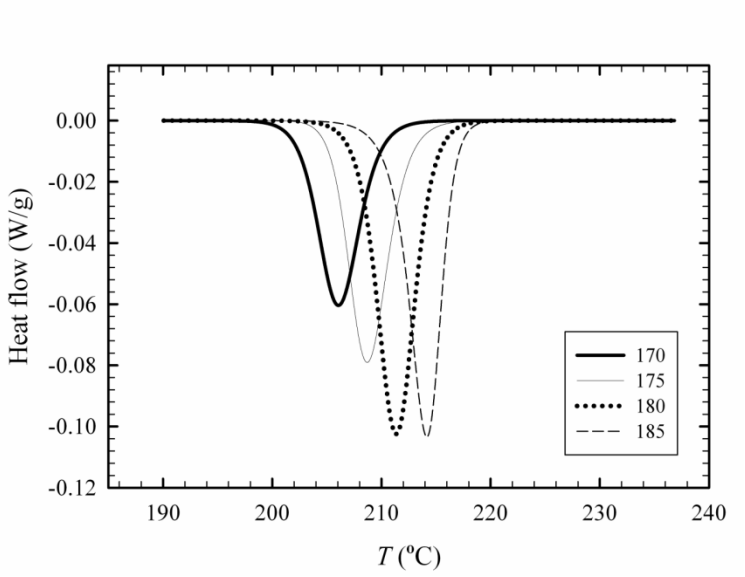

10-1

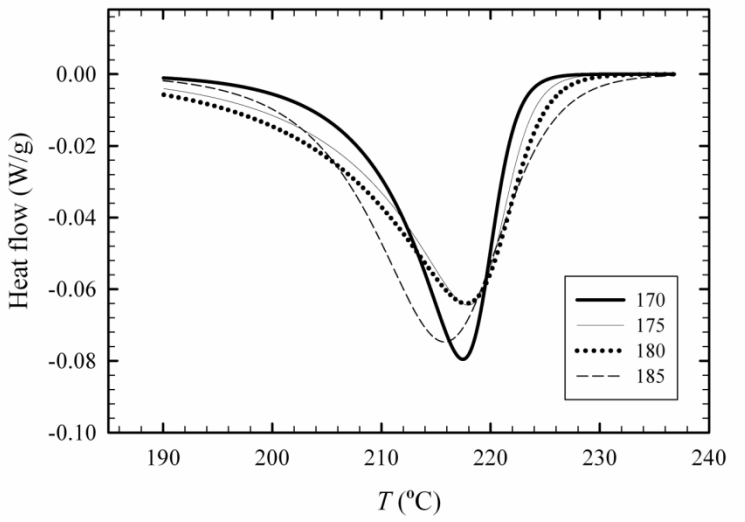

10-2

Figure 3.10 Deconvoluted melting peaks for different isothermal crystallization temperatures, 1: lower temperature melting peaks; 2: higher temperature melting peaks

3.3.4 Optical Microscopy

To further our understanding of crystalline morphology evolution and to elucidate the double melting peak phenomena, the 5% PDLA samples were characterized by optical microscopy observations in two different thermal procedures. In the first procedure, spherulite density of 5% PDLA blend was compared with that of neat PLLA. The specimen were melted at

240 ^{o}C for 2 min to remove the thermal history, cooled at 40 ^{o}C/min to 180 ^{o}C, crystallized for 3 min to generate some stereocomplex nuclei, cooled at 40 ^{o}C/min to 140 ^{o}C and then isothermally crystallized for 10 min. In Figure 3.11, the optical micrographs after this stage are illustrated. It is clear from these two images that a small amount of stereocomplex crystallites produced at higher temperatures had a profound nucleating effect for PLA homocrystallization. Neat PLA developed only few spherulites which did not grow much in size in the 10 min isothermal crystallization at 140 ^{o}C. On the other hand, 5% PDLA blend resulted in a much higher number of spherulites which almost covered all the surface area for the same crystallization time period.

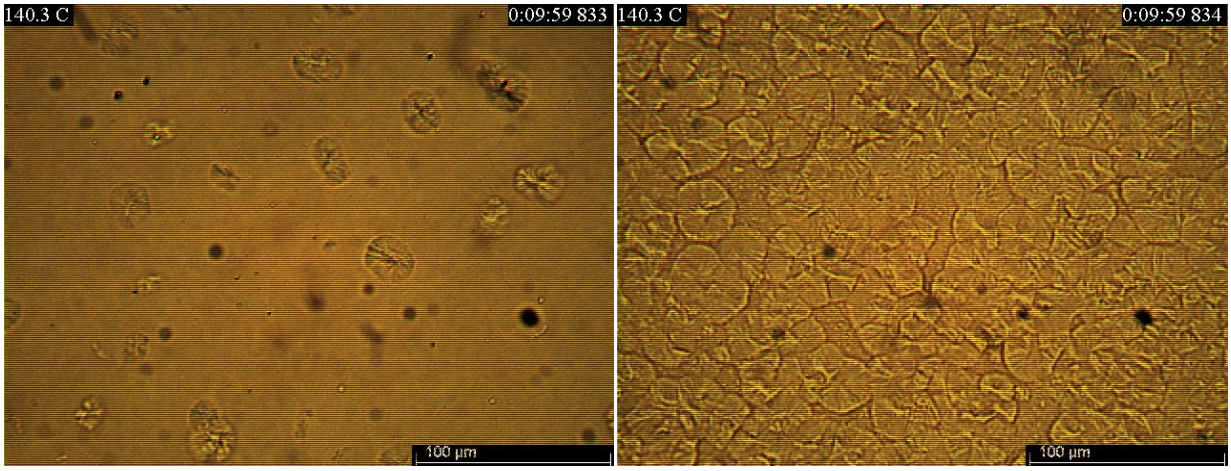

11-1 11-2

Figure 3.11 Optical micrographs of specimen after first thermal procedure, 1: neat PLLA; 2: 5% PDLA blend

Figure 3.12 represents the second thermal procedure followed to further investigate the stereocomplex formation and Figure 3.13 presents optical micrographs obtained at different stages of the thermal history. The samples were first heated to 240 ^{o}C to melt and remove thermal history and then cooled at 40 ^{o}C/min to 180 ^{o}C and isothermally crystallized for 30 min. Figure 3.13-1 illustrates the crystalline morphology at the end of this stage where stereocomplex spherulites were uniformly grown to about 40 µm in diameter. Subsequently, samples were cooled at 20 ^{o}C/min to 100 ^{o}C and held for 3 min. Figure 3.13-2 is taken during the cooling procedure at 120 ^{o}C. A trans-crystalline layer is developed on the surface of PLA stereocomplex spherulites during the cooling procedure which proves that the stereocomplex surface can initiate trans-crystallinity. As well, Figure 3.13-3 which shows the crystal morphology after 3 min at 100 ^{o}C is another demonstration of homocrystallization nucleated by stereocomplex. In this image, stereocomplex

spherulites are still detectable while a great number of small homocrystal spherulites covering the whole surface area were nucleated by much smaller stereocomplex crystallites. To further observe the crystalline morphology after re-melting the homocrystals, samples were heated back to 180 ^{o}C and kept for about 4 min to completely melt the homocrystals. Figure 3.13-4 illustrates the crystalline morphology at this point. In addition to the stereocomplex spherulites, an interconnected structure appeared in the bulk of the sample illustrated by bright lines connected throughout the sample. This is believed to be generated by the connection of small stereocomplexed regions, similar to a 3D network. Another interesting point is the existence of a very thin transparent layer around the stereocomplex spherulites. This is probably due to diffusion of PDLA chains to the stereocomplex spherulites. This migration leads to a depletion of this component in the boundary layer and thus leads to fully amorphous shells around the spherulites. Finally, the observed morphology was heated at a rate of 5 ^{o}C/min to 240 ^{o}C to carefully observe its melting behavior. The optical micrograph in Figure 3.13-5 was captured during this heating stage at 216 ^{o}C. At this temperature the network like structure had vanished while the stereocomplex spherulites were still present. It is noteworthy that the melting behavior observed in the final heating stage matches very well with the double melting peak behavior previously mentioned in DSC analysis. Thus, it can be assumed that the lower temperature melting peak is associated to the network structure and the higher temperature peak is the characteristic peak for spherulite melting. It could be argued that the thermal history in the DSC and optical microscopy tests were not identical. To remove any doubts on the relation between the two observed textures and the double melting peak, DSC tests were re-made with exactly the same thermal history as for the optical observation procedure 2. An identical double melting peak behavior was found confirming the previous results. To the authors' knowledge, it is the first time that this double melting peak behavior can be clearly associated to distinct crystalline morphologies in PLA stereocomplexes.

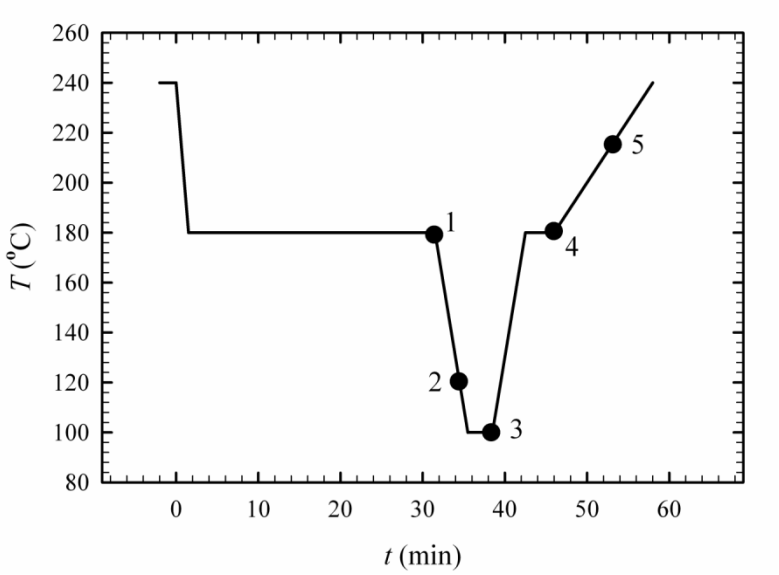

Figure 3.12 Second thermal procedure for optical microscopy observations

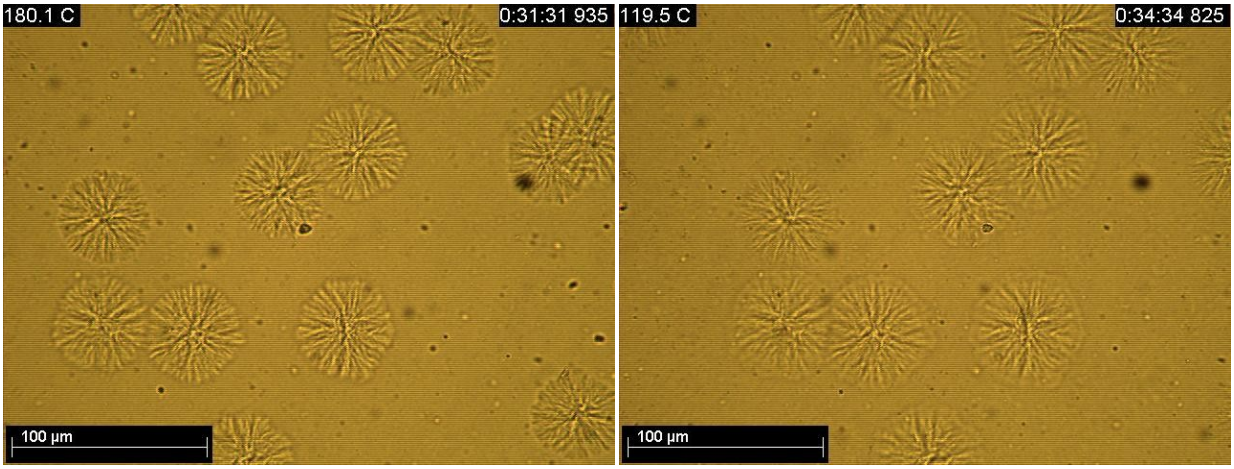

13-1 13-2

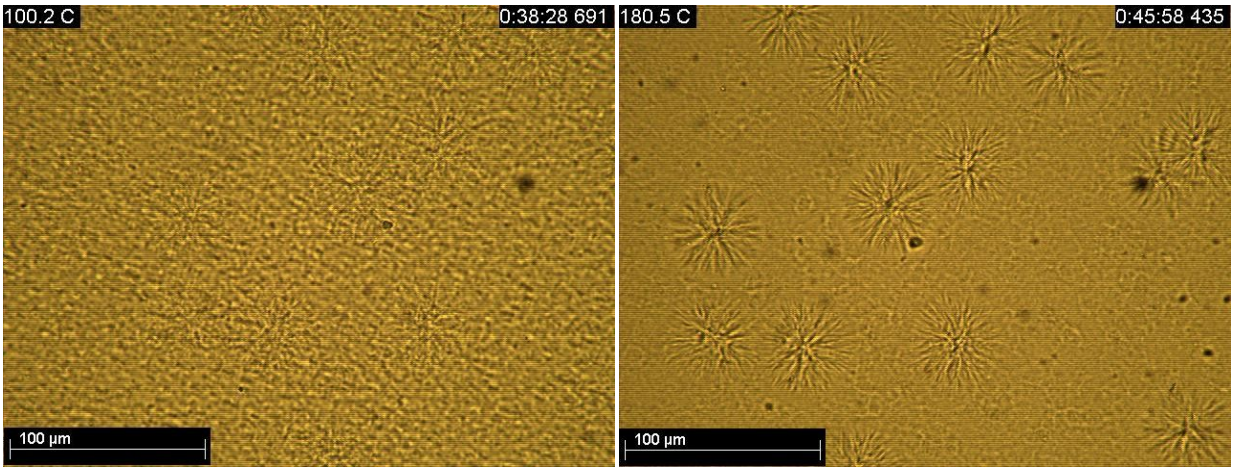

13-3 13-4

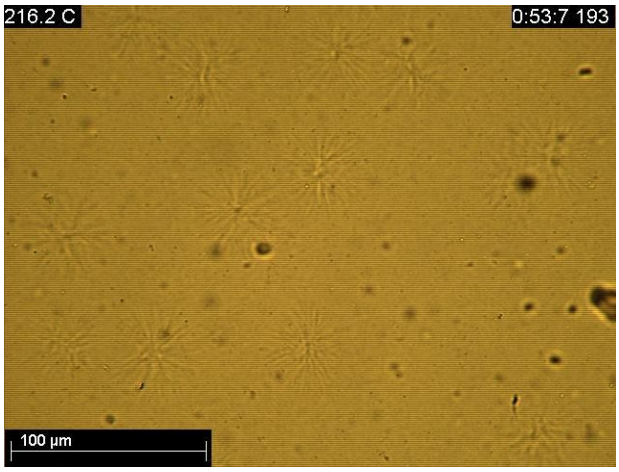

13-5

Figure 3.13 Optical micrographs obtained during the thermal procedure described in Figure 3.12

3.3.5 Discussion

It is interesting to reflect on the relations between the rheological response and the crystalline morphology developments in light of this dual network/spherulitic stereocomplex structure. Spherulitic structures will act as particulates with their volume fraction directly related to the crystalline content and to the amount or ratio of amorphous material that can be trapped within the complex spherulitic structure. In the earlier calculations to evaluate the effect of the solid crystalline fraction on the material viscosity, it was assumed that 100% of the PDLA was involved in stereocomplex formation. However, considering that the stereocomplex yield in this study was less than 50%, it is clear that the Krieger-Dougherty model predictions presented in Figure 3.3 were made using an overestimated solid content. Even if the apparent solid content would be increased due to an amorphous portion within the spherulites, the observed blend viscosities could not be predicted from a viscosity model based solely on a solid volume fraction. Furthermore, one should note that the large viscosity increase observed at low oscillation frequency in Figure 3.4 was caused by only 4.5% solid content rather than the 10% expected in the ideal stereocomplex formation situation. Only solid particulates with strong tendency for agglomeration or network formation show such large effects at concentration below 5%. It is also noteworthy that from our optical microscopy observations, the formation of the stereocomplex spherulites is a lengthy process. Around 30 minutes at 180^{o}C were required to develop the spherulites in Figure 3.13-1 for example. Network formation on the other hand is associated to a lower melting point structure and can appear more rapidly as we increase the undercooling. The

rheological procedure consisted in rapidly heating amorphous sample to 180°C and then monitoring the oscillatory response. In this context, the initial response is more directly related to the network formation rather than to spherulite formation.

It was noted in the comparison of calorimetric and rheological responses (Figure 3.8) that in the initial crystallization minutes, the crystalline growth based on the viscous response was greater than that measured from the standard calorimetric method. This may well be related to a non-linear relation between the blend viscosity and the crystalline content when a physical network structure is established. In that situation, the rheological response will be greater than the one expected from a suspension rheology model (i.e. a nearly linear relation between viscosity and solid content at low solid content). A rheological model that can accurately describe the behavior of the material during the early stages of the network formation would be useful and thus, further efforts in that direction should be made. Interestingly, the strong viscosity–crystallinity dependence may provide a more sensitive means to monitor the onset of the network formation compared to calorimetry or x-ray diffraction.

3.4 Conclusions

This work has shown the existence of a dual network/spherulitic crystalline morphology during PLA stereocomplex formation in the melt state. This dual structure can be witnessed directly by optical microscopy where the stereocomplex spherulites take on the usual radiated structure while the so-called network crystallinity is a less organized worm-like structure. The melting endotherm associated with the spherulites was around 218 °C while that of the network structure was significantly lower and was in direct relation with the crystallisation temperature. Typical half-time for completion of the overall stereocomplexation was between 300 and 500 s and the efficiency of stereocomplex formation was around 45%. The nucleating role of the stereocomplex for PLA homocrystallization was demonstrated by XRD and by optical microscopy characterizations. Specifically, a trans-crystalline layer of PLA homocrystals was grown on the surface of stereocomplex spherulites. Future efforts should focus on the kinetics and efficiency of stereocomplex formation at elevated temperatures in the melt state to benefit from this phenomenon in actual PLA melt-processing applications.

Chapter 4. Effect of nucleation and plasticization on the stereocomplex formation between enantiomeric poly(lactic acid)s

Avant-propos

Auteurs et affiliation:

Sajjad Saeidlou: *Département de génie chimique et de génie biotechnologique, Faculté de genie, Université de Sherbrooke*

Michel A. Huneault: *Département de génie chimique et de génie biotechnologique, Faculté de genie, Université de Sherbrooke*

Hongbo Li: *National Research Council of Canada*

Chul B. Park: *Department of Mechanical and Industrial Engineering, University of Toronto*

Date d'acception: 15 août 2013

État de l'acceptation: version finale publiée

Revue: Polymer

Référence: *Polymer*, 2013. **54**: p. 5762-5770.

Titre français: Effet de la nucléation et de la plastification sur la formation de stéréocomplexes entre les énantiomères de poly (acide lactique)

Contribution au document: Évaluation de l'effet de nucleation et de plastification sur la formation des stéréocomplexes et sur leur structure crystalline.

Résumé français: *L'effet de la nucléation et de la plastification sur la formation de stéréocomplexes entre le poly(L-acide lactique) (PLLA) et le poly(D-acide lactique) (PDLA) a été étudié dans les mélanges où le PDLA est ajouté en tant que phase mineure dans une phase principale de PLLA. L'utilisation de petites quantités de PDLA est destinée à créer une phase cristalline de stéréocomplexe ayant un point de fusion élevé qui peut servir d'agent de nucléation pour la phase majoritaire de PLLA. Des mélanges contenant 5% de PDLA, de 1% de talc ou de phosphonate organique comme agent de nucléation et de 5% de polyéthylène glycol comme plastifiant ont été préparés par mélange à l'état fondu. Leur comportement de cristallisation a été étudié par calorimétrie différentielle à balayage (DSC) en utilisant différentes histoires*

thermiques. Deux endothermes de fusion du stéréocomplexe ont été trouvés. Le pic de température et l'enthalpie de ces deux endothermes ont été corrélés à la température de cristallisation isotherme. Les différents endothermes ont également été associés à deux morphologies cristallines différentes observées par microscopie optique et nommées structure en réseau et structure sphérulitique. L'influence de la plastification et de la nucléation hétérogène sur ces morphologies a été étudiée par microscopie optique et des observations calorimétriques.

Effect of nucleation and plasticization on the stereocomplex formation between enantiomeric poly(lactic acid)s

Sajjad Saeidlou[a], Michel A. Huneault[a,*], Hongbo Li [b], Chul B. Park [c]

[a]Department of Chemical and Biotechnological Engineering, Université de Sherbrooke, Sherbrooke, QC J1K 2R1, Canada

[b]National Research Council of Canada, 75 de Mortagne, Boucherville, QCJ4B 6Y4, Canada

[c]Department of Mechanical and Industrial Engineering, University of Toronto, 5 King's College Road, Toronto, ON M5S 3G8, Canada

Abstract. *The effect of nucleation and plasticization on the stereocomplex formation between poly(L-lactic acid) (PLLA) and poly(D-lactic acid) (PDLA)was investigated in blends where PDLA is added as a minor phase in a major phase of PLLA. The use of small amounts of PDLA is aimed at creating a high melting point stereocomplex phase that in turn can serve as nucleating agent for the major phase of PLLA. Blends containing 5% PDLA with talc or organic phosphonate as nucleants and polyethylene glycol as plasticizer were prepared via melt-blending. Their crystallization behavior was investigated through Differential Scanning Calorimetry (DSC) using various thermal histories. Two peculiar stereocomplex melting endotherms were found. The peak temperature and enthalpy of these two endotherms were correlated to prior isothermal crystallization temperature. The different endotherms were also associated with two different crystalline morphologies observed by optical microscopy and referred to as Network and Spherulitic morphologies. The influence of plasticization and of heterogeneous nucleation on these morphologies was investigated through optical microscopy and calorimetric observations.*

Keywords: PLA stereocomplex, Crystallization kinetics, Nucleation and plasticization

4.1 Introduction

Poly(lactic acid) (PLA) is a thermoplastic polyester which was initially employed for specialty biomedical purposes due to its biocompatibility and bioresorbability. Thanks to its compostability and recent developments enabling its production from a renewable feedstock, PLA

utilization has increased dramatically with applications in packaging, textiles and molded articles [1, 8, 9]. Despite the good mechanical, optical and barrier properties, PLA has a low heat resistance as a result of low glass transition temperature, slow crystallization and low achievable crystallinity in conventional melt processing technologies. Lactic acid has a chiral carbon atom which gives rise to two enantiomeric forms, *L*-lactic acid and *D*-lactic acid. As a result, PLA can have a wide range of properties from amorphous to semi-crystalline forms, depending on the proportion and distribution of *L* and *D* units in the PLA chain. Ikada *et al.* found that this stereochemical aspect can lead to an interesting phenomenon where *L*- and *D*-rich PLA chains called PLLA and PDLA respectively, co-crystallize and form a stereocomplex with a melting point about 50 ^{o}C higher than PLLA or PDLA homocrystals [10]. Characteristics of the two components; i.e., the molecular weight, optical purity and chain architecture (linear or branched), as well as the blend preparation and crystallization conditions have influence over the kinetics and extent of stereocomplex formation between PLLA and PDLA. Several reports exist on the quantification of the role of these parameters as well as the understanding of stereocomplex formation mechanism [24, 67, 192-194, 198, 200-202, 213-222]. Furthermore, due to the higher melting point of stereocomplex compared to PLA homocrystal, it is possible to preserve it in molten PLA. This provides the opportunity of using PLA stereocomplex as a nucleation site for PLA homocrystallization [79, 80, 122, 144, 146, 147, 205, 216]. Other possible applications of stereocomplexation include improvement of thermo-mechanical [75, 223] and rheological properties [147, 203, 216]. More elaborated applications in carbon nanotubes-PLA nanocomposites [224, 225], increased interfacial adhesion in rubber toughened PLA [226], biodegradable hydrogels [227, 228] and nanoparticle formation [229-231] have also been reported recently. The fact that two different chains, i.e., PLLA and PDLA, must combine to form the stereocrystals imposes a larger diffusion path than in the regular chain folding crystallization mechanism. Therefore, stereocomplex formation compared to homocrystallization suffers from a larger kinetic barrier and this must be taken into account since stereocomplexation and homocrystal formation will be in competition upon cooling of the material. Due to the same kinetic issue, most of the prior research was done on blends prepared via solution mixing rather than through melt-mixing which would be the preferred method from an industrial application point of view. An approach to face this problem is to use stereoblock PLAs (PLLA-b-PDLA copolymers). However, since PLLA and PDLA blocks are connected to each other, their free

movement is constrained, thus stereocomplex formation is slower in this kind of materials relative to comparable PLLA/PDLA blends and leads to lower amounts of stereocomplex [232, 233]. It is possible to decouple stereocomplexation and homocrystallization by carrying out the stereocomplex formation at elevated temperatures where there is no overlap with homocrystallization. This is done obviously at the expense of a lower rate of stereocomplex formation since undercooling is reduced.

There has been a tremendous research effort dedicated to the PLA crystallization and this has been reviewed elsewhere [6]. Combination of nucleation and plasticization was shown to be necessary in order to increase the crystallization rate of PLA and obtain crystallized parts in a typical industrial molding process [76]. However, very little literature has been dedicated to the improvement of PLA stereocomplexation in the molten state [121]. In a previous study on the stereocomplex formation for melt mixed PLLA/PDLA blends at high temperatures, a peculiar dual network/spherulitic crystalline morphology was revealed [216]. In the current work, the effect of nucleation and plasticization on stereocomplex formation and on this network/spherulitic dual morphology is investigated.

4.2 Experimental

4.2.1 Materials

PLLA and PDLA were semi-crystalline commercial grades provided respectively by NatureWorks LLC and Hycail. According to the producers they contained 2% *D*- units and 0.5% *L*- units, respectively. Molecular weights of the polylactides were measured via a ViscotekTDAmax GPC apparatus (Malvern Instruments Ltd) equipped with a triple detection system. The measured weight-averaged molecular weight (M_w) and polydispersity index (M_w/M_n) were 109 kg/mol and 1.57 for PLLA and 61 kg/mol and 2.1 for PDLA. A high molecular weight PDLA (M_w = 174 kg/mol, PDI = 1.4) was also used for comparison but unless mentioned otherwise, the results presented in this paper are for the lower molecular weight PDLA. Polyethylene glycol (PEG) is a common plasticizer for PLA and is employed in different studies for enhancing its crystallization behavior. Therefore, to investigate the effect of plasticization on stereocomplex formation, a PEG with a nominal molecular weight of 3350 g/mol (Carbowax 3350) supplied by Dow Chemicals was selected. Talc (Mistron Vapor R) with a mean particle size

of 2 μm supplied by Luzenac America and an aromatic phosphonate (Ecopromote-NP) from Nissan Chemical Industries, LTD with a particle size of 0.1-0.2 μm were used as nucleating agents.

4.2.2 Blend preparation

Prior to blend preparation, all the materials were vacuum dried at 50 ^{o}C for 2 days. Different formulations were prepared via a melt-blending technique using a HAAKE MiniLab conical twin-screw micro compounder (Thermo Scientific). Mixing was carried out at 180 ^{o}C for 5 minutes at a rotation speed of 100 rpm. Neat PLLA was processed at the same operating conditions and was used as a reference (L). The extruded blends were also dried in the same conditions prior to characterizations. Table 4.1 summarizes the concentration of each component in the prepared formulations. Letters D, T, A and P in formulation designations refer to PDLA, talc, aromatic phosphonate and PEG, respectively. The number after each letter corresponds to the concentration of that component in weight %.

Table 4.1 Composition of the studied blends in wt. %

Designation	*PDLA*	*Talc*	*Aromatic Phosphonate*	*PEG*
L	0	0	0	0
D5	5	0	0	0
D5P5	5	0	0	5
D5P10	5	0	0	10
T1	0	1	0	0
A1	0	0	1	0
D5T1	5	1	0	0
D5A1	5	0	1	0
D5T1P5	5	1	0	5
D5A1P5	5	0	1	5
D5T1P10	5	1	0	10
D5A1P10	5	0	1	10

4.2.3 Differential Scanning Calorimetry (DSC)

Dynamic and isothermal characterizations were performed using a DSC Q2000 differential scanning calorimeter (TA instruments). Thermal history of the blends was removed by heating them to 240 ^{o}C and maintaining this temperature for 2 min. Afterwards, specimens were cooled to

room temperature at a rate of 10 ^{o}C/min and their crystallization from the melt was observed in the cooling cycle. In isothermal mode, removal of the thermal history was followed by rapid cooling to various isothermal crystallization temperatures (T_{iso}) ranging from 160 to 190 ^{o}C. Isothermal crystallization (i.e., stereocomplex formation) was carried out until its completion. Finally, samples were heated back to 240 ^{o}C at a rate of 10 ^{o}C/min to evaluate the stereocomplex melting behavior. A non-linear fitting software (PeakFit v4) was employed to deconvolute the overlapping double melting peaks. Pearson IV peak function with standard least-squares minimization was used to find the optimum fit.

4.2.4 Hot-stage Optical Microscopy

Optical microscopy (OPTIPHOT-2) was employed to observe the effect of isothermal crystallization temperature and additives on PLA stereocomplex crystalline morphology. Thin films were prepared by hot-pressing blend granules. A programmable hot-stage (Mettler FP82HT) was used to perform the thermal procedures.

4.3 Results and discussion

4.3.1 Non-isothermal DSC

Effect of PEG (plasticizer): The addition of a plasticizer increases chain mobility and facilitates its transfer to crystallization sites. It is typically most effective at lower crystallization temperatures where chains are restricted in motion. Figure 4.1 presents the DSC thermograms of neat PLLA and its blends with 5 wt.% PDLA, without and with PEG. Neat PLLA showed a small crystallization peak at 95 ^{o}C, while the other three blends had two crystallization peaks due to the presence of PDLA. For 5% PDLA without PEG (D5), the stereocomplex formation peak was small with an enthalpy of 2.4 J/g at 143.5 ^{o}C, and the presence of plasticizer increased stereocomplex enthalpy to 3.6 and 3.9 for 5 and 10% PEG respectively with no significant change in peak temperature. While larger homocrystallization peaks are expected in presence of the plasticizer, one could assume that the plasticizer will not significantly affect stereocomplex formation as it occurs at much higher temperatures compared to homocrystallization. However, results lead to the opposite conclusion. This can be explained considering the chain hindrance caused by stereocomplex formation. During the initial stages of stereocomplex formation, chain branching and a network-like structure forms due to the stereocomplex crystallite formation that

restricts chain mobility even at high temperatures [216]. Therefore, the presence of a plasticizer is helpful to counteract this negative aspect. Furthermore, the combination of plasticizer and the stereocomplex formed at higher temperatures that can act as a nucleating agent improves PLA homocrystallization even more, as expected from the synergistic effect of the nucleating agent and plasticizer on PLA crystallization. The 5% PDLA alone could not increase the homocrystallization compared to neat PLLA due to insufficient amount of stereocomplex and chain mobility issue at low crystallization temperature. On the other hand, presence of both PDLA and PEG enhanced homocrystallization as shown by the enthalpy increase from 3.4 J/g to 23 and 26 J/g and increasing peak temperature by 7 and 13 ^{o}C for D5P5 and D5P10 samples, respectively. Assuming a melting enthalpy of 146 J/g for 100% crystalline PLA ($\Delta H_{m,100}$) in the stereocomplex form [191], the maximum stereocomplex formation enthalpy at 5% PDLA content is 14.6 J/g for optically pure PLLA and PDLA ($2\times[PDLA]\times\Delta H_{m,100}$). Therefore the stereocomplex yield was increased from 16% for D5 sample to 26% by incorporating up to 10% plasticizer.

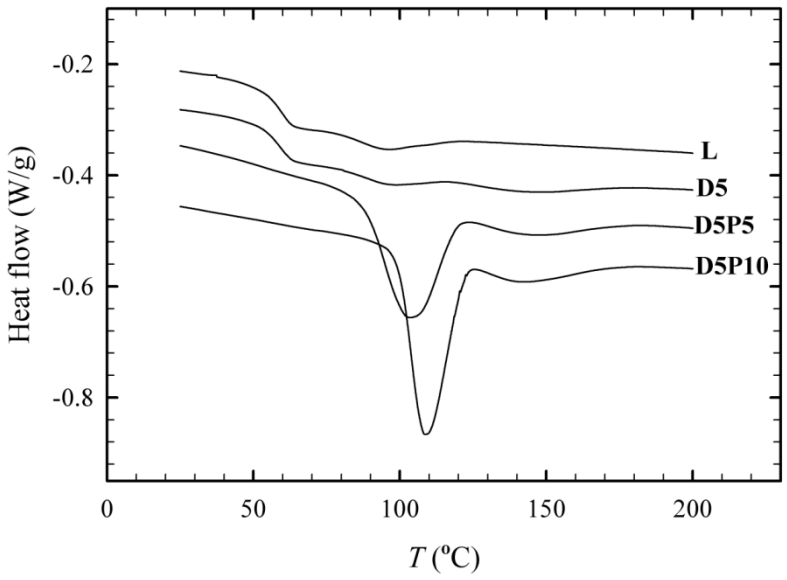

Figure 4.1 DSC cooling thermograms of neat PLLA (L), PLLA/5%PDLA (D5), PLLA/5%PDLA/5%PEG (D5P5) and PLLA/5%PDLA/10%PEG (D5P10)

Effect of nucleating agents: Influence of 1% talc or aromatic phosphonate on crystallization behavior of PLA blends is illustrated in Figure 4.2, where DSC cooling cycles of six samples are compared. Two types of crystallization peaks appear in these thermograms, those at higher temperatures, ranging from 143.5 ^{o}C (for D5) to 170.5 ^{o}C (for D5A1), are associated to stereocomplex formation and lower temperature peaks are related to homocrystallization. In terms

of stereocomplex formation both nucleating agents revealed significant increase in enthalpy and crystallization temperature. Stereocomplex enthalpy was increased to 7 and 7.5 J/g (corresponding to 48-51% stereocomplex crystallinity) and stereocomplex formation peak temperature was increased by 20 and 27 ^{o}C to 163.5 and 170.5 ^{o}C using 1% talc and 1% aromatic phosphonate, respectively. Another interesting result is the effect of aromatic phosphonate on PLA homocrystallization. A very sharp peak appeared at 128 ^{o}C with an enthalpy of 35.2 J/g. This is equal to complete crystallization at 33 ^{o}C higher temperature compared to the neat PLLA crystallization. Meanwhile, in the absence of PDLA (blends T1 and A1) homocrystallization peaks appeared at the same temperature as when both PDLA and nucleating agent were present. Therefore, talc and aromatic phosphonate have the main contribution in nucleation of homocrystallization.

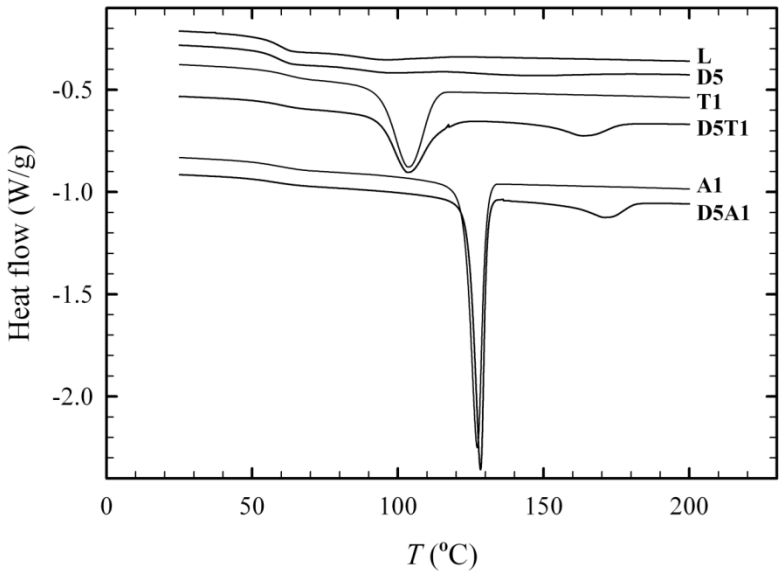

Figure 4.2 DSC cooling thermograms of neat PLLA (L), PLLA/5%PDLA (D5), PLLA/ 1% talc (T1), PLLA/5%PDLA/1%talc (D5T1), PLLA/ 1%aromatic phosphonate (A1) and PLLA/5%PDLA/1%aromatic phosphonate (D5A1)

Combined effect of nucleation and plasticization: Figure 4.3 and Figure 4.4 present the DSC thermograms of all studied formulations in the stereocomplex formation and homocrystallization regions, respectively. Since the role of the plasticizer is to facilitate chain movements at lower temperatures, higher improvements are observed for homocrystallization than for stereocomplex formation. More specifically, homocrystallization peak temperature and enthalpy were increased by 11 ^{o}C (from 103 to 114 ^{o}C) and 7.5 J/g when adding 10% PEG (i.e.

D5T1P10 compared to D5T1) while for aromatic phosphonate nucleated blend (D5A1) where homocrystallization is almost completed at a higher temperature, only a 2 ^{o}C increase in homocrystallization peak temperature was observed upon addition of the plasticizer. It is noteworthy that many studies have reported 130 ^{o}C as the optimum temperature for PLA spherulite growth rate [40, 60, 62, 87, 89]. Thus, if a nucleating agent like the aromatic phosphonate can nucleate PLA homocrystallization at this temperature it would result in a rapid crystallization. Similarly, for stereocomplex formation where peaks were shifted by 20 and 27 ^{o}C to 163.5 and 170.5 ^{o}C with 1% talc and aromatic phosphonate, further addition of plasticizer only increased peak temperature by 3.5 and 2 ^{o}C, respectively. Stereocomplex formation enthalpy was also increased to 7.7 and 8 J/g in presence of the plasticizer (D5T1P10 and D5A1P10 samples).

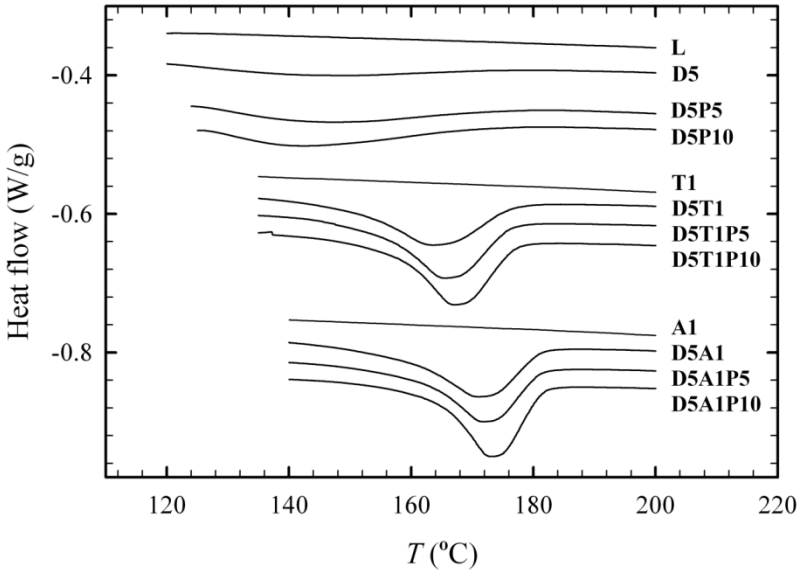

Figure 4.3 DSC cooling thermograms of all formulations in the stereocomplex formation region

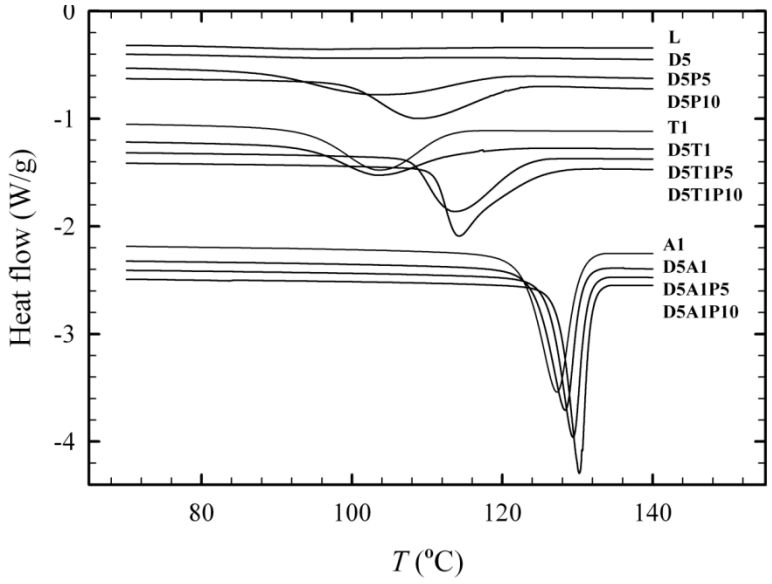

Figure 4.4 DSC cooling thermograms of all formulations in the homocrystallization region

4.3.2 Isothermal stereocomplex crystallization

Selected formulations were isothermally crystallized in the temperature range of 160 to 190 ^{o}C to study the effect of nucleation and plasticization on isothermal stereocomplexation kinetics and subsequent melting behavior. Figure 4.5 presents the crystallization peaks and the corresponding relative degree of stereocomplexation for the unmodified 5% PDLA blend (D5), the plasticized blend (D5P10), the aromatic phosphonate nucleated blend (D5A1) and for the plasticized/nucleated blend (D5A1P10). Successive curves represent 5 ^{o}C increments in isothermal crystallization temperature. Commonly, for all four samples, increasing the isothermal crystallization temperature resulted in widening of the peaks and in a slower stereocomplex formation. The aromatic phosphonate is the most efficient additive for enhancing the stereocomplex formation kinetics. PEG addition also increased the crystallization rate to some extent.

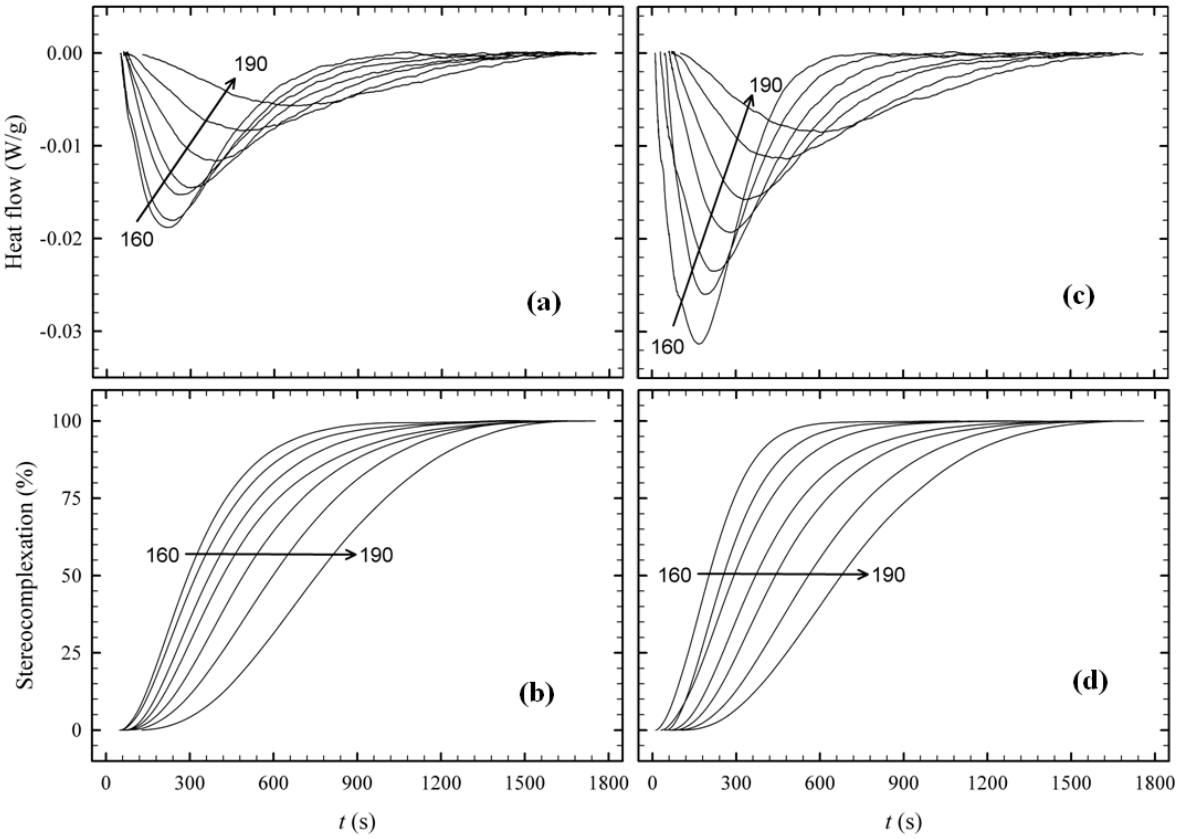
Heat flow (W/g)
0.00
-0.01
-0.02
-0.03
190
160
(a)
(c)
Stereocomplexation (%)
100
75
50
25
0
160
190
(b)
(d)
0
300
600
900
1200
1500
1800
t (s)

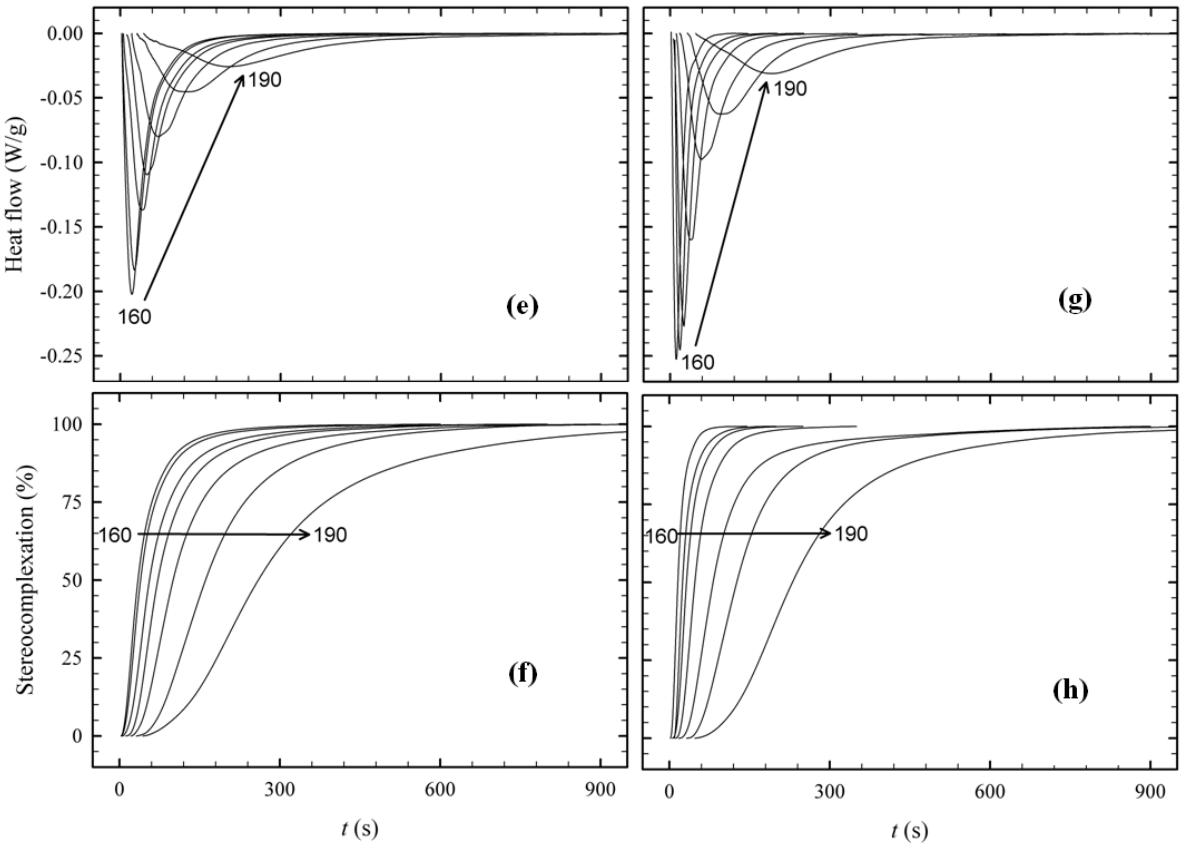

Figure 4.5 Isothermal crystallization peaks and corresponding relative degree of stereocomplexation for (a,b): D5, (c,d): D5P10, (e,f): D5A1 and (g,h): D5A1P10

To better illustrate the effect of temperature and formulation on the kinetics, stereocomplex formation half-time ($t_{1/2}$) is plotted versus the isothermal crystallization temperature in Figure 4.6. The $t_{1/2}$ is the time required to reach 50% relative degree of stereocomplex formation. For the blend without modifier (D5), $t_{1/2}$ is reduced from 12.6 min to 5 min by decreasing T_{iso} from 190 to 160 ^{o}C. For the blend with 10% PEG, the half-time ranged from 11.3 to 3.4 min in the same temperature interval showing some improvement in stereocomplex formation rate. In presence of aromatic phosphonate, the $t_{1/2}$ at 160 ^{o}C was remarkably reduced to 0.58 min and to 0.27 min with further addition of 10% PEG. Interestingly, the plasticizer was more effective in accelerating stereocomplex formation at lower temperatures and as the isothermal crystallization temperature was raised, data for plasticized and non-plasticized samples converged.

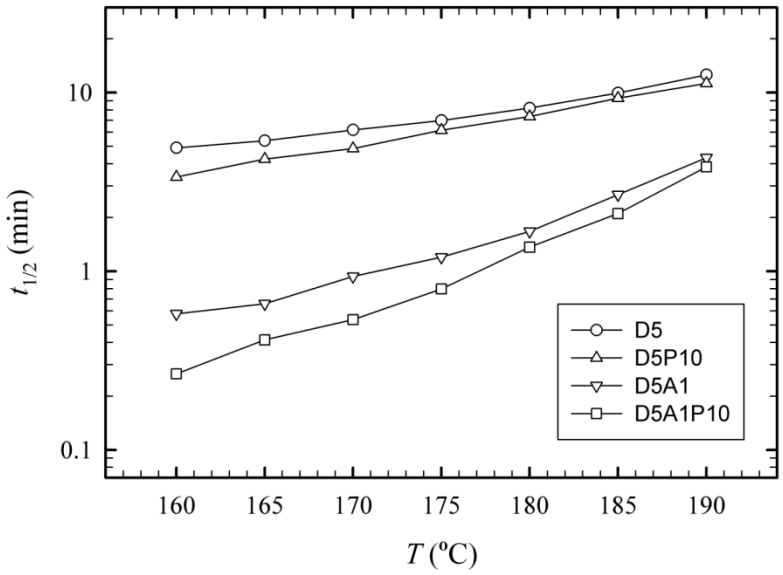

Figure 4.6 Stereocomplex formation half-time ($t_{1/2}$) as a function of isothermal crystallization temperature

4.3.3 PLA stereocomplex melting behavior

The melting behavior of isothermally crystallized blends was observed in a subsequent heating cycle at a rate of 10 °C/min. Figure 4.7 presents melting peaks for the unmodified 5% PDLA blend (D5) obtained after isothermal crystallization in the temperature range of 160-190 °C (5 °C increments) as an example. Curves are shifted vertically for the sake of better illustration.

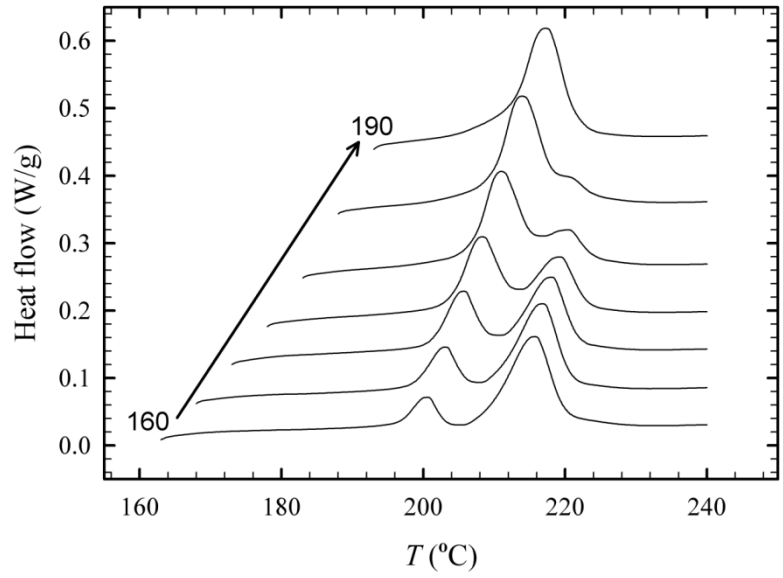

Figure 4.7 Melting behavior of the unmodified 5%PDLA blend (D5) after isothermal crystallization at 160-190 °C

In all four investigated blends, a double stereocomplex melting peak was observed, as it was reported earlier for PLLA/PDLA blends [216]. This phenomenon is related to the formation of a dual network/spherulite stereocomplex crystalline morphology and probably to a larger lamellae thickness in the spherulitic structure. Melt re-crystallization was ruled out as the cause of this behavior since double melting behavior was not dependent on heating rate for samples melted at heating rates between 5 to 40 ^{o}C/min. The position and amplitude of the two peaks varied depending on the isothermal crystallization temperature and presence of plasticizer and nucleating agent. In Figure 4.8, deconvoluted melting peaks obtained for different isothermal crystallization temperatures are illustrated for sample D5. Figure 4.8-a shows the lower temperature melting peaks associated to network structure and Figure 4.8-b shows the higher melting temperature peaks which are related to spherulite melting. Clearly, by increasing the isothermal crystallization temperature (T_{iso}), both the network and spherulite melting peaks shift to higher temperatures. However, the portion of network structure is increased in the final morphology at the expense of the spherulitic structure. The sum of melting enthalpies from the two peaks for all isothermal crystallization temperatures is around 7.5 J/g which is equal to 50% stereocomplex crystallinity.

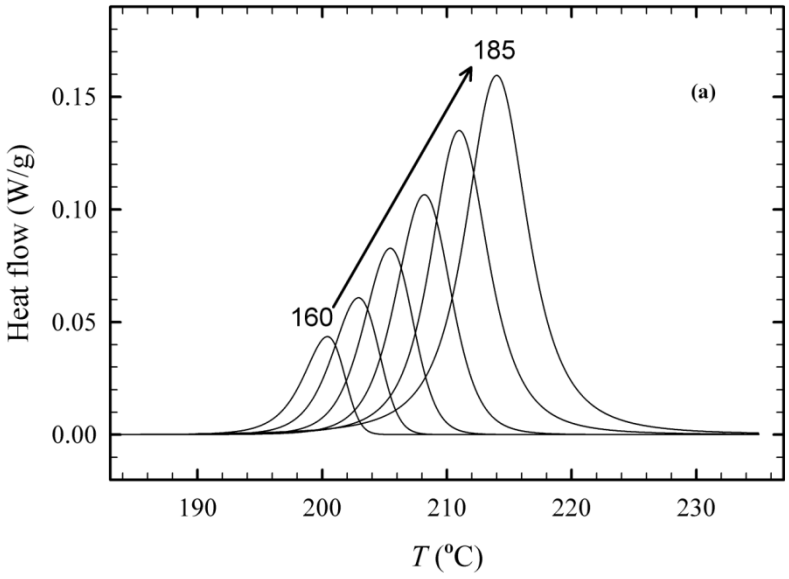

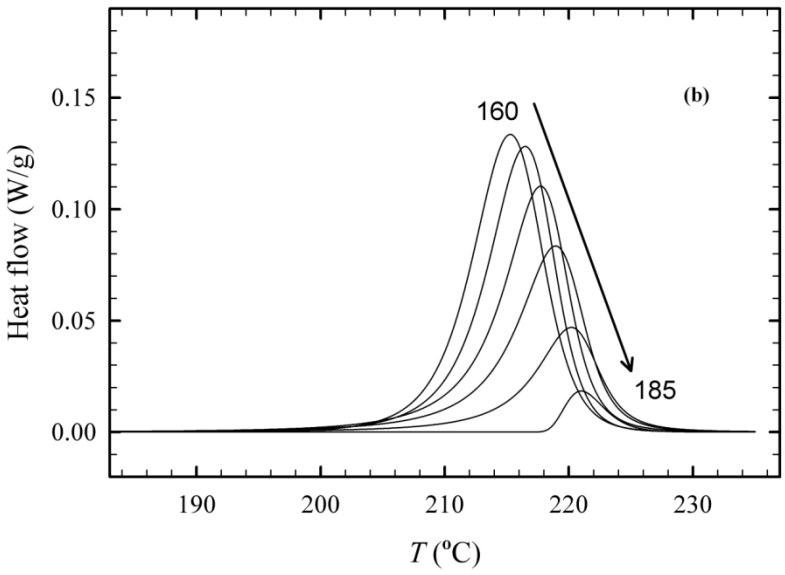

Figure 4.8 Effect of isothermal crystallization temperature on the melting behavior of PLLA with 5% PDLA (D5): (a) network structure melting and (b) spherulitic structure melting

Figure 4.9 known as Hoffman-Weeks plot, shows the variation of melting point versus crystallization temperature for the two melting peaks to obtain the stereocomplex equilibrium melting temperature. Melting temperature for both peaks increases linearly with isothermal crystallization temperature. However, the slope for lower temperature peak is higher which results in an equilibrium melting point of 248 ^{o}C compared to 232 ^{o}C obtained from the higher melting peak. Tsuji and Ikada [24] reported equilibrium melting point for 1:1 blends of PLLA and PDLA with different optical purities with the same method ranging from 214 to 263 ^{o}C, showing that estimated T_m^0 depends on the optical purity of PLA. Therefore, the two melting peaks which resulted in different T_m^0 of stereocomplex may have been originated from segregated PLLA and PDLA chain segments with different optical purities.

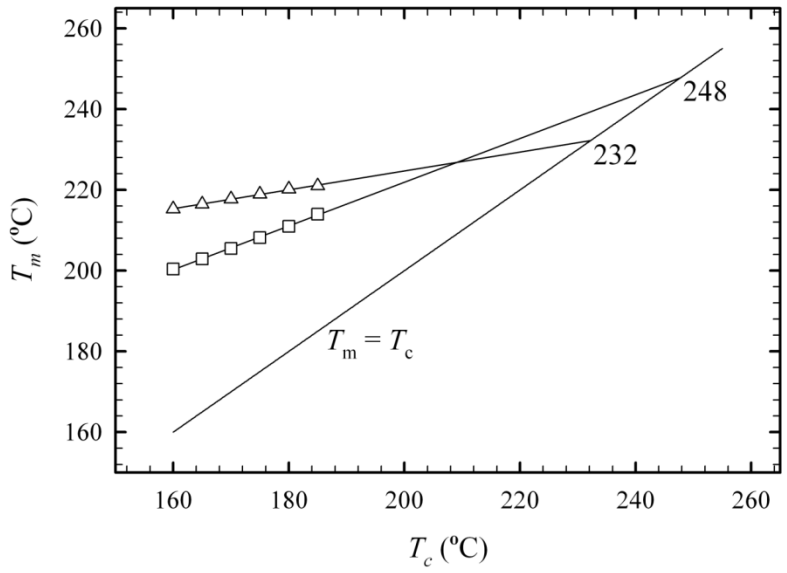

Figure 4.9 Hoffman-Weeks plot for the two stereocomplex melting peaks

A similar dual-peak melting behavior with increasing T_{iso} was observed for the other three blends. In Figure 4.10, melting peaks of D5, D5P10, D5A1 and D5A1P10 obtained after isothermal crystallization at 170 and 180 ^{o}C are compared as an example. Aromatic phosphonate addition (D5A1) resulted in a lower melting temperature spherulite and network compared to the reference 5% PDLA blend (D5). Spherulite melting peak temperature was reduced by 3 ^{o}C while network melting peak temperature was reduced only one degree. Addition of 10% PEG on the other hand shifted the melting peaks slightly to lower temperature as T_{iso} was increased. The more significant plasticizer effect however was increasing the enthalpy of the spherulite peak which is clear by comparing sample D5 with D5P10 and D5A1 with D5A1P10 blends. The sum of melting enthalpies from network and spherulite peaks for D5P10 blend was about 8.8 J/g which is equal to 60% stereocomplex crystallinity, showing a 10% increase in total stereocomplex formation.

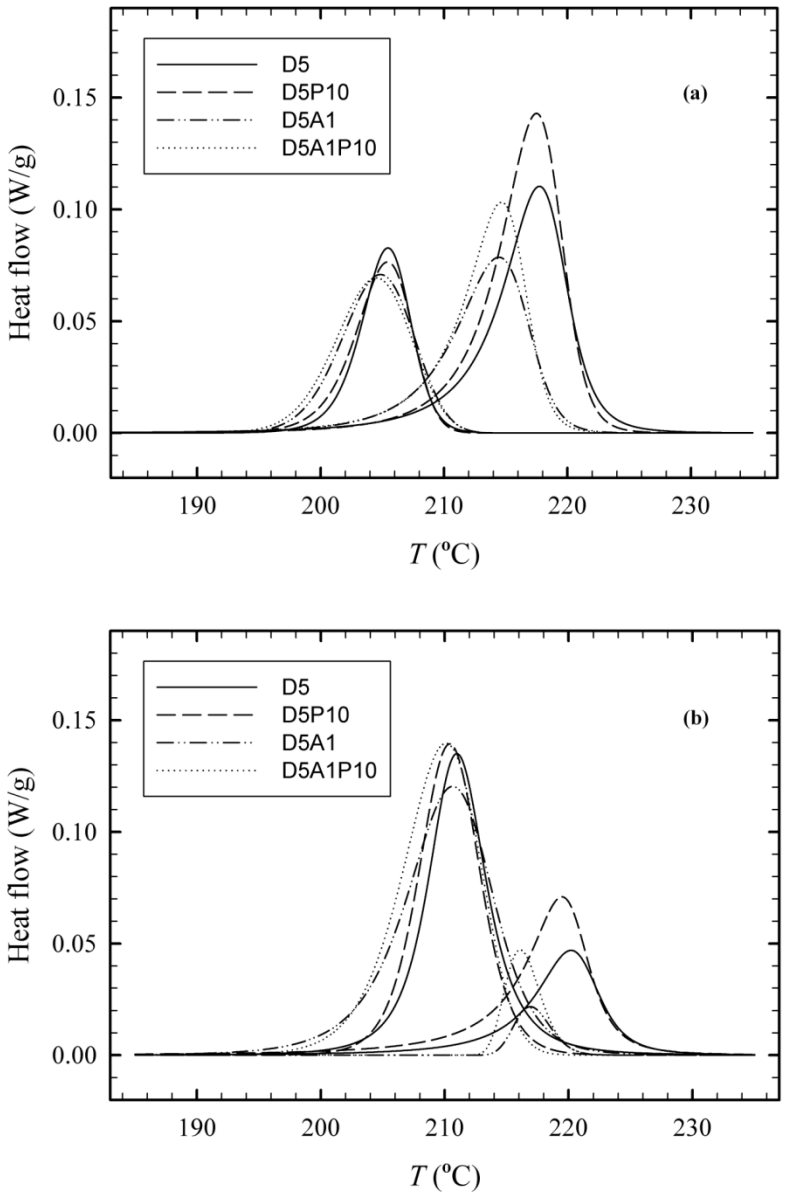

Figure 4.10 Effect of nucleating agent and plasticizer on the PLA stereocomplex network and spherulite melting peaks after isothermal crystallization at (a) 170 °C and (b) 180 °C

In addition, to understand the role of PDLA molecular weight on stereocomplexation, a higher molecular weight PDLA (M_w = 174 kg/mol, PDI = 1.4) was used for comparison. Figure 4.11 shows melting peaks obtained for a blend containing 5% of this higher molecular weight PDLA. The same double melting behavior is observed and the trend in their position and size variation with isothermal crystallization temperature is similar to that observed in Figure 4.7. On the other hand, due to the much higher molecular weight of PDLA,

stereocomplex formation is less favored and the melting enthalpy of stereocomplex formed is around 1.5 J/g compared to 7.5 J/g in case of lower molecular weight PDLA.

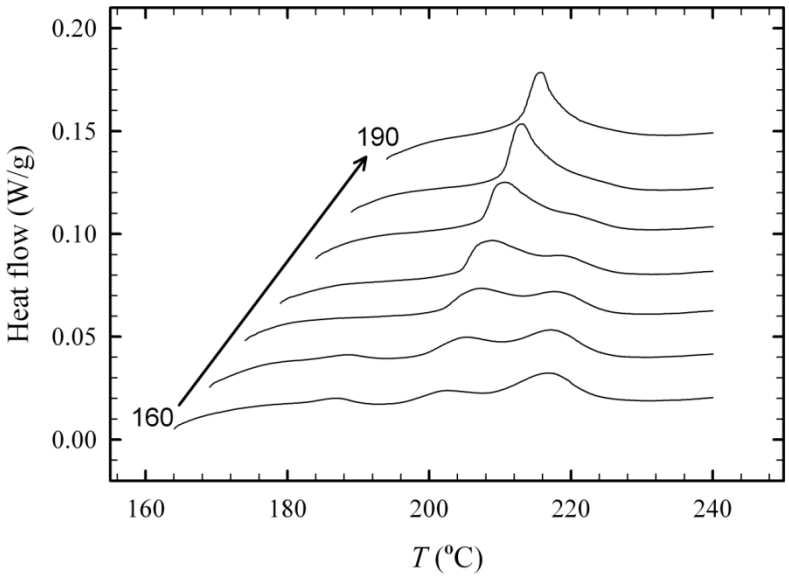

Figure 4.11 Melting behavior of the blend with 5% high molecular weight PDLA after isothermal crystallization at 160-190 °C

4.3.4 Optical microscopy observations

Optical microscopy observations were performed to correlate the crystalline morphology with isothermal DSC characterizations. After removing thermal history by keeping the samples at 240 °C for 2 min, thin films were isothermally crystallized at desired T_{iso} long enough (based on DSC results, Figure 4.5) to complete stereocomplex formation. Then samples were cooled to 110 °C, kept at this temperature for few minutes and finally heated back to 200 °C to observe the final morphology. As it was explained in an earlier work [216], this cooling and heating cycle was necessary for better visualization of the network morphology. Figure 4.12 shows the images captured at 200 °C for D5 blend isothermally crystallized at different temperatures. According to these images, by increasing T_{iso} from 160 to 190 °C, the number of stereocomplex spherulites is reduced slightly, the final spherulite size is reduced considerably, and stereocomplex lamellae are less packed in spherulite morphology and grow laterally on existing lamellae. Especially at T_{iso} equal to 190 °C some irregular lamellae aggregates are observed. These phenomena lead to less stereocomplex in the spherulite morphology and higher portion of network structure. Therefore, optical microscopy observations are consistent with isothermal DSC characterization results where network peak grows and spherulite peak shrinks with increasing T_{iso}.

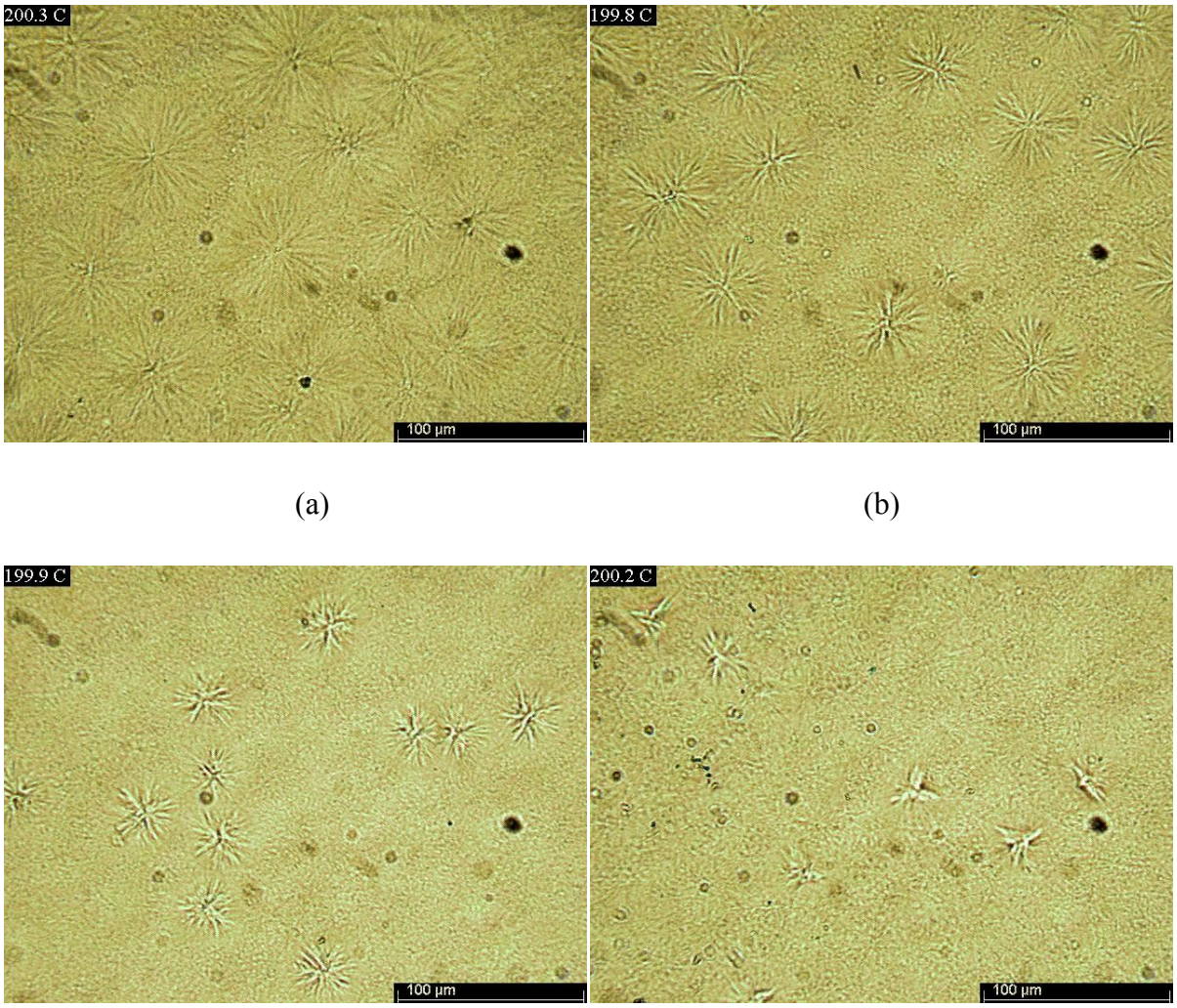

Figure 4.12 Final stereocomplex crystalline morphology of D5 blend at 200 °C, isothermally crystallized at (a) 160 °C, (b) 170 °C, (c) 180 °C and (d) 190 °C

Furthermore, to investigate the influence of nucleation and plasticization, the final stereocomplex morphologies after isothermal crystallization at 180 °C were compared. Micrographs taken at 200 °C are presented in Figure 4.13 for the same blend series as in previous figures (D5, D5P10, D5A1 and D5A1P10). Interestingly, four distinct morphologies were observed for the four blends. Comparing Figure 4.13-a with Figure 4.13-b suggests that the presence of plasticizer decreases the stereocomplex spherulite density while results in larger spherulites. On the contrary, presence of the aromatic phosphonate (Figure 4.13-c) greatly influenced the morphology leading to a dense mixture of stereocomplex network and very fine spherulites which are difficult to distinguish. Finally, presence of both plasticizer and nucleating

agent (Figure 4.13-d) ended in an intermediate morphology with a lower spherulite density and larger spherulites compared to D5A1 sample.

The achieved results are of great significance and could lead to the use of a minor stereocomplex phase as means for accelerating homocrystallization, for generating high melting point physical cross-links in an otherwise amorphous matrix or for increasing melt elasticity of PLA in melt processing applications. The stereocomplexation half-time was reduced by an order of magnitude which makes it possible to produce PLA stereocomplex efficiently in the timeframe of melt processing techniques. As well, a variety of stereocomplex morphologies can be produced in a controlled manner by varying temperature as well as nucleating agent and plasticizer concentration.

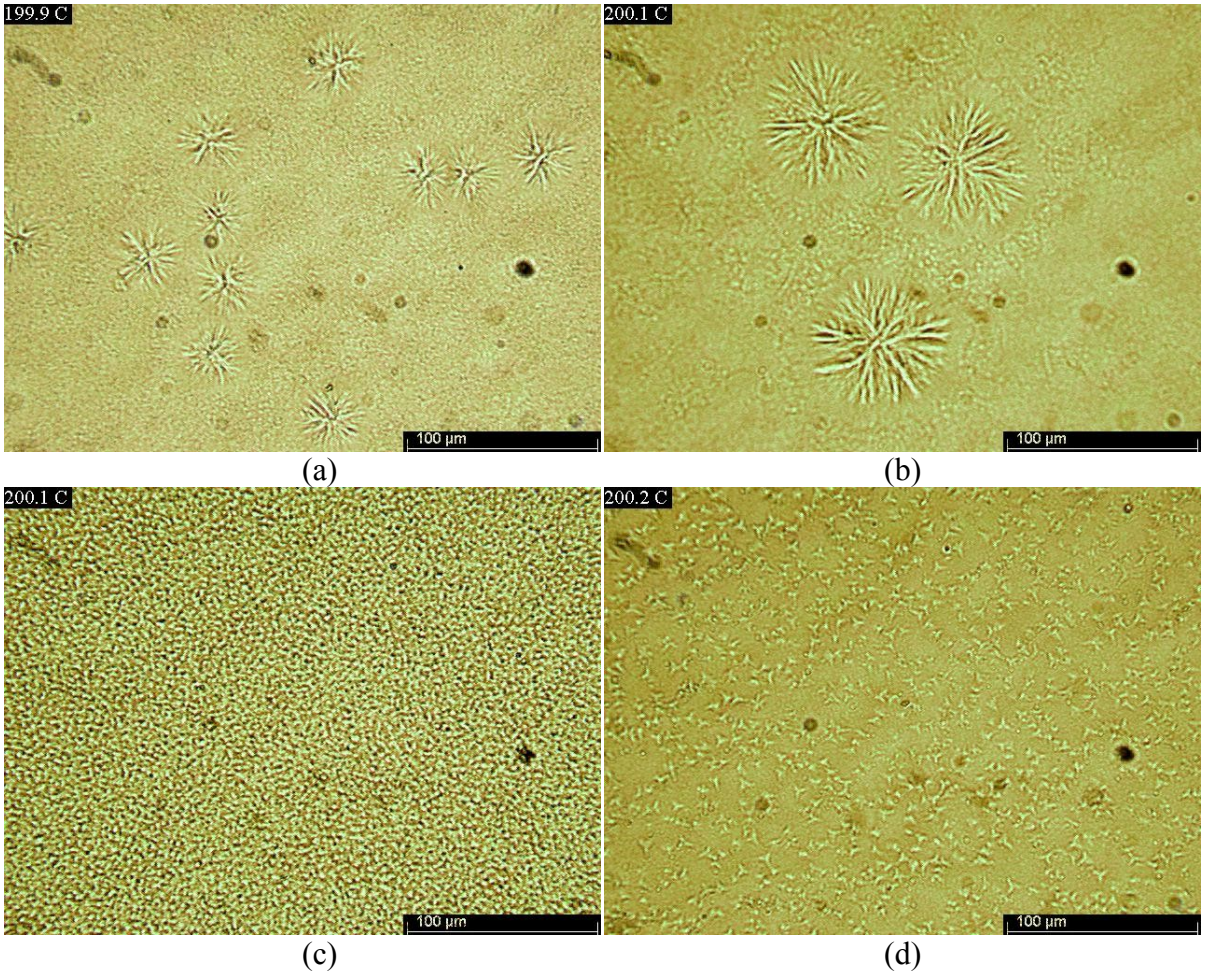

Figure 4.13 Final stereocomplex crystalline morphology at 200 °C, blends isothermally crystallized at 180 °C: (a) D5, (b) D5P10, (c) D5A1 and (d) D5A1P10

4.4 Conclusions

Both talc and aromatic phosphonate can nucleate PLA homocrystallization as well as stereocomplex formation, with aromatic phosphonate being the most efficient. The addition of a plasticizer such as PEG further lowers the stereocomplex formation time even though stereocomplexation is carried out at a much higher temperature than the homocrystallization. This emphasizes the importance of dynamic limitations in the stereocomplexation process. The stereocomplexation half-time can be reduced by an order of magnitude when properly combining heterogeneous nucleation and plasticization. Two types of stereocomplex morphologies, a lower melting-point network morphology and a higher melting-point spherulitic morphology, can coexist and are observable under optical microscope. The ratio of the two morphologies can be controlled by changing the temperature at which the stereocomplex is formed. Lower formation temperatures favor the spherulitic morphology at the expense of the network one. The presence of a plasticizer increases the spherulite size and reduces their number. The presence of nucleating agents, already known to nucleate homocrystallization, also increases dramatically the stereocomplex nucleation density leading accordingly to a reduction in spherulite size. In the current study, the spherulite size was lowered below the measuring limit of optical microscopy. These findings are of great interest because they show that stereocomplex formation in the melt state is feasible within an acceptable timeframe for industrial melt processes. Since the stereocomplexation and homocrystallization are enhanced by the same nucleants and plasticizers, these additives will provide high stereocomplexation rates and high homocrystallization level at the same time.

Chapter 5. Poly(lactic acid) stereocomplex formation: application to PLA rheological property modification

Avant-propos

Auteurs et affiliation:

Sajjad Saeidlou: *Département de génie chimique et de génie biotechnologique, Faculté de genie, Université de Sherbrooke*

Michel A. Huneault: *Département de génie chimique et de génie biotechnologique, Faculté de genie, Université de Sherbrooke*

Hongbo Li: *National Research Council of Canada*

Chul B. Park: *Department of Mechanical and Industrial Engineering, University of Toronto*

Date de soumission: 7 janvier 2014

Revue: Journal of Applied Polymer Science

Titre français: Modification rhéologique du PLA via la formation de stéréocomplexes

Contribution au document: Les effets de la formation des stéréocomplexes sur les propriétés rhéologiques sont examinés.

Résumé français: *La formation de stéréocomplexes de PLA en conditions isothermes a été étudiée en absence et en présence d'un agent de nucléation d'un point de vue rhéologique grâce à la sensibilité des propriétés viscoélastiques à des changements structurels au cours de ce processus. Le PDLA en concentrations faibles a été mélangé avec le PLLA à l'état fondu pour la formation de stéréocomplexes. Des échantillons amorphes ont été préparés et la cristallisation a été réalisée dans un rhéomètre à des températures élevées afin de simuler des conditions de mise en forme à l'état fondu. La stereocomplexation a été explorée au cours du temps en mesurant les paramètres rhéologiques en mode de cisaillement oscillatoire à faible déformation en utilisant la géométrie des plaques parallèles. Les données cinétiques obtenues par ce moyen ont été comparées aux données des études calorimétriques. Cette comparaison met en évidence une tendance différente en fonction de la méthode de caractérisation. De plus, après la fin de la cristallisation, la structure cristalline finale a été sondée sur une large gamme de fréquences pour étudier le rôle de la modification rhéologique du PDLA sur une phase principale de PLLA.*

Des différences entre les caractéristiques rhéologiques des mélanges asymétriques de PLLA / PDLA et PLLA ont été associées à des changements structurels qui se produisent en raison de la formation de stéréocomplexes.

Poly(lactic acid) stereocomplex formation: application to PLA rheological property modification

***Sajjad Saeidlou*[a], *Michel A. Huneault*[a,*], *Hongbo Li*[b], *Chul B. Park*[c]**

[a]*Department of Chemical and Biotechnological Engineering, Université de Sherbrooke, Sherbrooke, QC J1K 2R1, Canada*

[b]*National Research Council of Canada, 75 de Mortagne, Boucherville, QCJ4B 6Y4, Canada*

[c]*Department of Mechanical and Industrial Engineering, University of Toronto, 5 King's College Road, Toronto, ON M5S 3G8, Canada*

Abstract. *PLA stereocomplex formation in isothermal conditions in the absence and presence of a nucleating agent was studied from a rheological point of view due to sensitivity of viscoelastic properties to structural changes during this process. PDLA was melt blended in low concentrations with PLLA to produce a stereocomplex. Amorphous samples were prepared and crystallization was carried out in a rheometer at high temperatures to simulate melt processing conditions. Stereocomplexation was explored over time by measuring rheological parameters in small deformation oscillatory shear mode at a low frequency using parallel plate geometry. Kinetic data obtained by this means was compared to data from calorimetric studies, showing a different trend depending on the characterization method. Moreover, after the completion of crystallization, final crystalline structure was probed over a wide range of frequencies to investigate the rheological modification role of PDLA on PLLA major component. Differences in rheological characteristics of asymmetric PLLA/PDLA blends compared to neat PLLA were associated to the structural changes happening due to the formation of the stereocomplex.*

Keywords: PLA stereocomplex, Rheology, Crystallization

5.1 Introduction

Poly(lactic acid) (PLA) is a fast growing bio-based and compostable polymer that has raised lots of interest recently. Due to the presence of a chiral carbon atom, lactic acid has two enantiomeric forms called L-lactic acid and D-lactic acid. This can lead to an interesting

phenomenon where L- and D-rich PLA chains called PLLA and PDLA respectively, co-crystallize and form a crystal structure known as a stereocomplex [10]. PLA stereocomplex is distinguished from PLLA or PDLA homocrystals by a 50 ^{o}C higher melting point. In the last decade, PLA has become widely available commercially as a cost-competitive biobased polymer with applications in packaging, textile and molded parts [1, 8, 9]. This has augmented the need to overcome PLA deficiencies such as low heat resistance, slow crystallization and low melt strength. Currently available PLA are mainly made from L-Lactic acid as this is the preferred form naturally obtained through fermentation routes. Progress has been made however to produce D-lactic acid and therefore could open the way to the use of PLA stereocomplex to solve the aforementioned obstacles [234-237]. Up to now, investigations have mainly focused on gaining an understanding of the stereocomplexation phenomenon with the emphasis on the crystallization mechanism and on the effect of different parameters such as molecular weight, optical purity as well as the blend preparation method and crystallization conditions [24, 67, 192-194, 198, 200-202, 213-222]. In terms of applications, PLA stereocomplex has been investigated as a nucleation site for PLA homocrystallization [79, 80, 122, 144, 146, 147, 205, 216], as a thermo-mechanical properties modifier [75, 223] as well as in PLA nanocomposites [224, 225, 238, 239]. However, very few reports exist on the improvement of PLA rheological properties with the use of a stereocomplex [203]. Despite good mechanical, optical and barrier properties, rheological properties of PLA are relatively inadequate for some processing techniques that require melt elasticity, i.e. the so-called melt strength. This is particularly limiting for processes such as film blowing and extrusion foaming where melt elasticity is required to retain film or foam structure prior to solidification. Thus, the first objective of this work was to explore the influence of stereocomplex on PLA melt rheology.

On the other hand it is also interesting to study the PLLA/PDLA co-crystallization by rheological measurements. Many reports exists on PLA crystallization mostly based on calorimetric studies, reviewed elsewhere [6]. Rheological monitoring of PLA homocrystallization as well has been done by a number of researchers [240-242], however there is no study on rheological monitoring of PLA stereocomplex formation. It is known that nucleation and plasticization have a significant effect on PLA homocrystallization [76]. In a previous study on the stereocomplex formation for melt mixed PLLA/PDLA blends it was shown that these

modification techniques are also helpful for acceleration of stereocomplex formation even at elevated temperatures, with nucleation having a major contribution [243]. Therefore, the second objective of this work was to probe the effect of a nucleating agent on stereocomplex formation through rheological measurements. Results have been compared to kinetic data obtained via calorimetry and the difference in the response of material is explained taking into account the evolution of PLA microstructure by stereocomplex formation from the melt.

5.2 Experimental

5.2.1 Materials

PLLA and PDLA were semi-crystalline commercial grades provided respectively by NatureWorks LLC and Hycail. According to the producers they contained 2% *D*- units and 0.5% *L*- units, respectively. Molecular weights of the polylactides were measured via a ViscotekTDAmax GPC apparatus (Malvern Instruments Ltd) equipped with a triple detection system. The measured weight-averaged molecular weight (M_w) and polydispersity index (M_w/M_n) were 109 kg/mol and 1.57 for PLLA and 61 kg/mol and 2.1 for PDLA. An aromatic phosphonate (Ecopromote-NP) from Nissan Chemical Industries, LTD with a particle size of 0.1-0.2 μm was used as nucleating agent.

5.2.2 Blend preparation

Different formulations were prepared via a melt-blending technique using a LabTech twin-screw extruder. Mixing was carried out at 180 ^{o}C at a rotation speed of 200 rpm and a feeding rate of 4 kg/hr. Neat PLLA was processed at the same operating conditions and was used as a reference. The extruded blends were vacuum dried at 55 ^{o}C for 2 days prior to characterization.

5.2.3 Rheological measurements

Extruded samples were compression molded to disk-shaped specimens using a Carver laboratory press. The molding temperature was set to 240 ^{o}C and the mold assembly was removed and quenched in liquid nitrogen to obtain amorphous samples. Dynamic melt rheological measurements were performed using an MCR 502 rheometer (Anton Paar) with parallel plate geometry. Plates diameter was 25 mm and gap size was set to 1.2 mm. Initially, dynamic strain sweep tests were performed on annealed samples to determine the linear viscoelastic region. For

the crystallization monitoring, time sweep characterization was done at a frequency of 1 Hz for 30 min. Then, to investigate the effect of the crystalline structure formed during the time sweep test on the rheological properties of the blend, frequency sweep tests were performed in the frequency range of 0.1-300 rad/s. All tests were conducted under a blanket of dry nitrogen to minimize hydrolytic degradation.

5.3 Results and discussion

5.3.1 Effect of stereocomplex on linear viscoelastic region

Figure 5.1 shows the variation of elastic modulus (G') as a function of applied strain (γ) obtained at a frequency of 1 Hz for annealed samples with different concentrations of PDLA. It is clear that increasing the PDLA content results in an increase in G' as more stereocomplex is formed. Moreover, the linear viscoelastic region is significantly reduced as the PDLA concentration is increased. For neat PLLA the higher limit is 45% whereas for a blend with 10% PDLA it is decreased to about 2%. Similar behavior is observed for the well dispersed carbon nanotubes (up to 7%) in PLA matrix [244]. Based on these results a low strain of 0.5% was chosen for the rheological measurements.

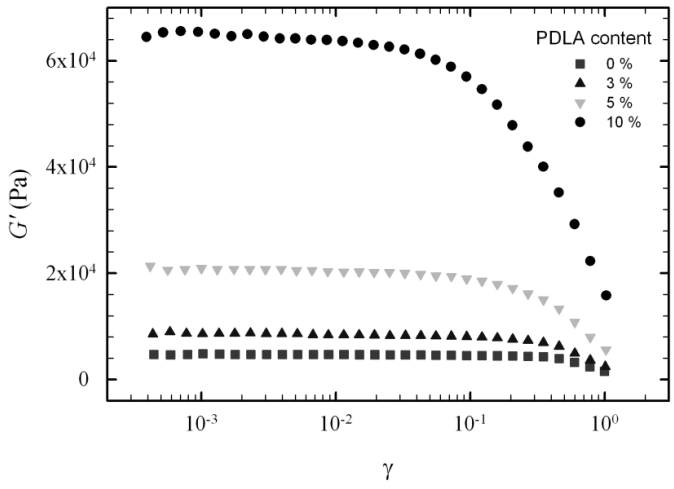

Figure 5.1 Elastic modulus as a function of strain for annealed samples with PDLA concentration between 0 to 10 wt.%.

5.3.2 Rheological monitoring of stereocomplex formation

Time sweep tests were performed on amorphous samples at 180 ^{o}C and a frequency of 1 Hz to monitor the variation of rheological properties with time which is an indication of

stereocomplex formation at the test temperature. In Figure 5.2, *G*' is plotted versus time for blends with different amounts of PDLA.

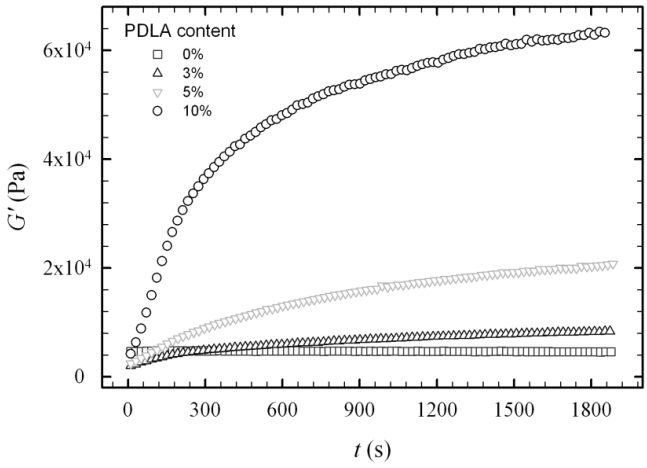

Figure 5.2 Elastic modulus as a function of time for initially amorphous samples with different PDLA concentrations

First of all, for neat PLLA variation of *G*' in the time frame of the test was small. Therefore the material was thermally stable at these conditions. By adding PDLA to PLLA, the initial value of *G*' decreased below that of neat PLLA. This was expected since PDLA has a lower molecular weight compared to PLLA. As time went by, *G*' gradually increased until it reached a plateau where variations of elastic modulus were small enough to assume that the stereocomplex formation was completed. The final value of the elastic modulus, $G'(\infty)$ depended on PDLA concentration and was in agreement with the values obtained for annealed samples in strain sweep tests.

To demonstrate the effect of stereocomplex formation in the test conditions on melt elasticity, phase angle (δ) as a function of time is presented in Figure 5.3 for the investigated blends. Neat PLLA showed a constant phase angle of 75^{o} in the absence of any PDLA to co-crystallize with. Meanwhile, PLLA/PDLA blends revealed a decrease in phase angle, indicating that stereocomplex structure formed and contributed to an increase in melt elasticity. Higher PDLA concentration resulted in a lower phase angle, reaching a value of 44^{o} for 10% PDLA.

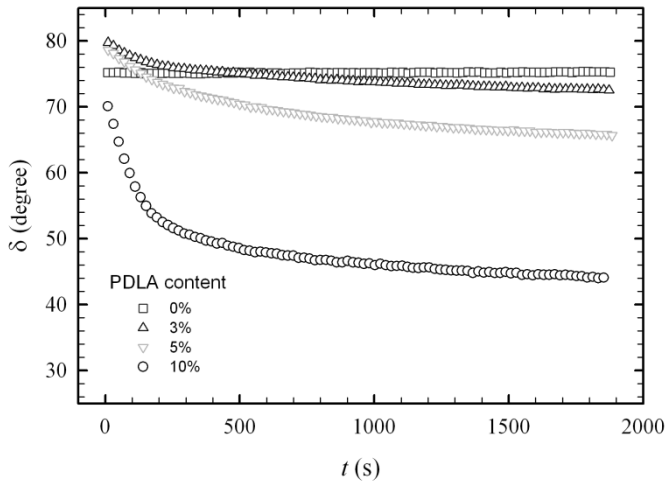

Figure 5.3 Variation of phase angle with time as an indication of stereocomplex formation

In prior work, It has been assumed that the amount of crystalline phase scales with G' based on the following equation [245]:

$$\chi(t) = \frac{G'(t) - G'(0)}{G'(\infty) - G'(0)} \qquad \textbf{Equation 5.1}$$

where χ is the relative crystallinity, $G'(t)$ is the elastic modulus at time t, $G'(0)$ is the initial elastic modulus and $G'(\infty)$ is its final value. Therefore, to investigate the kinetics of stereocomplex formation based on rheological data, χ is plotted versus crystallization time in Figure 5.4.

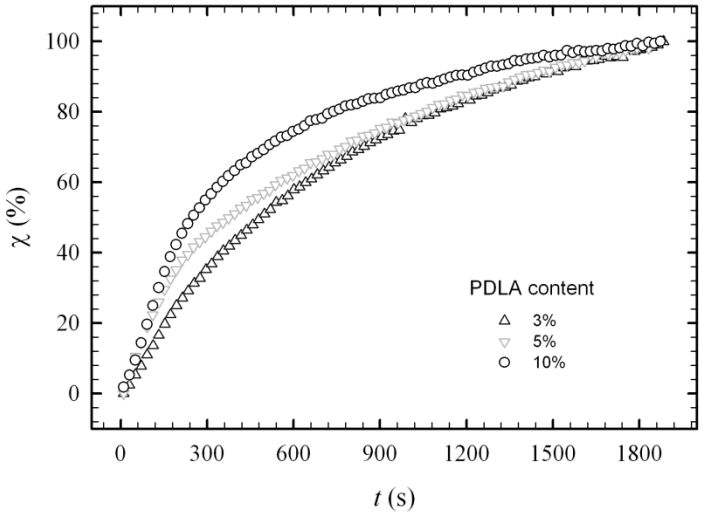

Figure 5.4 Relative crystallinity as a function of time for blends with 3, 5 and 10% PDLA.

From this figure it can be seen that crystallization rate depends on PDLA concentration and as the PDLA amount in the blend is increased, the stereocomplex formation rate is increased. Stereocomplex formation half-time ($t_{1/2}$) was between 3.8 to 8.3 min depending on PDLA concentration.

Comparing rheology with DSC: It is interesting to compare the kinetic data obtained from rheological measurements with those from calorimetry [243]. In Figure 5.5, kinetic curves corresponding to stereocomplex formation at 180 ^{o}C for the blend with 5% PDLA are compared.

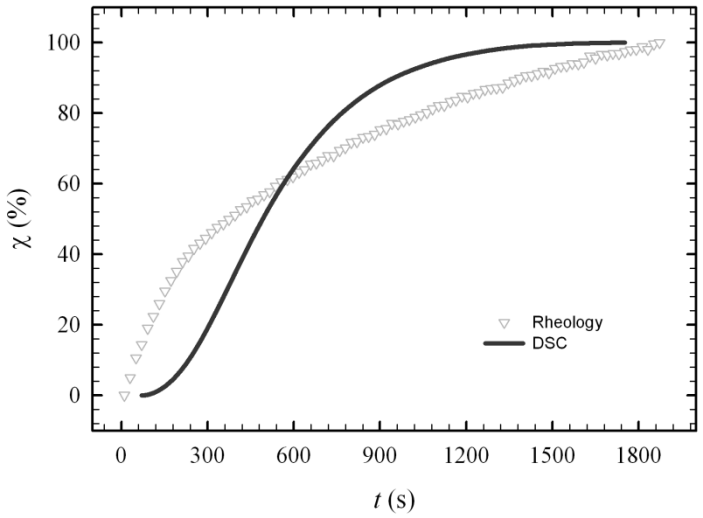

Figure 5.5 Comparison of relative crystallinity as a function of time for 5% PDLA blend obtained by rheological and calorimetric measurements at T_c = 180 °C

The relative crystallinity obtained from rheological measurements was higher compared to that obtained from DSC until 50% stereocomplex formation, after which it falls below the DSC curve. This discrepancy may be explained by considering the specific case of stereocomplex formation and of the complex crystalline structure formed in isothermal conditions. It was shown that a dual network/spherulitic crystalline morphology is formed by co-crystallization of PLLA and PDLA chains [216, 243]. Spherulites are higher order structures which takes longer time to produce and grow. On the other hand, network structure is composed of smaller crystallites formed at a shorter time scale at different spots where PLLA and PDLA chains are in the vicinity of each other. Therefore, the effect of enantiomeric chains connection to each other is more significant on melt rheology at the initial stages of stereocomplexation. Physical connection of two chains results in an apparent increase in molecular weight. Also the chain structure evolves from a linear to a branched structure. Furthermore, if more than two chains are involved in stereocomplexation, physical cross-linking may occur. All these reasons result in an increase in elasticity and PLA viscosity, thus a higher rheological response in the earlier stages of crystallization.

Effect of nucleating agent: It has been shown through calorimetric studies that an aromatic phosphonate has a significant nucleating effect on PLA stereocomplex formation [243]. This was further investigated by tracing the variation of elastic modulus with time in the presence of this material. Figure 5.6 shows G' as a function of time for three samples. The straight line corresponds to the sample without PDLA having 1% nucleating agent. Thus, the material is thermally stable in the presence of nucleating agent with no significant decrease in G' after about 30 min. The curve presented with downward triangle symbol is related to the blend with 5% PDLA as illustrated in Figure 5.2 and is shown for the sake of comparison. Finally, the blend with 5% PDLA and 1% nucleating agent is presented with open circles. The initial point for the sample with PDLA and nucleating agent was higher compared to the other two blends, suggesting that the stereocomplex formation had already progressed to some extend from the time that sample was placed in the rheometer until time sweep test was started. In addition, the plateau was reached much faster compared to the unmodified blend.

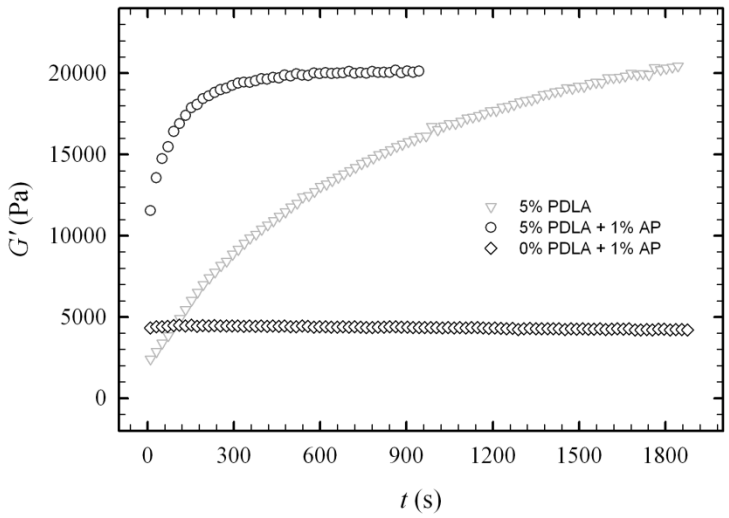

Figure 5.6 Elastic modulus as a function of time for amorphous samples: 1% nucleating agent without and with 5% PDLA and 5% PDLA blend without nucleating agent

G' values for the nucleated sample are transformed to relative crystallinity according to Equation 5.1 and compared in Figure 5.7 to unmodified blend's relative crystallinity obtained from rheology and DSC characterization. To find the initial point for the nucleated sample, data were extrapolated to the initial value of elastic modulus for the unmodified blend. Similar to the unmodified blend, the kinetic curve for the blend containing 1% aromatic phosphonate and 5% PDLA obtained from DSC characterization is illustrated. Based on Figure 5.7, it can be concluded that heterogeneous nucleation was highly effective to enhance the stereocomplex formation at high temperatures. Stereocomplex formation half-time was reduced from 375 s for unmodified blend to 50 s in the presence of aromatic phosphonate. For the nucleated sample as well, the rheological data showed an earlier increase in relative crystallinity compared to DSC curve. However, since the stereocomplex formation was much faster in this case compared to the unmodified blend, this difference is not as notable.

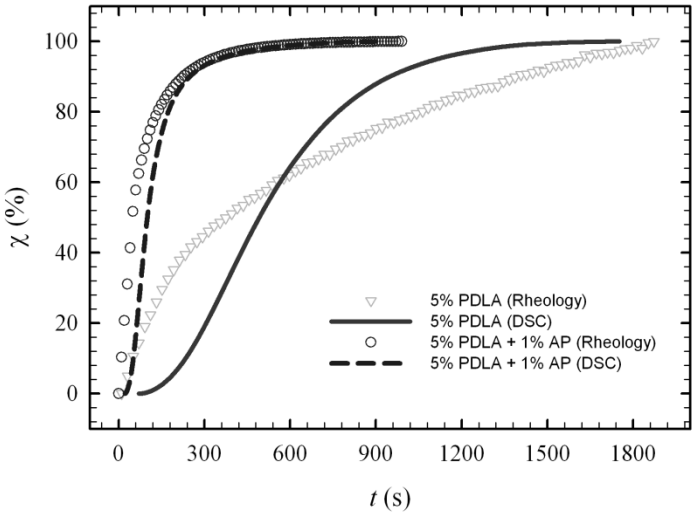

Figure 5.7 Comparison of relative crystallinity as a function of time for 5% PDLA blends without and with nucleating agent obtained by rheological and calorimetric measurements at 180 ^{o}C

5.3.3 Effect of stereocomplex on PLA rheological properties

To investigate the effect of stereocomplex on the rheological properties of PLA, frequency sweep tests were performed on samples which had already completed stereocomplexation in isothermal time sweep tests. In Figure 5.8, complex viscosity is plotted as a function of oscillation frequency for neat PLLA as well as blends with 3, 5 and 10% PDLA.

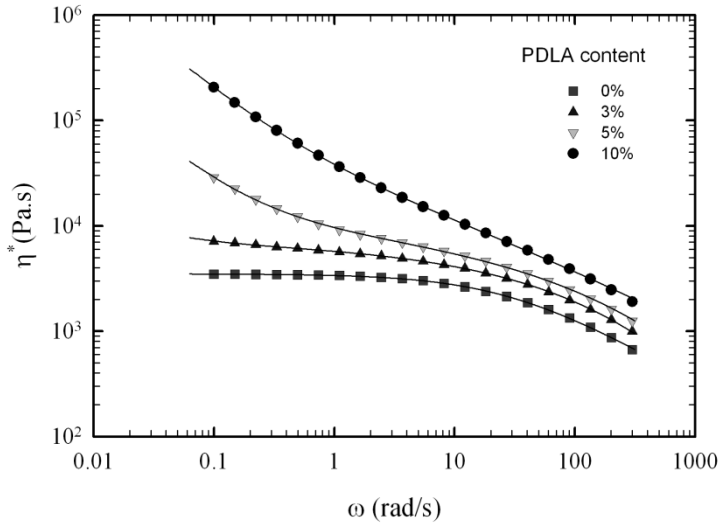

Figure 5.8 Complex viscosity vs. frequency at 180 ^{o}C for neat PLLA and blends with 3, 5 and 10% PDLA after completion of stereocomplex formation.

PLLA showed a η*- ω relationship typical of linear polymers with a Newtonian plateau at low frequencies. However as soon as PDLA was introduced to PLLA, the complex viscosity data was shifted upward, especially at lower frequency region. This behavior was more evident for 5 and 10% PDLA blends where complex viscosity does not stabilize to a viscosity plateau value at low frequency, thus showing a significant frequency dependent behavior.

To further analyze the crystalline morphology present in our blend, the viscosity increase ratio of the investigated blends was compared with predictions from a solution viscosity model. If the stereocomplex is present in the form of isolated and non-interacting "solid particulates" in an amorphous matrix of PLA, the effect of crystallinity should be similar to the effect of adding a solid filler. The experimental viscosity increase ratio was compared to prediction from Krieger-Dougherty model at the frequency of 0.1 rad/s. This model is used to predict the viscosity of concentrated suspensions:

$$\frac{\eta}{\eta_0} = \left(1 - \frac{\varphi}{\varphi_{max}}\right)^{-A\varphi_{max}}$$ **Equation 5.2**

where η is the viscosity of the suspension, η_0 is the matrix phase viscosity, φ is the volume fraction of solid particles, φ_{max} is the maximum packing equal to 0.61 and *A* is a constant equal to 3.28. The first question arising with the use of a solution model is how to calculate the volumetric solid fraction. Since one PDLA chain crystallizes with one PLLA chain, in an ideal situation for 100% stereocomplex yield, the stereocomplex content can be assumed as two times the PDLA concentration. However, it was shown previously that stereocomplexation efficiency is around 50%. Therefore, we can assume that the "solid fraction" to be used in the Krigher-Dougherty model corresponds roughly to the PDLA (weight) fraction. One obvious simplification is made in this process. It is to neglect the density difference between the crystalline and amorphous phases since the volume fraction of denser crystalline matter should be slightly smaller than the weight fraction. Comparing the Krieger-Dougherty prediction with experimental data shows that the effect of PDLA addition on the blend viscosity is substantially higher than that obtained from a suspension model. For example, at a PDLA content of 10%, the model predicted a 1.5 times increase in viscosity while experimental data showed a value of 60 times increase. This clearly confirms that the huge viscosity increase observed in presence of the stereocomplex cannot be

simply explained by the presence of non-interacting solid spherulites dispersed in a matrix of amorphous PLA. It must therefore be concluded that the solid crystalline fraction present in the PLLA matrix are not isolated crystallites or spherulites and must have some level of interaction, possibly through a network tying PLA chains at a much finer level and that can explain the dramatic viscosity increase.

Accordingly, it was assumed that the PLA melt containing stereocomplex structure had a yield stress to describe the significant viscosity increase at low frequencies. Equation 5.3 which is the Carreau-Yasuda model with an extra term accounting for the yield stress was employed to fit the complex viscosity data.

$$|\eta^*(\omega)| = \frac{\sigma_0}{\omega} + \eta_0[1 + (\lambda\omega)^a]^{\frac{(n-1)}{a}} \qquad \textbf{Equation 5.3}$$

where η^* is the complex viscosity, σ_0 is the yield stress, ω is the frequency, η_0 is the zero-shear viscosity, λ is the characteristic relaxation time, a is the Yasuda parameter and n is the shear thinning index. Solid lines presented in Figure 5.8 represent the predictions of Equation 5.3. As it is clear from the figure, Equation 5.3 predicts very well the complex viscosity data. Predicted yield stress is plotted as a function of PDLA concentration in Figure 5.9. The blend with 3% PDLA had a yield stress of 12 Pa and by increasing the PDLA content to 5%, an upward trend was observed in yield stress value. Based on the presented data points, a rheological percolation was assumed at 4.5% PDLA content where the horizontal line connecting the first two points crosses the diagonal line connecting the last two points.

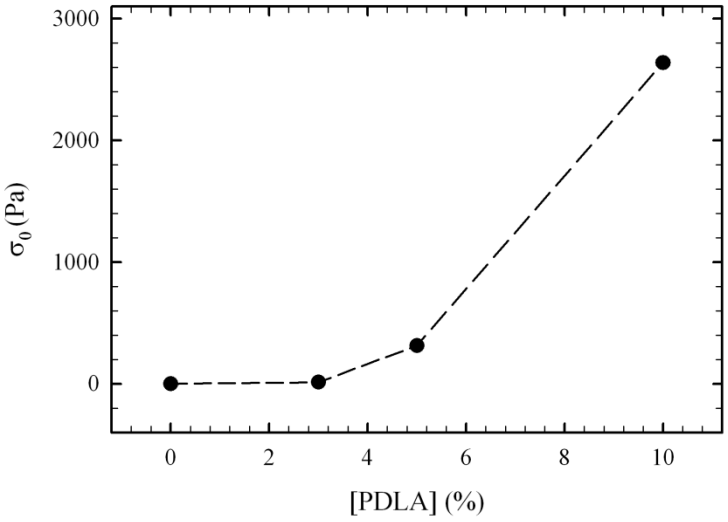

Figure 5.9 Yield stress as a function of PDLA concentration

Comparison of the material functions such as storage and loss moduli in relation to material composition is a proper approach to understand the role of the stereocomplex structure and its concentration on PLA viscoelastic behavior. Therefore, in Figure 5.10 the variation of elastic and loss moduli as a function of frequency is compared for neat PLLA and PLLA/PDLA blends with different PDLA contents after being crystallized in time sweep tests.

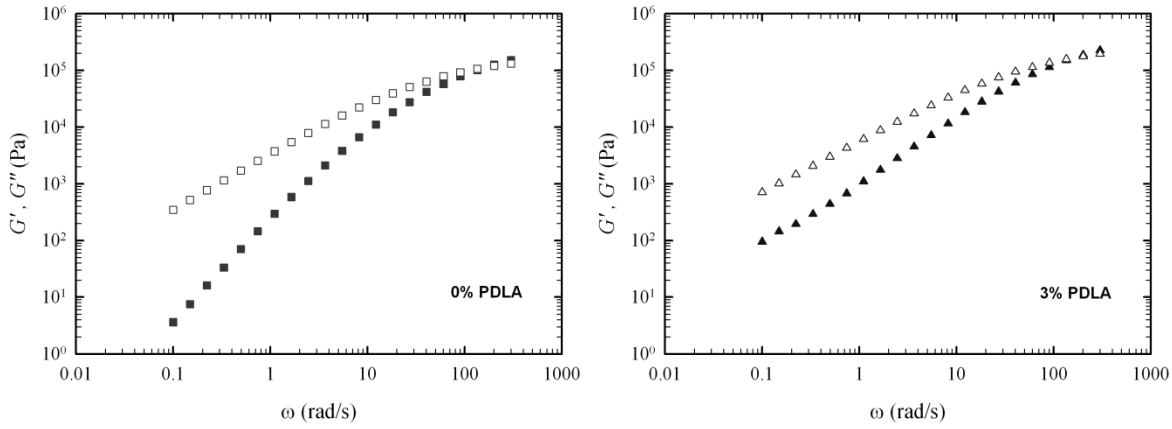

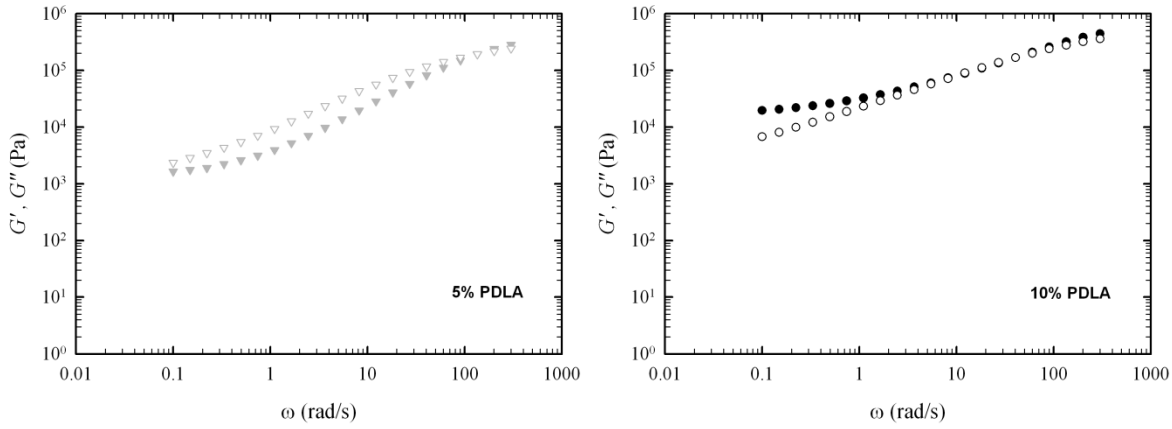

Figure 5.10 Elastic (filled symbols) and loss (open symbols) moduli as a function of frequency for neat PLLA and blends with 3, 5 and 10% PDLA

For neat PLLA a *G*'-*G*'' relationship typical of linear polymers is observed where at low frequencies *G*' is proportional to ω^2 and *G*'' is proportional to ω. When 3% of PLLA is replaced by PDLA, both dynamic moduli shift up and *G*' becomes closer to *G*''. Further addition of PDLA (5 and 10%) results in higher *G*' and *G*'' values and *G*' becomes more independent of the frequency. At 5% PDLA concentration *G*' and *G*'' get too much close to each other at 0.1 rad/s, it seems they cross at a lower frequency. In the case of 10% PDLA, the elastic nature of the material becomes more significant. *G*' is above *G*'' at frequencies below 5 and above 60 rad/s and between these frequencies *G*' and *G*'' overlay. The high increase in *G*' at low frequencies suggest that there is a structure forming in the presence of PDLA and the microstructure is changing progressively.

Cole-Cole plots are commonly used in the literature to describe the viscoelastic properties of heterogeneous polymeric systems and the transformation in their microstructure as a result of temperature variation, branching or structure formation. Therefore, these plots are presented in Figure 5.11 for better illustration of this change in microstructure. Figure 5.11-a is the plot of *G*' versus *G*'' and Figure 5.11-b η'' versus η' for the four studied blends. For the neat PLLA *G*' versus *G*'' and η'' versus η' show linear and semi-circular behavior, respectively, which is expected from the linear chain structure of the PLA. On the other hand, by increasing the PDLA content in the blends, *G*' versus *G*'' shifts upwards and deviates from neat PLA showing that the microstructure is evolving. The same conclusion can be drawn from η'' versus η' plot where addition of PDLA results in a tale in semi-circular behavior which shifts upward as the PDLA content is increased

from 3 to 10%. This deviating behavior is also observed in the composites of PLA with structuring materials such as silica and carbon nanotubes [244, 246].

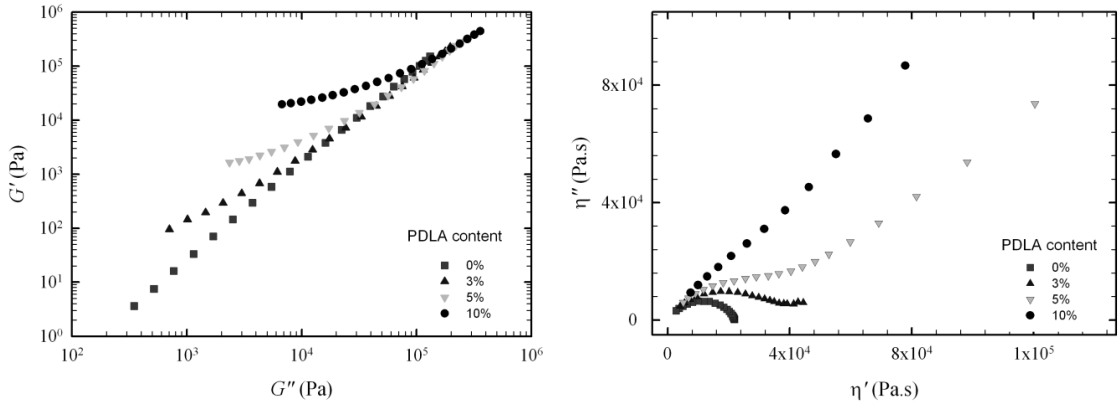

Figure 5.11 Cole-Cole plots for neat PLLA and blends with 3, 5 and 10% PDLA: (a) *G*' versus *G*'' and (b) *η*'' versus *η*'

5.4 Conclusions

Rheological monitoring of PLA stereocomplex formation kinetics at high temperatures was performed for the first time for asymmetric PLLA/PDLA blends. Crystallization half-time was in the range of 4-8 minutes showing a dependency on PDLA concentration. It was shown that the elastic modulus was more sensitive to crystallization in the early stages of the crystallization process. This was associated to interaction or network formation between the crystallites resulting in apparent molecular weight increase and branching. In addition, it was shown that crystallization kinetics can be significantly increased in the presence of an aromatic phosphonate which was employed as a nucleating agent. Frequency sweep tests performed on crystallized specimens showed a remarkable increase in viscosity and elasticity of the blend as PDLA content was increased above 3%. Complex viscosity vs. frequency data could be predicted quite well with the Carreau-Yasuda model with an extra term accounting for a yield stress. Based on the plot of the yield stress as a function of PDLA content, a rheological percolation is achieved at 4.5% PDLA content. Low frequency region data in the complex viscosity and dynamic moduli graphs as well as cole-cole plots also suggest the transformation of chain microstructure from a linear to a branched architecture in the presence of a small concentration of PDLA.

Chapter 6. Enhanced foaming behavior of poly(lactic acid) in the presence of PLA stereocomplex

6.1 Introduction

An emerging trend in the polymer area is to replace fossil based polymers with biopolymers. Among the bio-based polymers, poly(lactic acid) has attracted so much attention due to its desirable mechanical and physical properties. Foaming of PLA could be desirable for many reasons. Foaming is a possible way to reduce material consumption, produce lighter products, provide materials with good insulating properties or in biomedical field, produce porous materials with controlled bioresorbability. Unfortunately, the linear structure of PLA molecules results in low elasticity which is not favorable for the foaming process. Therefore, PLA foaming remains a challenge process with a narrow processing window. Several attempts have been made to improve PLA foamability by adding minerals such as clay and silica, inducing chain branching through multifunctional chain extenders and partial crystallization [31, 247-251]. However, PLA foaming in the presence of a minor stereocomplex phase has not been studied. In rheological measurements, it was observed that stereocomplex structure had a notable effect on PLA elasticity. Thus it is interesting to investigate the influence of stereocomplex structure on PLA foaming behavior and employ it as a processing modifier. Specifically, it is of high interest to elaborate on PLA modification by itself to produce entirely bio-based and biocompatible foams.

6.2 Experimental

6.2.1 Materials

PLLA and PDLA were the same grades as previously used in this work, provided respectively by NatureWorks LLC and Hycail. According to the producers, they contained 2% *D*- units and 0.5% *L*- units, respectively. Molecular weights of the polylactides were measured via a ViscotekTDAmax GPC apparatus (Malvern Instruments Ltd) equipped with a triple detection system. The measured weight-averaged molecular weight (M_w) and polydispersity index (M_w/M_n) were 109 kg/mol and 1.57 for PLLA and 61 kg/mol and 2.1 for PDLA.

6.2.2 Blending and sample preparation

Prior to blend preparation, PLLA and PDLA were vacuum dried at 50 ^{o}C for 2 days. Two samples were prepared via a melt-blending technique using a HAAKE MiniLab conical twin-screw micro compounder (Thermo Scientific). The first sample was neat PLLA used as a reference and the second sample was a PLLA/PDLA blend with 5% PDLA. Mixing was carried out at 180 ^{o}C for 5 minutes at a rotation speed of 100 rpm. CO_2 was used as foaming agent as it is a safe, inexpensive gas with high solubility in PLA.

For foam visualization experiments, films with approximately 200 μm thickness were prepared by hot pressing technique using a Carver laboratory press and circular specimens with a diameter of 5 mm were punched out of the films. For batch foaming experiments rectangular specimens were prepared with a thickness of 1mm.

6.2.3 Foaming visualization

Figure 6.1 is a schematic illustration of the foaming visualization setup. The setup consists of a high temperature, high pressure chamber (up to 2500 psi and 250 ^{o}C), a pressure drop rate control system with a pressure data acquisition system, a gas supply system including a gas reservoir and a syringe pump to reach desired pressure, and an optical system including an objective lens, light source and a high speed camera with a maximum speed of 120,000 fps.

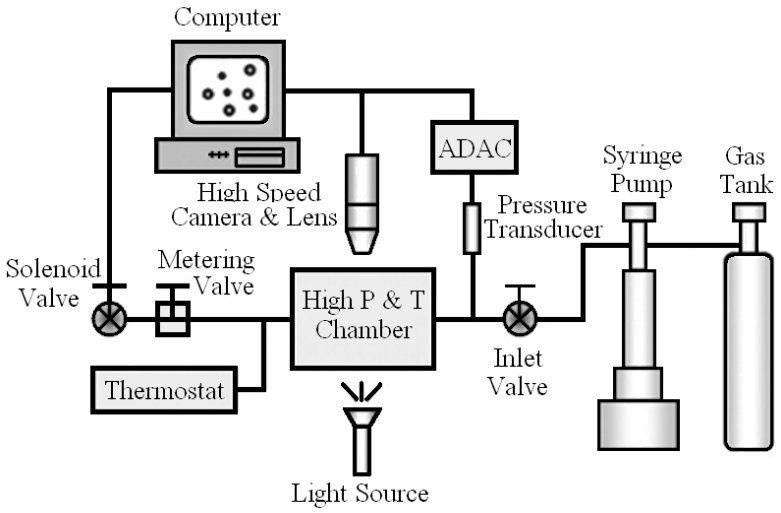

Figure 6.1 Schematic of the foaming visualization system [252]

Samples were first heated to 180 ^{o}C and remained at that temperature for 2 min to remove traces of homocrystals. Next, they were brought to foaming temperature and pressure and saturated for 30 min. Finally, pressure release valve was activated and images were captured. Figure 6.2 shows the pressure drop profile based on the chosen saturation pressures. A one second delay was intentionally given after the pressure release was triggered for better illustration of pressure profile.

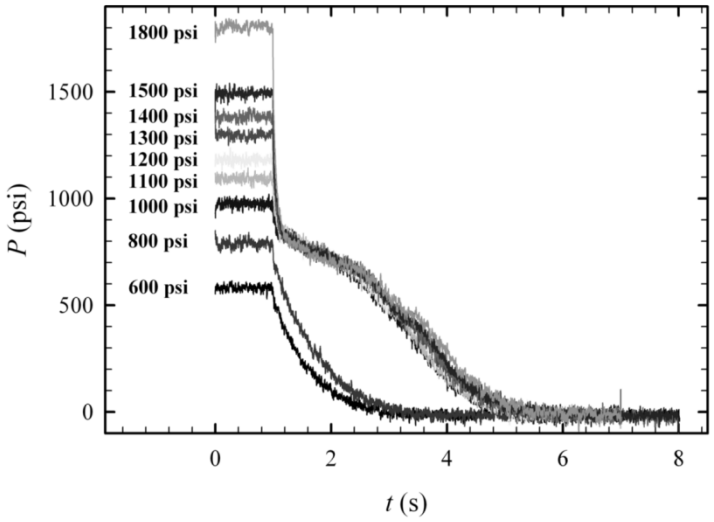

Figure 6.2 Pressure drop profile for different saturation pressures

6.2.4 Batch foaming

Batch foaming was done based on the following procedure. A high pressure PAAR autoclave was used to saturate the specimens at room temperature. Samples were placed in the autoclave and pressure was raised to saturation pressure. Based on the pressure and sample thickness, enough time was given to make sure that specimens are saturated with CO_2. Then, samples were removed from the autoclave and placed in a silicon oil bath with a pre-adjusted temperature. Finally foamed samples were quenched in a cold water bath.

6.3 Results and discussion

6.3.1 Foam visualization

A wide range of foaming temperature and pressure was investigated to compare the samples with and without stereocomplex. Pressure was changed between 600 and 1800 psi and

temperature was varied from 160 to 180 ^{o}C. Lower temperatures were avoided to eliminate the chance of homocrystallization. Figure 6.3 shows the effect of pressure on cell nucleation for neat PLLA. Tests are done at 180 ^{o}C and each image covers a 1mm × 1mm area.

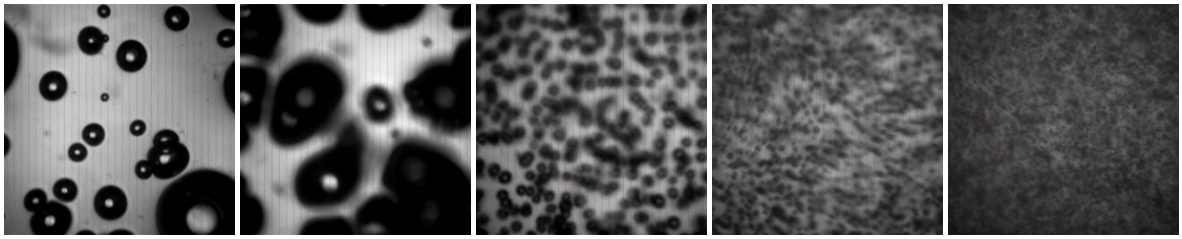

1200 psi 1300 psi 1400 psi 1500 psi 1800 psi

Figure 6.3 Effect of saturation pressure on cell density at 180 ^{o}C for neat PLLA

It is clear from this figure that by increasing saturation pressure, cell density increased significantly as the CO_2 concentration was increased in the system. Therefore to have a better comparison of the samples with and without stereocomplex a saturation pressure of 1100 psi was chosen, just above the CO_2 critical pressure (1070 psi).

In order to determine the foaming temperature for the comparison of neat PLLA with 5% PDLA blend, the latter was examined at a saturation pressure of 1100 psi at three different temperatures. Figure 6.4 shows the images obtained from these tests.

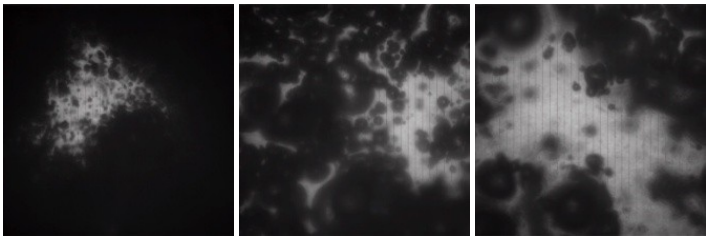

160 ^{o}C 170 ^{o}C 180 ^{o}C

Figure 6.4 Effect of foaming temperature on cell density at 1100 psi for 5% PDLA blend

According to Figure 6.4, reducing foaming pressure from 180 to 170 ^{o}C resulted in a slight increase in cell density, while going further down to 160 ^{o}C had a huge effect on cell nucleation. It seems that cell nucleation mechanism was changed by lowering temperature and a much higher cell density was obtained. Therefore it was decided to compare the two materials at this foaming temperature.

In Figure 6.5, cell nucleation and growth is compared for neat PLLA and PLLA with 5 wt.% PDLA at previously determined conditions, i.e. foaming temperature of 160 ^{o}C and saturation pressure of 1100 psi. The upper row shows images associated to PLLA and the lower row shows the images for the blend containing stereocomplex. Number above or below each image indicate the elapsed time in ms.

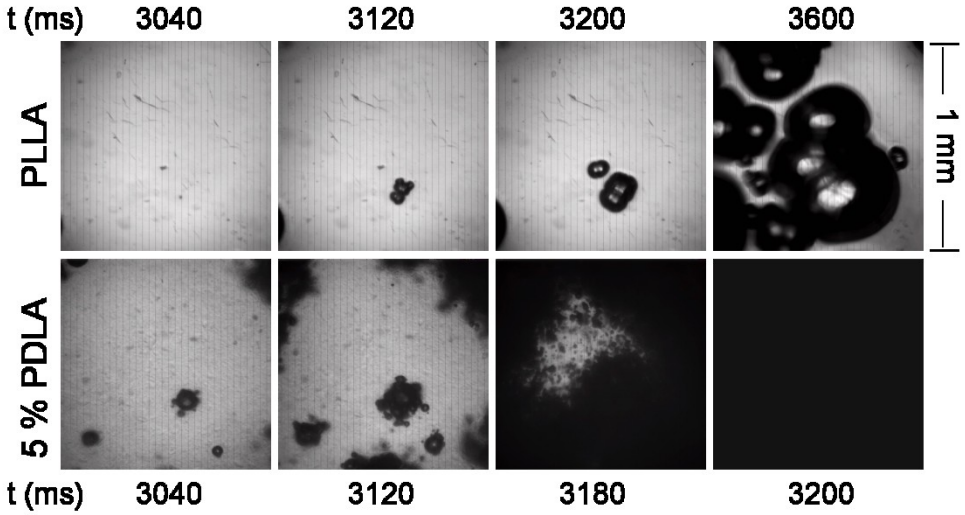

Figure 6.5 Comparison of cell nucleation and growth for neat PLLA and PLLA with 5% PDLA at 160 ^{o}C and 1100 psi

Based on the images presented in Figure 6.5, neat PLLA had a very low cell density at the specified conditions which grew to big cells after formation in about half a second. On the other hand, PLLA containing stereocomplex showed a completely different behavior. Although cell nucleation started at comparable times with neat PLLA, in about 0.2 s after, the entire surface was covered with a lot of small cells. New cells emerged in a matter of milliseconds around initial cells and propagated from all directions. This shows clearly that foaming mechanism was different between the two samples and when the stereocomplex was present in the system, due to the elasticity of the material, the stress generated in the flow field around the growing cells rapidly transferred to the neighboring areas and new cells were produced by the induced fluctuations.

6.3.2 Batch foaming

Batch foaming tests were performed to confirm the finding of foaming visualization experiments. Specimens were saturated at 800 psi and foamed at 160 ^{o}C. SEM images of the

foamed samples are compared in Figure 6.6. Neat PLLA resulted in a coarser cell morphology with a distribution of small and larger cells. On the other hand, cell morphology for PLLA with stereocomplex was more homogeneous with much finer cells in the range of few microns in diameter. This is in agreement with the results from foaming visualization experiments, showing a higher cell density and smaller cell size in the presence of PLA stereocomplex.

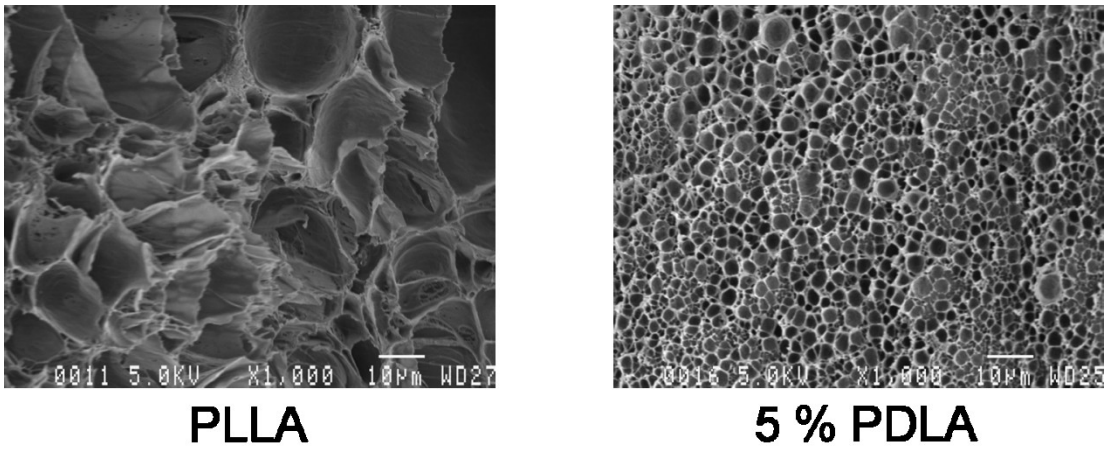

Figure 6.6 SEM images of neat PLLA and PDLA with 5% PDLA foamed in a batch foaming process.

6.4 Conclusions

Foaming visualization and batch foaming experiments were performed on neat PLLA and PLLA with 5% PDLA to investigate the effect of foaming temperature, saturation pressure, and stereocomplex structure on PLA foaming behavior. In the foaming visualization experiments, increasing the saturation pressure and decreasing the foaming temperature had positive effect on cell nucleation. Cell density increased dramatically at pressures above 1400 psi for both samples while at a pressure just above the critical pressure of CO_2, a reduction in temperature from 170 to 160 ^{o}C changed the cell nucleation mechanism to stress induced cell nucleation and propagation for blend containing PDLA. Morphology of the foamed specimen obtained in a batch foaming experiment also supported the significant difference between neat PLLA and 5%PDLA/PLLA blends, showing much finer and more homogeneous cell morphology. It is believed that the remarkable enhancement is due to the formation of the stereocomplex prior to foaming which acts as a bubble nucleating agent as well as rheology modifier.

Chapter 7. Conclusions and recommendations

7.1 Conclusions

7.1.1 (Français)

Dans cette thèse, la cinétique de formation de stéréocomplexes à l'état fondu dans des mélanges asymétriques de PLLA / PDLA avec une faible concentration de PDLA a été étudiée. Dans la première phase du projet, l'existence d'une morphologie cristalline double réseau / sphérulites a été révélée par microscopie optique et indirectement par DSC et par mesures rhéologiques. Le pic de fusion associé à des sphérulites était à des températures plus élevées par rapport à celle de la structure du réseau et les deux étaient en relation directe avec la température de cristallisation. C'est la première fois que ce comportement a été décrit dans les publications scientifiques. Il a également été montré que le demi-temps typique de formation des stéréocomplexes se situe entre 300 et 500 s et que l'efficacité de la formation était d'environ 50%. En plus, le rôle de la nucléation du stéréocomplexe sur l'homo-cristallisation du PLA a été évalué par diffraction des rayons X et par microscopie optique. Une région transcristalline à la surface de sphérulites de stéréocomplexe a été clairement démontrée et c'est aussi une contribution originale de ce travail.

Dans la deuxième phase du projet, l'objectif était d'accélérer la cinétique de formation de stéréocomplexe à températures élevées pour être en mesure de profiter de ce phénomène dans les applications réelles de mise en forme à l'état fondu. Il a été montré que le talc et le phosphonate aromatique peuvent nucléer l'homo-cristallisation du PLA ainsi que la formation de stéréocomplexe, le phosphonate aromatique étant le plus efficace. Très peu de littérature existe sur l'utilisation de phosphonate aromatique dans les polymères et ce fut le premier rapport montrant la grande efficacité de ce composé pour la formation de stéréocomplexe. En plus, il a été trouvé que même si la formation de stéréocomplexe est effectuée à une température beaucoup plus élevée que l'homo-cristallisation, la présence d'un plastifiant tel que le PEG contribue encore à réduire le temps de formation de stéréocomplexe. Au moyen de la nucléation et de la plastification, la mi-temps de formation de stéréocomplexe a été réduit d'un ordre de magnitude, ce qui montre que la formation de stéréocomplexe à l'état fondu est possible dans un délai acceptable pour les processus de mise en forme industriels. Aussi dans la deuxième phase, une investigation plus approfondie a été faite sur la morphologie cristalline double montrant que le ratio entre les deux morphologies

peut être contrôlé; des températures de cristallisation inférieures favorisent la morphologie sphérulitique par rapport à la morphologie de réseau. La plastification et la nucléation hétérogène ont affecté significativement la morphologie de stéréocomplexe. L'agent plastifiant augmente la taille de sphérulites et réduit leur nombre tandis que la tendance inverse est observée lors de l'ajout d'un agent de nucléation.

Dans la troisième étape du projet, le suivi rhéologique de formation de stéréocomplexe de PLA a révélé une dépendance de la cinétique sur la concentration de PDLA. Les courbes cinétiques obtenues par des mesures rhéologiques ont été différentes de celles obtenues par caractérisation DSC en ce sens qu'une cristallisation plus rapide a été détectée dans les étapes initiales. Ce comportement est associé à des changements dans la masse moléculaire apparente, la ramification, et formation de la structure de réseau. Les caractérisations supplémentaires des échantillons cristallisés dans les tests de balayage de fréquences ont suggéré qu'une phase mineure de stéréocomplexe peut agir comme un modificateur des propriétés rhéologiques de PLA. Une augmentation remarquable de la viscosité et de l'élasticité du mélange a été détectée lorsque la quantité de PDLA a été augmentée au-dessus de 3%. Les données de viscosité complexe et des modules dynamiques dans le domaine des fréquences faibles ainsi que des graphiques Cole-Cole suggèrent la transformation de la microstructure à chaîne linéaire vers une architecture ramifiée, en présence d'une faible concentration de PDLA.

Dans la dernière partie du projet, l'utilisation d'une phase mineure de stéréocomplexe sur le procédé de moussage de PLA a été explorée en comparant le PLLA avec un mélange 95/5 de PLLA / PDLA dans la visualisation de moussage et moussage en mode discontinu. Dans un procédé de moussage basé sur la chute rapide de pression de dioxyde de carbone d'un échantillon saturé, il a été trouvé que la densité des cellules a été augmentée en augmentant la pression de saturation et en réduisant la température de moussage. Il était intéressant de noter qu'en présence de stéréocomplexes de PLA, une réduction de la température de 170 à 160 ° C a changé le mécanisme de moussage de la nucléation homogène vers un mécanisme de nucléation et de propagation de cellules induites par la contrainte. Cette différence considérable dans le comportement de moussage des échantillons a été confirmé par les images MEB d'échantillons moussées dans un procédé discontinu, montrant une morphologie cellulaire plus homogène et plus fine dans le mélange de PLLA / PDLA. Donc, une petite quantité de PDLA peut remarquablement améliorer le moussage du PLA.

7.1.2 (English)

In this thesis, kinetics of stereocomplex formation from the melt in asymmetric PLLA/PDLA blends with low PDLA concentrations was investigated. In the first phase of the project, the existence of a dual Network / Spherulitic crystalline morphology was revealed by optical microscopy and indirectly through DSC and rheological measurements. The melting endotherm associated with the spherulites was at higher temperatures compared to that of the network structure, and both were in direct relation with the crystallisation temperature. It was the first time that this behaviour was described in the scientific literature. It was also shown that the typical half-time for completion of the overall stereocomplexation was between 300 and 500 s and that the efficiency of stereocomplex formation was around 50%. In addition, the nucleation role of the stereocomplex for PLA homocrystallization was assessed by XRD and by optical microscopy characterizations. An original transcrystalline region at the surface of stereocomplex spherulites was clearly demonstrated and is also an original contribution of this work.

In the second phase of the project, it was intended to enhance the stereocomplexation kinetics at elevated temperatures to be able to take advantage of this phenomenon in actual melt processing applications. It was shown that talc and aromatic phosphonate can nucleate PLA homocrystallization as well as stereocomplex formation, with aromatic phosphonate being the most efficient. Very little literature exists on the use of aromatic phosphonate in polymers and this was the first report showing the high efficiency of this compound for stereocomplex formation. In addition, it was found that even though stereocomplexation is carried out at a much higher temperature than the homocrystallization, the presence of a plasticizer such as PEG further lowers the stereocomplex formation time. By means of nucleation and plasticization, the half-time of stereocomplexation was reduced by an order of magnitude, showing that stereocomplex formation in the melt state is feasible within an acceptable timeframe for industrial melt processes. Also in the second phase, more investigation was done on the dual stereocomplex crystalline morphology showing that the composition ratio between the two morphologies can be controlled; lower crystallization temperatures favor the spherulitic morphology at the expense of the network one. Both plasticization and heterogeneous nucleation affected stereocomplex morphology significantly. The plasticizer increases the spherulite size and reduces their number while the opposite trend is observed when adding a nucleating agent.

In the third stage of the project, rheological monitoring of PLA stereocomplex formation revealed a dependency of kinetics on PDLA concentration. Kinetic curves obtained by rheological measurements were different from those obtained by DSC characterization in the sense that a faster crystallization was detected at the initial stages of crystallization. This behaviour is associated to the changes in apparent molecular weight, branching and a network structure formation. Further characterizations of crystallized specimen in frequency sweep tests suggested the suitability of a stereocomplex minor phase as a PLA rheological property modifier. A remarkable increase in viscosity and elasticity of the blend was detected as PDLA content increased above 3%. Low frequency region data in complex viscosity and dynamic moduli graphs as well as cole-cole plots suggest the transformation of chain microstructure from linear to branched architecture in the presence of a small concentration of PDLA.

In the final section of the project, the use of a stereocomplex minor phase on the PLA foaming process was explored by comparing neat PLLA with a 95/5 PLLA/PDLA blend in foaming visualization and batch foaming experiments. In a foaming process based on rapid pressure drop of a carbon dioxide saturated specimen, it was found that cell density was increased by increasing saturation pressure and reducing foaming temperature. Interestingly, in the presence of the PLA stereocomplex, a reduction in temperature from 170 to 160 ^{o}C changed the cell nucleation mechanism from a homogeneous mechanism to a stress induced cell nucleation and propagation. This considerable difference in the foaming behavior of the two specimens was confirmed by SEM images of samples foamed in a batch process, showing much finer and more homogeneous cell morphology in PLLA/PDLA blend. Thus a small amount of PDLA could remarkably enhance PLA foaming.

7.2 Recommendations

The following topics are suggested for further research:

1. *Stereocomplex formation in rapid expansion of supercritical solutions (RESS) continuous process:* Based on the literature it is known that the challenge in stereocomplex formation is kinetics rather than thermodynamics and there is a competition between homocrystallization and stereocomplexation. It was also shown that using organic solvents for increasing the chain mobility can help to increase the ratio of stereocomplex over homocrystals. Besides, it was found that the presence of plasticizer enhanced the

kinetics of stereocomplex formation. Thus, it is desired to maximize the chain mobility throughout stereocomplex formation. RESS process is a possible method. It is an interesting process to produce polymer micro-particles [253]. Especially, employing CO_2 is an interesting choice due to its mild supercritical conditions leading to low operating temperatures and pressures. Furthermore, using an environment friendly gas instead of organic solvents is another advantage of CO_2. On the other hand, CO_2 has illustrated plasticization effect in PLA crystallization. Putting these facts together, one can assume that using RESS is a potential solution to produce rapidly and efficiently stereocomplexed PLA in a continuous way. Furthermore, the final product shape which is a powder with micron size particles is suitable for other applications. For example it might be a nucleating agent for PLA homocrystallization and stereocomplex formation in the melt state as a high concentration source of pre-crystallized stereocomplex.

2. *Improvement of PLA foaming behavior in the presence of PLA stereocomplex:* Some preliminary experiments has been done to investigate PLA foaming behavior in the presence of stereocomplex. Initial stage of the foaming process, i.e. cell nucleation and growth was recorded via a high speed camera. Accordingly, stereocomplex structure was potent to increase cell density by stress induced nucleation. Batch foaming experiments also supported the significant positive influence of stereocomplex on final foam morphology. Therefore, PLA foaming in the presence of stereocomplex needs to be explored in more details.
3. *Effect of shear and extensional flow fields on PLA stereocomplex formation:* It is known that shear and elongational flow have influence over crystallization of polymers. Various reports exist on this subject. However, PLA stereocomplex formation is a new topic that has not be systematically investigated. As for other slowly crystallizing polyesters, strain induced crystallization could be a way to efficiently produce materials with high crystalline content. It is highly recommended that stereocomplex formation is explored in shear and elongational flow fields as it is directly related to the kinetics of crystallization. Potential applications include stereocomplex formation in injection molding, fiber spinning, foaming and extrusion processes.

References

1. **Auras, R., Harte, B., and Selke, S., *An overview of polylactides as packaging materials.* Macromolecular Bioscience, 2004. 4: p. 835-864.**
2. **Gupta, A.P. and Kumar, V., *New emerging trends in synthetic biodegradable polymers - Polylactide: A critique.* European Polymer Journal, 2007. 43: p. 4053-4074.**
3. **Madhavan Nampoothiri, K., Nair, N.R., and John, R.P., *An overview of the recent developments in polylactide (PLA) research.* Bioresource Technology, 2010. 101: p. 8493-8501.**
4. **Rasal, R.M., Janorkar, A.V., and Hirt, D.E., *Poly(lactic acid) modifications.* Progress in Polymer Science (Oxford), 2010. 35: p. 338-356.**
5. **Liu, H. and Zhang, J., *Research progress in toughening modification of poly(lactic acid).* Journal of Polymer Science, Part B: Polymer Physics, 2011. 49: p. 1051-1083.**
6. **Saeidlou, S., Huneault, M.A., Li, H., and Park, C.B., *Poly(lactic acid) crystallization.* Progress in Polymer Science, 2012. 37: p. 1657-1677.**
7. **Ulery, B.D., Nair, L.S., and Laurencin, C.T., *Biomedical applications of biodegradable polymers.* Journal of Polymer Science, Part B: Polymer Physics, 2011. 49: p. 832-864.**
8. **Lim, L.T., Auras, R., and Rubino, M., *Processing technologies for poly(lactic acid).* Progress in Polymer Science (Oxford), 2008. 33: p. 820-852.**
9. **Gupta, B., Revagade, N., and Hilborn, J., *Poly(lactic acid) fiber: An overview.* Progress in Polymer Science (Oxford), 2007. 32: p. 455-482.**
10. **Ikada, Y., Jamshidi, K., Tsuji, H., and Hyon, S.H., *Stereocomplex formation between enantiomeric poly(lactides).* Macromolecules, 1987. 20: p. 904-906.**
11. **Lasprilla, A.J.R., Martinez, G.A.R., Lunelli, B.H., Jardini, A.L., and Filho, R.M., *Poly-lactic acid synthesis for application in biomedical devices - A review.* Biotechnology Advances, 2012. 30: p. 321-328.**
12. **Harris, A.M. and Lee, E.C., *Improving mechanical performance of injection molded PLA by controlling crystallinity.* Journal of Applied Polymer Science, 2008. 107: p. 2246-2255.**
13. **Perego, G., Cella, G.D., and Bastioli, C., *Effect of molecular weight and crystallinity on poly(lactic acid) mechanical properties.* Journal of Applied Polymer Science, 1996. 59: p. 37-43.**
14. **Li, S. and McCarthy, S., *Influence of crystallinity and stereochemistry on the enzymatic degradation of poly(lactide)s.* Macromolecules, 1999. 32: p. 4454-4456.**
15. **Drieskens, M., Peeters, R., Mullens, J., Franco, D., Iemstra, P.J., and Hristova-Bogaerds, D.G., *Structure versus properties relationship of poly(lactic acid). I. effect of crystallinity on barrier properties.* Journal of Polymer Science, Part B: Polymer Physics, 2009. 47: p. 2247-2258.**
16. **Garlotta, D., *A literature review of poly(lactic acid).* Journal of Polymers and the Environment, 2001. 9: p. 63-84.**
17. **Sodergard, A. and Stolt, M., *Properties of lactic acid based polymers and their correlation with composition.* Progress in Polymer Science (Oxford), 2002. 27: p. 1123-1163.**
18. **Mehta, R., Kumar, V., Bhunia, H., and Upadhyay, S.N., *Synthesis of poly(lactic acid): A review.* Journal of Macromolecular Science - Polymer Reviews, 2005. 45: p. 325-349.**
19. **Chabot, F., Vert, M., Chapelle, S., and Granger, P., *CONFIGURATIONAL STRUCTURES OF LACTIC ACID STEREOCOPOLYMERS AS DETERMINED BY 13C-{1H} n.m.r.* Polymer, 1983. 24: p. 53-59.**
20. **Tsuji, H. and Ikada, Y., *Stereocomplex formation between enantiomeric poly(lactic acid)s. X. Binary blends from poly(D-lactide-co-glycolide) and poly(L-lactide-co-glycolide).* Journal of Applied Polymer Science, 1994. 53: p. 1061-1071.**
21. **Wisniewski, M., Borgne, A.L., and Spassky, N., *Synthesis and properties of (D)- and (L)-lactide stereocopolymers using the system achiral Schiff's base/aluminium methoxide as initiator.* Macromolecular Chemistry and Physics, 1997. 198: p. 1227-1238.**
22. **Sarasua, J.-R., Prud'homme, R.E., Wisniewski, M., Le Borgne, A., and Spassky, N., *Crystallization and melting behavior of polylactides.* Macromolecules, 1998. 31: p. 3895-3905.**
23. **Inkinen, S., Hakkarainen, M., Albertsson, A.-C., and Sodergard, A., *From lactic acid to poly(lactic acid) (PLA): Characterization and analysis of PLA and Its precursors.* Biomacromolecules, 2011. 12: p. 523-532.**
24. **Tsuji, H. and Ikada, Y., *Crystallization from the melt of poly(lactide)s with different optical purities and their blends.* Macromolecular Chemistry and Physics, 1996. 197: p. 3483-3499.**

25. **Kricheldorf, H.R. and Serra, A., *POLYLACTONES - 6. INFLUENCE OF VARIOUS METAL SALTS ON THE OPTICAL PURITY OF POLY(L-LACTIDE).* Polymer Bulletin, 1985. 14: p. 497-502.**
26. **Spinu, M., *Star-shaped hydroxyacid polymers*, 1993, E. I. Du Pont de Nemours and Company (Wilmington, DE): United States, 5225521.**
27. **Kim, S.H., Han, Y.-K., Ahn, K.-D., Kim, Y.H., and Chang, T., *Preparation of star-shaped polylactide with pentaerythritol and stannous octoate.* Die Makromolekulare Chemie, 1993. 194: p. 3229-3236.**
28. **Korhonen, H., Helminen, A., and Seppala, J.V., *Synthesis of polylactides in the presence of co-initiators with different numbers of hydroxyl groups.* Polymer, 2001. 42: p. 7541-7549.**
29. **Pitet, L.M., Hait, S.B., Lanyk, T.J., and Knauss, D.M., *Linear and branched architectures from the polymerization of lactide with glycidol.* Macromolecules, 2007. 40: p. 2327-2334.**
30. **Wolf, F.K. and Frey, H., *Inimer-Promoted synthesis of branched and hyperbranched polylactide copolymers.* Macromolecules, 2009. 42: p. 9443-9456.**
31. **Mihai, M., Huneault, M.A., and Favis, B.D., *Rheology and extrusion foaming of chain-branched poly(lactic acid).* Polymer Engineering and Science, 2010. 50: p. 629-642.**
32. **Lehermeier, H.J. and Dorgan, J.R., *Melt rheology of poly(lactic acid): Consequences of blending chain architectures.* Polymer Engineering and Science, 2001. 41: p. 2172-2184.**
33. **Sodergard, A. and Nasman, J.H., *Stabilization of poly(L-lactide) in the melt.* Polymer Degradation and Stability, 1994. 46: p. 25-30.**
34. **Soedergaard, A., Niemi, M., Selin, J.-F., and Naesman, J.H., *Changes in Peroxide Melt-Modified Poly(L-lactide).* Industrial & Engineering Chemistry Research, 1995. 34: p. 1203-1207.**
35. **De Santis, P. and Kovacs, A.J., *Molecular conformation of poly(S-lactic acid).* Biopolymers, 1968. 6: p. 299-306.**
36. **Kalb, B. and Pennings, A.J., *GENERAL CRYSTALLIZATION BEHAVIOUR OF POLY(L-LACTIC ACID).* Polymer, 1980. 21: p. 607-612.**
37. **Hoogsteen, W., Postema, A.R., Pennings, A.J., Brinke, G.t., and Zugenmaier, P., *Crystal structure, conformation, and morphology of solution-spun poly(L-lactide) fibers.* Macromolecules, 1990. 23: p. 634-642.**
38. **Kobayashi, J., Asahi, T., Ichiki, M., Oikawa, A., Suzuki, H., Watanabe, T., Fukada, E., and Shikinami, Y., *Structural and optical properties of poly lactic acids.* Journal of Applied Physics, 1995. 77: p. 2957-2973.**
39. **Zhang, J., Duan, Y., Sato, H., Tsuji, H., Noda, I., Yan, S., and Ozaki, Y., *Crystal modifications and thermal behavior of poly(L-lactic acid) revealed by infrared spectroscopy.* Macromolecules, 2005. 38: p. 8012-8021.**
40. **Kawai, T., Rahman, N., Matsuba, G., Nishida, K., Kanaya, T., Nakano, M., Okamoto, H., Kawada, J., Usuki, A., Honma, N., Nakajima, K., and Matsuda, M., *Crystallization and Melting Behavior of Poly (l-lactic Acid).* Macromolecules, 2007. 40: p. 9463-9469.**
41. **Zhang, J., Tashiro, K., Tsuji, H., and Domb, A.J., *Disorder-to-order phase transition and multiple melting behavior of poly(L-lactide) investigated by simultaneous measurements of WAXD and DSC.* Macromolecules, 2008. 41: p. 1352-1357.**
42. **Cocca, M., Lorenzo, M.L.D., Malinconico, M., and Frezza, V., *Influence of crystal polymorphism on mechanical and barrier properties of poly(l-lactic acid).* European Polymer Journal, 2011. 47: p. 1073-1080.**
43. **Eling, B., Gogolewski, S., and Pennings, A.J., *BIODEGRADABLE MATERIALS OF POLY(L-LACTIC ACID) - 1. MELT-SPUN AND SOLUTION-SPUN FIBRES.* Polymer, 1982. 23: p. 1587-1593.**
44. **Puiggali, J., Ikada, Y., Tsuji, H., Cartier, L., Okihara, T., and Lotz, B., *The frustrated structure of poly(L-lactide).* Polymer, 2000. 41: p. 8921-8930.**
45. **Cartier, L., Okihara, T., Ikada, Y., Tsuji, H., Puiggali, J., and Lotz, B., *Epitaxial crystallization and crystalline polymorphism of polylactides.* Polymer, 2000. 41: p. 8909-8919.**
46. **Okihara, T., Tsuji, M., Kawaguchi, A., Katayama, K.-i., Tsuji, H., Hyon, S.-H., and Ikada, Y., *Crystal structure of stereocomplex of poly(L-lactide) and poly(D-lactide).* Journal of Macromolecular Science - Physics, 1991. B30: p. 119-140.**
47. **Cartier, L., Okihara, T., and Lotz, B., *Triangular polymer single crystals: stereocomplexes, twins, and frustrated structures.* Macromolecules, 1997. 30: p. 6313-6322.**
48. **Abe, H., Kikkawa, Y., Inoue, Y., and Doi, Y., *Morphological and Kinetic Analyses of Regime Transition for Poly[(S)-lactide] Crystal Growth.* Biomacromolecules, 2001. 2: p. 1007-1014.**

49. **Dorgan, J.R., Janzen, J., Clayton, M.P., Hait, S.B., and Knauss, D.M., *Melt rheology of variable L-content poly(lactic acid).* Journal of Rheology, 2005. 49: p. 607-619.**
50. **Jamshidi, K., Hyon, S.H., and Ikada, Y., *Thermal characterization of polylactides.* Polymer, 1988. 29: p. 2229-2234.**
51. **Witzke, D.R., *Introduction to properties, engineering, and prospects of polylactide polymers*, 1997, Michigan State University: Michigan.**
52. **Zhao, Y.-L., Cai, Q., Jiang, J., Shuai, X.-T., Bei, J.-Z., Chen, C.-F., and Xi, F., *Synthesis and thermal properties of novel star-shaped poly(L-lactide)s with starburst PAMAM-OH dendrimer macroinitiator.* Polymer, 2002. 43: p. 5819-5825.**
53. **Nofar, M., Zhu, W., Park, C.B., and Randall, J., *Crystallization kinetics of linear and long-chain-branched polylactide.* Industrial and Engineering Chemistry Research, 2011. 50: p. 13789-13798.**
54. **Kolstad, J.J., *Crystallization kinetics of poly(L-lactide-co-meso-lactide).* Journal of Applied Polymer Science, 1996. 62: p. 1079-1091.**
55. **Bigg, D.M., *Polylactide copolymers: Effect of copolymer ratio and end capping on their properties.* Advances in Polymer Technology, 2005. 24: p. 69-82.**
56. **Hartmann, M., *High molecular weight polylactic acid polymers*, in *Biopolymers from renewable resources*, D. Kaplan, Editor 1998, Springer-Verlag: Berlin/Heidelberg. p. 367–411.**
57. **Hoffman, J.D. and Weeks, J.J., *Melting process and equilibrium melting temperature of polychlorotrifluoroethylene.* Journal of Research of the National Institute of Standards and Technology, 1962. 66A: p. 13-28.**
58. **Baur, V.H., *Einfluß der sequenzlängenverteilung auf das schmelz-ende von copolymeren.* Die Makromolekulare Chemie, 1966. 98: p. 297-301.**
59. **Flory, P.J., *Theory of crystallization in copolymers.* Faraday Society -- Transactions, 1955. 51: p. 848-857.**
60. **Huang, J., Lisowski, M.S., Runt, J., Hall, E.S., Kean, R.T., Buehler, N., and Lin, J.S., *Crystallization and microstructure of poly(L-lactide-co-meso-lactide) copolymers.* Macromolecules, 1998. 31: p. 2593-2599.**
61. **Baratian, S., Hall, E.S., Lin, J.S., Xu, R., and Runt, J., *Crystallization and solid-state structure of random polylactide copolymers: Poly(L-lactide-co-D-lactide)s.* Macromolecules, 2001. 34: p. 4857-4864.**
62. **Vasanthakumari, R. and Pennings, A.J., *Crystallization kinetics of Poly(L-lactic acid).* Polymer, 1983. 24: p. 175-178.**
63. **Fischer, E.W., Sterzel, H.J., and Wegner, G., *Investigation of the structure of solution grown crystals of lactide copolymers by means of chemical reactions.* Colloid & Polymer Science, 1973. 251: p. 980-990.**
64. **Tsuji, H. and Ikada, Y., *Blends of isotactic and atactic poly(lactide). I. Effects of mixing ratio of isomers on crystallization of blends from melt.* Journal of Applied Polymer Science, 1995. 58: p. 1793-1802.**
65. **Iannace, S. and Nicolais, L., *Isothermal crystallization and chain mobility of poly(L-lactide).* Journal of Applied Polymer Science, 1997. 64: p. 911-919.**
66. **Tsuji, H. and Ikada, Y., *Properties and morphologies of poly(L-lactide): 1. Annealing condition effects on properties and morphologies of poly(L-lactide).* Polymer, 1995. 36: p. 2709-2716.**
67. **Tsuji, H. and Ikada, Y., *Stereocomplex formation between enantiomeric poly(lactic acid)s. 9. Stereocomplexation from the melt.* Macromolecules, 1993. 26: p. 6918-6926.**
68. **Miyata, T. and Masuko, T., *Crystallization behaviour of poly(L-lactide).* Polymer, 1998. 39: p. 5515-5521.**
69. **Abe, H., Harigaya, M., Kikkawa, Y., Tsuge, T., and Doi, Y., *Crystal growth and solid-state structure of poly(lactide) stereocopolymers.* Biomacromolecules, 2005. 6: p. 457-467.**
70. **Tsuji, H. and Ikada, Y., *Stereocomplex formation between enantiomeric poly(lactic acid)s. 6. Binary blends from copolymers.* Macromolecules, 1992. 25: p. 5719-5723.**
71. **Ahmed, J., Zhang, J.X., Song, Z., and Varshney, S.K. *Thermal properties of polylactides: Effect of molecular mass and nature of lactide isomer*. 2009. Van Godewijckstraat 30, Dordrecht, 3311 GZ, Netherlands: Springer Netherlands.**
72. **Pan, P., Kai, W., Zhu, B., Dong, T., and Inoue, Y., *Polymorphous Crystallization and Multiple Melting Behavior of Poly(l-lactide): Molecular Weight Dependence.* Macromolecules, 2007. 40: p. 6898-6905.**
73. **Yasuniwa, M., Sakamo, K., Ono, Y., and Kawahara, W., *Melting behavior of poly(l-lactic acid): X-ray and DSC analyses of the melting process.* Polymer, 2008. 49: p. 1943-1951.**

74. **Kim, E.S., Kim, B.C., and Kim, S.H., *Structural Effect of Linear and Star-Shaped Poly(L-lactic acid) on Physical Properties.* Journal of Polymer Science, Part B: Polymer Physics, 2004. 42: p. 939-946.**
75. **Tsuji, H. and Ikada, Y., *Stereocomplex formation between enantiomeric poly(lactic acid)s. XI. Mechanical properties and morphology of solution-cast films.* Polymer, 1999. 40: p. 6699-6708.**
76. **Li, H. and Huneault, M.A., *Effect of nucleation and plasticization on the crystallization of poly(lactic acid).* Polymer, 2007. 48: p. 6855-6866.**
77. **Hu, Y., Hu, Y.S., Topolkaraev, V., Hiltner, A., and Baer, E., *Crystallization and phase separation in blends of high stereoregular poly(lactide) with poly(ethylene glycol).* Polymer, 2003. 44: p. 5681-5689.**
78. **Kulinski, Z. and Piorkowska, E., *Crystallization, structure and properties of plasticized poly(L-lactide).* Polymer, 2005. 46: p. 10290-10300.**
79. **Tsuji, H., Takai, H., and Saha, S.K., *Isothermal and non-isothermal crystallization behavior of poly(l-lactic acid): Effects of stereocomplex as nucleating agent.* Polymer, 2006. 47: p. 3826-3837.**
80. **Schmidt, S.C. and Hillmyer, M.A., *Polylactide Stereocomplex Crystallites as Nucleating Agents for Isotactic Polylactide.* Journal of Polymer Science, Part B: Polymer Physics, 2001. 39: p. 300-313.**
81. **Kikkawa, Y., Abe, H., Fujita, M., Iwata, T., Inoue, Y., and Doi, Y., *Crystal Growth in Poly(L-lactide) Thin Film Revealed by in situ Atomic Force Microscopy.* Macromolecular Chemistry and Physics, 2003. 204: p. 1822-1831.**
82. **Yuryev, Y., Wood-Adams, P., Heuzey, M.-C., Dubois, C., and Brisson, J., *Crystallization of polylactide films: An atomic force microscopy study of the effects of temperature and blending.* Polymer, 2008. 49: p. 2306-2320.**
83. **Yasuniwa, M., Tsubakihara, S., Iura, K., Ono, Y., Dan, Y., and Takahashi, K., *Crystallization behavior of poly(l-lactic acid).* Polymer, 2006. 47: p. 7554-7563.**
84. **Li, X.-J., Li, Z.-M., Zhong, G.-J., and Li, L.-B., *Steady-shear-induced isothermal crystallization of poly(L-lactide) (PLLA).* Journal of Macromolecular Science, Part B: Physics, 2008. 47: p. 511-522.**
85. **Lauritzen Jr, J.I. and Hoffman, J.D., *EXTENSION OF THEORY OF GROWTH OF CHAIN-FOLDED POLYMER CRYSTALS TO LARGE UNDERCOOLINGS.* Journal of Applied Physics, 1973. 44: p. 4340-4352.**
86. **Hoffman, J.D., Davis, T.G., and Lauritzen Jr, J.I., *The Rate of Crystallization of Linear Polymers With Chain Folding*, in *Treatise on Solid State Chemistry: Vol. 3: Crystalline and Noncrystalline Solids*, N.B. Hannay, Editor 1976, Plenum Press: New York. p. 497-614.**
87. **Di Lorenzo, M.L., *Determination of spherulite growth rates of poly(L-lactic acid) using combined isothermal and non-isothermal procedures.* Polymer, 2001. 42: p. 9441-9446.**
88. **Tsuji, H., Miyase, T., Tezuka, Y., and Saha, S.K., *Physical properties, crystallization, and spherulite growth of linear and 3-arm poly(L-lactide)s.* Biomacromolecules, 2005. 6: p. 244-254.**
89. **He, Y., Fan, Z., Wei, J., and Li, S., *Morphology and melt crystallization of poly(L-lactide) obtained by ring opening polymerization of L-lactide with zinc catalyst.* Polymer Engineering and Science, 2006. 46: p. 1583-1589.**
90. **Di Lorenzo, M.L., *Crystallization behavior of poly(l-lactic acid).* European Polymer Journal, 2005. 41: p. 569-575.**
91. **Pan, P., Zhu, B., Kai, W., Dong, T., and Inoue, Y., *Effect of crystallization temperature on crystal modifications and crystallization kinetics of poly(L-lactide).* Journal of Applied Polymer Science, 2008. 107: p. 54-62.**
92. **Tsuji, H., Sugiura, Y., Sakamoto, Y., Bouapao, L., and Itsuno, S., *Crystallization behavior of linear 1-arm and 2-arm poly(l-lactide)s: Effects of coinitiators.* Polymer, 2008. 49: p. 1385-1397.**
93. **Bouapao, L., Tsuji, H., Tashiro, K., Zhang, J., and Hanesaka, M., *Crystallization, spherulite growth, and structure of blends of crystalline and amorphous poly(lactide)s.* Polymer, 2009. 50: p. 4007-4017.**
94. **Tsuji, H., Tezuka, Y., Saha, S.K., Suzuki, M., and Itsuno, S., *Spherulite growth of l-lactide copolymers: Effects of tacticity and comonomers.* Polymer, 2005. 46: p. 4917-4927.**
95. **Hoffman, J.D., Miller, R.L., Marand, H., and Roitman, D.B., *Relationship between the lateral surface free energy and the chain structure of melt-crystallized polymers.* Macromolecules, 1992. 25: p. 2221-2229.**
96. **Tonelli, A.E. and Flory, P.J., *The Configurational Statistics of Random Poly(lactic acid) Chains. I. Experimental Results.* Macromolecules, 1969. 2: p. 225-227.**
97. **Brant, D.A., Tonelli, A.E., and Flory, P.J., *The Configurational Statistics of Random Poly(lactic acid) Chains. II. Theory.* Macromolecules, 1969. 2: p. 228-235.**

98. **Grijpma, D.W., Penning, J.P., and Pennings, A.J., *Chain entanglement, mechanical properties and drawability of poly(lactide).* Colloid and Polymer Science, 1994. 272: p. 1068-1081.**
99. **Joziasse, C.A.P., Veenstra, H., Grijpma, D.W., and Pennings, A.J., *On the chain stiffness of poly(lactide)s.* Macromolecular Chemistry and Physics, 1996. 197: p. 2219-2229.**
100. **Cooper-White, J.J. and Mackay, M.E., *Rheological properties of poly(lactides). Effect of molecular weight and temperature on the viscoelasticity of poly(l-lactic acid).* Journal of Polymer Science, Part B: Polymer Physics, 1999. 37: p. 1803-1814.**
101. **Blomqvist, J., *RIS Metropolis Monte Carlo studies of poly(L-lactic), poly(L,D-lactic) and polyglycolic acids.* Polymer, 2001. 42: p. 3515-3521.**
102. **Dorgan, J.R., Janzen, J., Knauss, D.M., Hait, S.B., Limoges, B.R., and Hutchinson, M.H., *Fundamental solution and single-chain properties of polylactides.* Journal of Polymer Science, Part B: Polymer Physics, 2005. 43: p. 3100-3111.**
103. **Zhou, W.Y., Duan, B., Wang, M., and Cheung, W.L., *Crystallization kinetics of poly(L-lactide)/carbonated hydroxyapatite nanocomposite microspheres.* Journal of Applied Polymer Science, 2009. 113: p. 4100-4115.**
104. **Shieh, Y.-T., Twu, Y.-K., Su, C.-C., Lin, R.-H., and Liu, G.-L., *Crystallization kinetics study of poly(L-lactic acid)/carbon nanotubes nanocomposites.* Journal of Polymer Science, Part B: Polymer Physics, 2010. 48: p. 983-989.**
105. **Day, M., Nawaby, A.V., and Liao, X. *A DSC study of the crystallization behaviour of polylactic acid and its nanocomposites*. 2006. Kluwer Academic Publishers.**
106. **Xiao, H.W., Li, P., Ren, X., Jiang, T., and Yeh, J.-T., *Isothermal crystallization kinetics and crystal structure of poly(lactic acid): Effect of triphenyl phosphate and talc.* Journal of Applied Polymer Science, 2010. 118: p. 3558-3569.**
107. **Urbanovici, E., Schneider, H.A., Brizzolara, D., and Cantow, H.J., *Isothermal melt crystallization kinetics of poly(L-lactic acid).* Journal of thermal analysis, 1996. 47: p. 931-939.**
108. **He, Y., Fan, Z., Hu, Y., Wu, T., Wei, J., and Li, S., *DSC analysis of isothermal melt-crystallization, glass transition and melting behavior of poly(l-lactide) with different molecular weights.* European Polymer Journal, 2007. 43: p. 4431-4439.**
109. **Pantani, R., De Santis, F., Sorrentino, A., De Maio, F., and Titomanlio, G., *Crystallization kinetics of virgin and processed poly(lactic acid).* Polymer Degradation and Stability, 2010. 95: p. 1148-1159.**
110. **Pei, A., Zhou, Q., and Berglund, L.A., *Functionalized cellulose nanocrystals as biobased nucleation agents in poly(l-lactide) (PLLA) - Crystallization and mechanical property effects.* Composites Science and Technology, 2010. 70: p. 815-821.**
111. **Wen, L. and Xin, Z., *Effect of a novel nucleating agent on isothermal crystallization of poly(L-lactic acid).* Chinese Journal of Chemical Engineering, 2010. 18: p. 899-904.**
112. **Li, Y., Chen, C., Li, J., and Sun, X.S., *Isothermal crystallization and melting behaviors of bionanocomposites from poly(lactic acid) and TiO2 nanowires.* Journal of Applied Polymer Science, 2012. 124: p. 2968-2977.**
113. **Cai, Y., Yan, S., Yin, J., Fan, Y., and Chen, X., *Crystallization behavior of biodegradable poly(L-lactic acid) filled with a powerful nucleating agent: N,N-Bis(benzoyl) suberic acid dihydrazide.* Journal of Applied Polymer Science, 2011. 121: p. 1408-1416.**
114. **De Santis, F., Pantani, R., and Titomanlio, G., *Nucleation and crystallization kinetics of poly(lactic acid).* Thermochimica Acta, 2011. 522: p. 128-134.**
115. **Legras, R., Mercier, J.P., and Nield, E., *Polymer crystallization by chemical nucleation.* Nature, 1983. 304: p. 432-434.**
116. **Legras, R., Bailly, C., Daumerie, M., Dekoninck, J.M., Mercier, J.P., Zichy, V., and Nield, E., *CHEMICAL NUCLEATION, A NEW CONCEPT APPLIED TO THE MECHANISM OF ACTION OF ORGANIC ACID SALTS ON THE CRYSTALLIZATION OF POLYETHYLENE TEREPHTHALATE AND BISPHENOL-A POLYCARBONATE.* Polymer, 1984. 25: p. 835-844.**
117. **Dekoninck, J.M., Legras, R., and Mercier, J.P., *Nucleation of poly(ethylene terephthalate) by sodium compounds: a unique mechanism.* Polymer, 1989. 30: p. 910-913.**
118. **Garcia, D., *HETEROGENEOUS NUCLEATION OF POLY(ETHYLENE TEREPHTHALATE).* Journal of polymer science. Part A-2, Polymer physics, 1984. 22: p. 2063-2072.**
119. **Zhang, J., *Effective nucleating chemical agents for the crystallization of poly(trimethylene terephthalate).* Journal of Applied Polymer Science, 2004. 93: p. 590-601.**

120. **Penco, M., Spagnoli, G., Peroni, I., Rahman, M.A., Frediani, M., Oberhauser, W., and Lazzeri, A.** ***Effect of nucleating agents on the molar mass distribution and its correlation with the isothermal crystallization behavior of poly(L -lactic acid)*****. in** ***Contributions from the 5th International Conference on Times of Polymers (TOP) and Composites, Ischia, Italy, June 20-23, 2010.*** **2011. P.O.Box 18667, Newark, NJ 07191-8667, United States: John Wiley and Sons Inc.**
121. **Urayama, H., Kanamori, T., Fukushima, K., and Kimura, Y.,** ***Controlled crystal nucleation in the melt-crystallization of poly(L-lactide) and poly(L-lactide)/poly(D-lactide) stereocomplex.*** **Polymer, 2003. 44: p. 5635-5641.**
122. **Anderson, K.S. and Hillmyer, M.A.,** ***Melt preparation and nucleation efficiency of polylactide stereocomplex crystallites.*** **Polymer, 2006. 47: p. 2030-2035.**
123. **Kawamoto, N., Sakai, A., Horikoshi, T., Urushihara, T., and Tobita, E.,** ***Nucleating agent for poly(L-lactic acid) - An optimization of chemical structure of hydrazide compound for advanced nucleation ability.*** **Journal of Applied Polymer Science, 2007. 103: p. 198-203.**
124. **Ke, T. and Sun, X.,** ***Melting behavior and crystallization kinetics of starch and poly(lactic acid) composites.*** **Journal of Applied Polymer Science, 2003. 89: p. 1203-1210.**
125. **Tsuji, H., Takai, H., Fukuda, N., and Takikawa, H.,** ***Non-isothermal crystallization behavior of poly(L-lactic acid) in the presence of various additives.*** **Macromolecular Materials and Engineering, 2006. 291: p. 325-335.**
126. **Pan, P., Liang, Z., Cao, A., and Inoue, Y.,** ***Layered Metal Phosphonate Reinforced Poly(l-lactide) Composites with a Highly Enhanced Crystallization Rate.*** **ACS Applied Materials & Interfaces, 2009. 1: p. 402-411.**
127. **Ogata, N., Jimenez, G., Kawai, H., and Ogihara, T.,** ***Structure and thermal/mechanical properties of poly(l-lactide)-clay blend.*** **Journal of Polymer Science, Part B: Polymer Physics, 1997. 35: p. 389-396.**
128. **Nam, J.Y., Sinha Ray, S., and Okamoto, M.,** ***Crystallization behavior and morphology of biodegradable polylactide/layered silicate nanocomposite.*** **Macromolecules, 2003. 36: p. 7126-7131.**
129. **Ray, S.S., Yamada, K., Okamoto, M., Fujimoto, Y., Ogami, A., and Ueda, K.,** ***New polylactide/layered silicate nanocomposites. 5. Designing of materials with desired properties.*** **Polymer, 2003. 44: p. 6633-6646.**
130. **Krikorian, V. and Pochan, D.J.,** ***Unusual crystallization behavior of organoclay reinforced poly(L-lactic acid) nanocomposites.*** **Macromolecules, 2004. 37: p. 6480-6491.**
131. **Krikorian, V. and Pochan, D.J.,** ***Crystallization behavior of poly(L-lactic acid) nanocomposites: Nucleation and growth probed by infrared spectroscopy.*** **Macromolecules, 2005. 38: p. 6520-6527.**
132. **Nam, P.H., Ninomiya, N., Fujimori, A., and Masuko, T.,** ***Crystallization characteristics of intercalated poly(L-lactide)/organo- modified montmorillonite hybrids.*** **Polymer Engineering and Science, 2006. 46: p. 39-46.**
133. **Bigg, D.M.** ***Controlling the performance and rate of degradation of polylactide copolymers*****. in** ***61st Annual Technical Conference ANTEC 2003, May 4, 2003 - May 8, 2003*****. 2003. Nashville, TN, United states: Society of Plastics Engineers.**
134. **Nam, J.Y., Okamoto, M., Okamoto, H., Nakano, M., Usuki, A., and Matsuda, M.,** ***Morphology and crystallization kinetics in a mixture of low-molecular weight aliphatic amide and polylactide.*** **Polymer, 2006. 47: p. 1340-1347.**
135. **Nakajima, H., Takahashi, M., and Kimura, Y.,** ***Induced crystallization of plla in the presence of 1,3,5-benzenetricarboxylamide derivatives as nucleators: Preparation of haze-free crystalline PLLA materials.*** **Macromolecular Materials and Engineering, 2010. 295: p. 460-468.**
136. **Li, H. and Huneault, M.A.,** ***Crystallization of PLA/Thermoplastic Starch Blends.*** **International Polymer Processing, 2008. 23: p. 412-418.**
137. **Qiu, Z. and Li, Z.,** ***Effect of orotic acid on the crystallization kinetics and morphology of biodegradable poly(l-lactide) as an efficient nucleating agent.*** **Industrial and Engineering Chemistry Research, 2011. 50: p. 12299-12303.**
138. **Moon, S.-I., Jin, F., Lee, C.-J., Tsutsumi, S., and Hyon, S.-H.** ***Novel carbon nanotube/poly(L-lactic acid) nanocomposites; their modulus, thermal stability, and electrical conductivity*****. 2005. Wiley-VCH Verlag.**
139. **Shieh, Y.-T. and Liu, G.-L.,** ***Effects of carbon nanotubes on crystallization and melting behavior of poly(L-lactide) via DSC and TMDSC studies.*** **Journal of Polymer Science, Part B: Polymer Physics, 2007. 45: p. 1870-1881.**

140. **Tsuji, H., Kawashima, Y., Takikawa, H., and Tanaka, S., *Poly(l-lactide)/nano-structured carbon composites: Conductivity, thermal properties, crystallization, and biodegradation.* Polymer, 2007. 48: p. 4213-4225.**

141. **Xu, H.-S., Dai, X.J., Lamb, P.R., and Li, Z.-M., *Poly(l-lactide) crystallization induced by multiwall carbon nanotubes at very low loading.* Journal of Polymer Science, Part B: Polymer Physics, 2009. 47: p. 2341-2352.**

142. **Li, Y., Wang, Y., Liu, L., Han, L., Xiang, F., and Zhou, Z., *Crystallization improvement of poly(L-lactide) induced by functionalized multiwalled carbon nanotubes.* Journal of Polymer Science, Part B: Polymer Physics, 2009. 47: p. 326-339.**

143. **Xu, J.-Z., Chen, T., Yang, C.-L., Li, Z.-M., Mao, Y.-M., Zeng, B.-Q., and Hsiao, B.S., *Isothermal crystallization of poly(l -lactide) induced by graphene nanosheets and carbon nanotubes: A comparative study.* Macromolecules, 2010. 43: p. 5000-5008.**

144. **Brochu, S., Prud'homme, R.E., Barakat, I., and Jerome, R., *Stereocomplexation and Morphology of Polylactides.* Macromolecules, 1995. 28: p. 5230-5239.**

145. **Fillon, B., Lotz, B., Thierry, A., and Wittmann, J.C., *Self-nucleation and enhanced nucleation of polymers. Definition of a convenient calorimetric efficiency scale and evaluation of nucleating additives in isotactic polypropylene (A phase).* Journal of Polymer Science, Part B: Polymer Physics, 1993. 31: p. 1395-1405.**

146. **Yamane, H. and Sasai, K., *Effect of the addition of poly(D-lactic acid) on the thermal property of poly(L-lactic acid).* Polymer, 2003. 44: p. 2569-2575.**

147. **Rahman, N., Kawai, T., Go Matsuba, K.N., Kanaya, T., Watanabe, H., Okamoto, H., Kato, M., Usuki, A., Matsuda, M., Nakajima, K., and Honma, N., *Effect of polylactide stereocomplex on the crystallization behavior of poly(L-lactic acid).* Macromolecules, 2009. 42: p. 4739-4745.**

148. **Tsuji, H. and Tezuka, Y., *Stereocomplex formation between enantiometric poly(lactic acid)s. 12. Spherulite growth of low-molecular-weight poly(lactic acid)s from the melt.* Biomacromolecules, 2004. 5: p. 1181-1186.**

149. **Qiu, Z. and Pan, H., *Preparation, crystallization and hydrolytic degradation of biodegradable poly(l-lactide)/polyhedral oligomeric silsesquioxanes nanocomposite.* Composites Science and Technology, 2010. 70: p. 1089-1094.**

150. **Pan, H. and Qiu, Z., *Biodegradable poly(L-lactide)/polyhedral oligomeric silsesquioxanes nanocomposites: Enhanced crystallization, mechanical properties, and hydrolytic degradation.* Macromolecules, 2010. 43: p. 1499-1506.**

151. **Yu, J. and Qiu, Z., *Preparation and properties of biodegradable poly(L-lactide)/octamethyl- polyhedral oligomeric silsesquioxanes nanocomposites with enhanced crystallization rate via simple melt compounding.* ACS Applied Materials and Interfaces, 2011. 3: p. 890-897.**

152. **Yu, J. and Qiu, Z., *Effect of low octavinyl-polyhedral oligomeric silsesquioxanes loadings on the melt crystallization and morphology of biodegradable poly(l-lactide).* Thermochimica Acta, 2011. 519: p. 90-95.**

153. **Wang, S., Han, C., Bian, J., Han, L., Wang, X., and Dong, L., *Morphology, crystallization and enzymatic hydrolysis of poly(L-lactide) nucleated using layered metal phosphonates.* Polymer International, 2011. 60: p. 284-295.**

154. **Pillin, I., Montrelay, N., and Grohens, Y., *Thermo-mechanical characterization of plasticized PLA: Is the miscibility the only significant factor?* Polymer, 2006. 47: p. 4676-4682.**

155. **Martin, O. and Averous, L., *Poly(lactic acid): Plasticization and properties of biodegradable multiphase systems.* Polymer, 2001. 42: p. 6209-6219.**

156. **Kulinski, Z., Piorkowska, E., Gadzinowska, K., and Stasiak, M., *Plasticization of poly(L-lactide) with poly(propylene glycol).* Biomacromolecules, 2006. 7: p. 2128-2135.**

157. **Sungsanit, K., Kao, N., and Bhattacharya, S.N., *Properties of linear poly(lactic acid)/polyethylene glycol blends.* Polymer Engineering and Science, 2012. 52: p. 108-116.**

158. **Hu, Y., Rogunova, M., Topolkaraev, V., Hiltner, A., and Baer, E., *Aging of poly(lactide)/poly(ethylene glycol) blends. Part 1. Poly(lactide) with low stereoregularity.* Polymer, 2003. 44: p. 5701-5710.**

159. **Hu, Y., Hu, Y.S., Topolkaraev, V., Hiltner, A., and Baer, E., *Aging of poly(lactide)/poly(ethylene glycol) blends. Part 2. Poly(lactide) with high stereoregularity.* Polymer, 2003. 44: p. 5711-5720.**

160. **Ran, X.-H., Jia, Z.-Y., Yang, Y.-M., and Dong, L.-S., *Flexible plasticized PLA with high crystallinity obtained by controlling the annealing temperature.* E-Polymers, 2010.**

161. **Xiao, H., Lu, W., and Yeh, J.-T., *Effect of plasticizer on the crystallization behavior of poly(lactic acid).* Journal of Applied Polymer Science, 2009. 113: p. 112-121.**
162. **Yang, S.-L., Wu, Z.-H., Meng, B., and Yang, W., *The effects of dioctyl phthalate plasticization on the morphology and thermal, mechanical, and rheological properties of chemical crosslinked polylactide.* Journal of Polymer Science, Part B: Polymer Physics, 2009. 47: p. 1136-1145.**
163. **Martino, V.P., Jimenez, A., and Ruseckaite, R.A., *Processing and characterization of poly(lactic acid) films plasticized with commercial adipates.* Journal of Applied Polymer Science, 2009. 112: p. 2010-2018.**
164. **Martino, V.P., Ruseckaite, R.A., and Jimenez, A. *Thermal and mechanical characterization of plasticized poly (L-lactide-co-D,L-lactide) films for food packaging*. 2006. Kluwer Academic Publishers.**
165. **Murariu, M., Da Silva Ferreira, A., Pluta, M., Bonnaud, L., Alexandre, M., and Dubois, P., *Polylactide (PLA)-CaSO4 composites toughened with low molecular weight and polymeric ester-like plasticizers and related performances.* European Polymer Journal, 2008. 44: p. 3842-3852.**
166. **Wang, N., Zhang, X., Yu, J., and Fang, J., *Study of the properties of plasticised poly(lactic acid) with poly(1,3-butylene adipate).* Polymers and Polymer Composites, 2008. 16: p. 597-604.**
167. **Labrecque, L.V., Kumar, R.A., Dave, V., Gross, R.A., and McCarthy, S.P., *Citrate esters as plasticizers for poly(lactic acid).* Journal of Applied Polymer Science, 1997. 66: p. 1507-1513.**
168. **Ljungberg, N. and Wesslen, B., *The effects of plasticizers on the dynamic mechanical and thermal properties of poly(lactic acid).* Journal of Applied Polymer Science, 2002. 86: p. 1227-1234.**
169. **Ljungberg, N. and Wesslen, B., *Preparation and properties of plasticized poly(lactic acid) films.* Biomacromolecules, 2005. 6: p. 1789-1796.**
170. **Ljungberg, N. and Wesslen, B., *Tributyl citrate oligomers as plasticizers for poly (lactic acid): Thermo-mechanical film properties and aging.* Polymer, 2003. 44: p. 7679-7688.**
171. **Ljungberg, N. and Wesslen, B., *Thermomechanical film properties and aging of blends of poly(lactic acid) and malonate oligomers.* Journal of Applied Polymer Science, 2004. 94: p. 2140-2149.**
172. **Jacobsen, S. and Fritz, H.G., *Plasticizing polylactide - the effect of different plasticizers on the mechanical properties.* Polymer Engineering and Science, 1999. 39: p. 1303-1310.**
173. **Lai, W.-C., Liau, W.-B., and Lin, T.-T., *The effect of end groups of PEG on the crystallization behaviors of binary crystalline polymer blends PEG/PLLA.* Polymer, 2004. 45: p. 3073-3080.**
174. **Lai, W.-C., Liau, W.-B., and Yang, L.-Y., *The effect of ionic interaction on the miscibility and crystallization behaviors of polyethylene glycol/ poly(L-lactic acid) blends.* Journal of Applied Polymer Science, 2008. 110: p. 3616-3623.**
175. **Piorkowska, E., Kulinski, Z., Galeski, A., and Masirek, R., *Plasticization of semicrystalline poly(l-lactide) with poly(propylene glycol).* Polymer, 2006. 47: p. 7178-7188.**
176. **Takada, M., Hasegawa, S., and Ohshima, M., *Crystallization kinetics of poly(L-lactide) in contact with pressurized CO2.* Polymer Engineering and Science, 2004. 44: p. 186-196.**
177. **Yu, L., Liu, H., Dean, K., and Chen, L., *Cold crystallization and postmelting crystallization of PLA plasticized by compressed carbon dioxide.* Journal of Polymer Science, Part B: Polymer Physics, 2008. 46: p. 2630-2636.**
178. **Reignier, J., Tatibouet, J., and Gendron, R., *Effect of dissolved carbon dioxide on the glass transition and crystallization of poly(lactic acid) as probed by ultrasonic measurements.* Journal of Applied Polymer Science, 2009. 112: p. 1345-1355.**
179. **Liao, X., Nawaby, A.V., and Whitfield, P.S., *Carbon dioxide-induced crystallization in poly(L-lactic acid) and its effect on foam morphologies.* Polymer International, 2010. 59: p. 1709-1718.**
180. **Mihai, M., Huneault, M.A., Favis, B.D., and Li, H., *Extrusion foaming of semi-crystalline PLA and PLA/thermoplastic starch blends.* Macromolecular Bioscience, 2007. 7: p. 907-920.**
181. **Mihai, M., Huneault, M.A., and Favis, B.D., *Crystallinity development in cellular poly(lactic acid) in the presence of supercritical carbon dioxide.* Journal of Applied Polymer Science, 2009. 113: p. 2920-2932.**
182. **Pluta, M., *Morphology and properties of polylactide modified by thermal treatment, filling with layered silicates and plasticization.* Polymer, 2004. 45: p. 8239-8251.**
183. **Ozkoc, G. and Kemaloglu, S., *Morphology, biodegradability, mechanical, and thermal properties of nanocomposite films based on PLA and plasticized PLA.* Journal of Applied Polymer Science, 2009. 114: p. 2481-2487.**

184. **Gumus, S., Ozkoc, G., and Aytac, A., *Plasticized and unplasticized PLA/organoclay nanocomposites: Short- and long-term thermal properties, morphology, and nonisothermal crystallization behavior.* Journal of Applied Polymer Science, 2012. 123: p. 2837-2848.**
185. **Li, M., Hu, D., Wang, Y., and Shen, C., *Nonisothermal crystallization kinetics of poly(lactic acid) formulations comprising talc with poly(ethylene glycol).* Polymer Engineering and Science, 2010. 50: p. 2298-2305.**
186. **Xiao, H., Yang, L., Ren, X., Jiang, T., and Yeh, J.-T., *Kinetics and crystal structure of poly(lactic acid) crystallized nonisothermally: Effect of plasticizer and nucleating agent.* Polymer Composites, 2010. 31: p. 2057-2068.**
187. **Li, Y., Wu, H., Wang, Y., Liu, L., Han, L., Wu, J., and Xiang, F., *Synergistic effects of PEG and MWCNTs on crystallization behavior of PLLA.* Journal of Polymer Science, Part B: Polymer Physics, 2010. 48: p. 520-528.**
188. **Li, X.-j., Zhong, G.-j., and Li, Z.-m., *Non-isothermal crystallization of poly(L-lactide) (PLLA) under quiescent and steady shear conditions.* Chinese Journal of Polymer Science, 2010. 28: p. 357-366.**
189. **Huang, S., Li, H., Jiang, S., Chen, X., and An, L., *Crystal structure and morphology influenced by shear effect of poly(l-lactide) and its melting behavior revealed by WAXD, DSC and in-situ POM.* Polymer, 2011. 52: p. 3478-3487.**
190. **Tsuji, H., *Poly(lactide) stereocomplexes: Formation, structure, properties, degradation, and applications.* Macromolecular Bioscience, 2005. 5: p. 569-597.**
191. **Tsuji, H., Horii, F., Nakagawa, M., Ikada, Y., Odani, H., and Kitamaru, R., *Stereocomplex formation between enantiomeric poly(lactic acid)s. 7. Phase structure of the stereocomplex crystallized from a dilute acetonitrile solution as studied by high-resolution solid-state carbon-13 NMR spectroscopy.* Macromolecules, 1992. 25: p. 4114-4118.**
192. **Tsuji, H., Horii, F., Hyon, S.-H., and Ikada, Y., *Stereocomplex formation between enantiomeric poly(lactic acid)s. 2. Stereocomplex formation in concentrated solutions.* Macromolecules, 1991. 24: p. 2719-2724.**
193. **Tsuji, H., Hyon, S.-H., and Ikada, Y., *Stereocomplex formation between enantiomeric poly(lactic acid)s. 4. Differential scanning calorimetric studies on precipitates from mixed solutions of poly(D-lactic acid) and poly(L-lactic acid).* Macromolecules, 1991. 24: p. 5657-5662.**
194. **Tsuji, H., Hyon, S.-H., and Ikada, Y., *Stereocomplex formation between enantiomeric poly(lactic acid)s. 3. Calorimetric studies on blend films cast from dilute solution.* Macromolecules, 1991. 24: p. 5651-5656.**
195. **Bouapao, L. and Tsuji, H., *Stereocomplex crystallization and spherulite growth of low molecular weight poly-(l-lactide) and poly(d-lactide) from the melt.* Macromolecular Chemistry and Physics, 2009. 210: p. 993-1002.**
196. **Masaki, D., Fukui, Y., Toyohara, K., Ikegame, M., Nagasaka, B., and Yamane, H., *Stereocomplex formation in the poly(L-lactic acid)/poly(D-lactic acid) melt blends and the melt spun fibers.* Sen-I Gakkaishi, 2008. 64: p. 212-219.**
197. **Saeidlou, S., Huneault, M.A., Li, H., and Park, C.B., *Poly(lactic acid) Crystallization.* Progress in Polymer Science, In press.**
198. **Brizzolara, D., Cantow, H.-J., Diederichs, K., Keller, E., and Domb, A.J., *Mechanism of the stereocomplex formation between enantiomeric poly(lactide)s.* Macromolecules, 1996. 29: p. 191-191.**
199. **Zhang, J., Sato, H., Tsuji, H., Noda, I., and Ozaki, Y., *Infrared spectroscopic study of CH3O=C interaction during poly(L-lactide)/Poly(D-lactide) stereocomplex formation.* Macromolecules, 2005. 38: p. 1822-1828.**
200. **He, Y., Xu, Y., Wei, J., Fan, Z., and Li, S., *Unique crystallization behavior of poly(l-lactide)/poly(d-lactide) stereocomplex depending on initial melt states.* Polymer, 2008. 49: p. 5670-5675.**
201. **Maillard, D. and Prud'homme, R.E., *Differences between crystals obtained in PLLA-rich or PDLA-rich stereocomplex mixtures.* Macromolecules, 2010. 43: p. 4006-4010.**
202. **Purnama, P. and Kim, S.H., *Stereocomplex formation of high-molecular-weight polylactide using Supercritical fluid.* Macromolecules, 2010. 43: p. 1137-1142.**
203. **Yamane, H., Sasai, K., Takano, M., and Takahashi, M., *Poly(D-lactic acid) as a rheological modifier of poly(L-lactic acid): Shear and biaxial extensional flow behavior.* Journal of Rheology, 2004. 48: p. 599-609.**

204. **Quynh, T.M., Mitomo, H., Zhao, L., and Tamada, M., *Properties of a poly(L-lactic acid)/poly(D-lactic acid) stereocomplex and the stereocomplex crosslinked with triallyl isocyanurate by irradiation.* Journal of Applied Polymer Science, 2008. 110: p. 2358-2365.**

205. **Narita, J., Katagiri, M., and Tsuji, H., *Highly enhanced nucleating effect of melt-recrystallized stereocomplex crystallites on poly(L-lactic acid) crystallization.* Macromolecular Materials and Engineering, 2011. 296: p. 887-893.**

206. **Xu, H., Teng, C., and Yu, M., *Improvements of thermal property and crystallization behavior of PLLA based multiblock copolymer by forming stereocomplex with PDLA oligomer.* Polymer, 2006. 47: p. 3922-3928.**

207. **Wang, X. and Prud'homme, R.E., *Differences between stereocomplex spherulites obtained in equimolar and non-equimolar poly(L -lactide)/Poly(D -lactide) blends.* Macromolecular Chemistry and Physics, 2011. 212: p. 691-698.**

208. **Han, C.D., *Rheology of Particulate-Filled Polymers, Nanocomposites, and Fiber-Reinforced Thermoplastic Composites*, in *Rheology and Processing of Polymeric Materials, Volume 1 - Polymer Rheology*2007, Oxford University Press. p. 547-622.**

209. **Fambri, L., Pegoretti, A., Fenner, R., Incardona, S.D., and Migliaresi, C., *Biodegradable fibres of poly(L-lactic acid) produced by melt spinning.* Polymer, 1997. 38: p. 79-85.**

210. **Mezghani, K. and Spruiell, J.E., *High speed melt spinning of poly(L-lactic acid) filaments.* Journal of Polymer Science, Part B: Polymer Physics, 1998. 36: p. 1005-1012.**

211. **Okuzaki, H., Kubota, I., and Kunugi, T., *Mechanical properties and structure of the zone-drawn poly(L-lactic acid) fibers.* Journal of Polymer Science, Part B: Polymer Physics, 1999. 37: p. 991-996.**

212. **Yasuniwa, M., Tsubakihara, S., Sugimoto, Y., and Nakafuku, C., *Thermal analysis of the double-melting behavior of poly(L-lactic acid).* Journal of Polymer Science, Part B: Polymer Physics, 2004. 42: p. 25-32.**

213. **Sarasua, J.-R., Rodriguez, N.L., Arraiza, A.L., and Meaurio, E., *Stereoselective crystallization and specific interactions in polylactides.* Macromolecules, 2005. 38: p. 8362-8371.**

214. **He, Y., Wu, T., Wei, J., Fan, Z., and Li, S., *Morphological investigation on melt crystallized polylactide homo- And stereocopolymers by enzymatic degradation with proteinase K.* Journal of Polymer Science, Part B: Polymer Physics, 2008. 46: p. 959-970.**

215. **Woo, E.M. and Chang, L., *Crystallization and morphology of stereocomplexes in nonequimolar mixtures of poly(l-lactic acid) with excess poly(d-lactic acid).* Polymer, 2011. 52: p. 6080-6089.**

216. **Saeidlou, S., Huneault, M.A., Li, H., Sammut, P., and Park, C.B., *Evidence of a dual network/spherulitic crystalline morphology in PLA stereocomplexes.* Polymer, 2012. 53: p. 5816-5824.**

217. **Li, Y. and Han, C., *Isothermal and nonisothermal cold crystallization behaviors of asymmetric poly(l -lactide)/Poly(d -lactide) blends.* Industrial and Engineering Chemistry Research, 2012. 51: p. 15927-15935.**

218. **Sun, J., Shao, J., Huang, S., Zhang, B., Li, G., Wang, X., and Chen, X., *Thermostimulated crystallization of polylactide stereocomplex.* Materials Letters, 2012. 89: p. 169-171.**

219. **Yang, C.-F., Huang, Y.-F., Ruan, J., and Su, A.-C., *Extensive development of precursory helical pairs prior to formation of stereocomplex crystals in racemic polylactide melt mixture.* Macromolecules, 2012. 45: p. 872-878.**

220. **Xiong, Z., Liu, G., Zhang, X., Wen, T., De Vos, S., Joziasse, C., and Wang, D., *Temperature dependence of crystalline transition of highly-oriented poly(l-lactide)/poly(d-lactide) blend: In-situ synchrotron X-ray scattering study.* Polymer (United Kingdom), 2013. 54: p. 964-971.**

221. **Liu, Y., Sun, J., Bian, X., Feng, L., Xiang, S., Sun, B., Chen, Z., Li, G., and Chen, X., *Melt stereocomplexation from poly(l-lactic acid) and poly(d-lactic acid) with different optical purity.* Polymer Degradation and Stability, 2013. 98: p. 844-852.**

222. **Sakamoto, Y. and Tsuji, H., *Stereocomplex crystallization behavior and physical properties of linear 1-Arm, 2-Arm, and branched 4-arm poly(L-lactide)/poly(D-lactide) blends: Effects of chain directional change and branching.* Macromolecular Chemistry and Physics, 2013. 214: p. 776-786.**

223. **Nagahama, K., Shimizu, K., Ichimura, S., Takahashi, A., Ouchi, T., and Ohya, Y., *Biodegradable stereocomplex materials of polylactide-grafted dextran exhibiting soft and tough properties in dry and wet states.* Journal of Polymer Science, Part A: Polymer Chemistry, 2012. 50: p. 2669-2676.**

224. **Brzezinski, M., Bogusawska, M., Ilcikova, M., Mosnacek, J., and Biela, T., *Unusual thermal properties of polylactides and polylactide stereocomplexes containing polylactide-functionalized multi-walled carbon nanotubes.* Macromolecules, 2012. 45: p. 8714-8721.**

225. **Quan, H., Zhang, S.-J., Qiao, J.-L., and Zhang, L.-Y., *The electrical properties and crystallization of stereocomplex poly(lactic acid) filled with carbon nanotubes.* Polymer (United Kingdom), 2012. 53: p. 4547-4552.**
226. **Ye, S., Ting Lin, T., Weei Tjiu, W., Kwan Wong, P., and He, C., *Rubber toughening of poly(lactic acid): Effect of stereocomplex formation at the rubber-matrix interface.* Journal of Applied Polymer Science, 2013. 128: p. 2541-2547.**
227. **Nouailhas, H., El Ghzaoui, A., Li, S., and Coudane, J., *Stereocomplex-induced gelation properties of polylactide/poly(ethylene glycol) diblock and triblock copolymers.* Journal of Applied Polymer Science, 2011. 122: p. 1599-1606.**
228. **Calucci, L., Forte, C., Buwalda, S.J., and Dijkstra, P.J., *Solid-state NMR study of stereocomplexes formed by enantiomeric star-shaped PEG-PLA copolymers in water.* Macromolecules, 2011. 44: p. 7288-7295.**
229. **Portinha, D., Bouteiller, L., Pensec, S., Richez, A., and Chassenieux, C., *Influence of preparation conditions on the self-assembly by stereocomplexation of polylactide containing diblock copolymers.* Macromolecules, 2004. 37: p. 3401-3406.**
230. **Kim, S.H., Tan, J.P.K., Nederberg, F., Fukushima, K., Yang, Y.Y., Waymouth, R.M., and Hedrick, J.L., *Mixed micelle formation through stereocomplexation between enantiomeric poly(lactide) block copolymers.* Macromolecules, 2009. 42: p. 25-29.**
231. **Tan, B.H., Hussain, H., Lin, T.T., Chua, Y.C., Leong, Y.W., Tjiu, W.W., Wong, P.K., and He, C.B., *Stable dispersions of hybrid nanoparticles induced by stereocomplexation between enantiomeric poly(lactide) star polymers.* Langmuir, 2011. 27: p. 10538-10547.**
232. **Tsuji, H., Wada, T., Sakamoto, Y., and Sugiura, Y., *Stereocomplex crystallization and spherulite growth behavior of poly(l-lactide)-b-poly(d-lactide) stereodiblock copolymers.* Polymer, 2010. 51: p. 4937-4947.**
233. **Rahaman, M.H. and Tsuji, H., *Isothermal crystallization and spherulite growth behavior of stereo multiblock poly(lactic acid)s: Effects of block length.* Journal of Applied Polymer Science, 2013.**
234. **Fukushima, K., Sogo, K., Miura, S., and Kimura, Y., *Production of D-lactic acid by bacterial fermentation of rice starch.* Macromolecular Bioscience, 2004. 4: p. 1021-1027.**
235. **Okano, K., Zhang, Q., Shinkawa, S., Yoshida, S., Tanaka, T., Fukuda, H., and Kondo, A., *Efficient production of optically pure D-lactic acid from raw corn starch by using a genetically modified L-lactate dehydrogenase gene-deficient and -amylase-secreting Lactobacillus plantarum strain.* Applied and Environmental Microbiology, 2009. 75: p. 462-467.**
236. **Mazumdar, S., Clomburg, J.M., and Gonzalez, R., *Escherichia coli strains engineered for homofermentative production of D-lactic acid from glycerol.* Applied and Environmental Microbiology, 2010. 76: p. 4327-4336.**
237. **Tashiro, Y., Kaneko, W., Sun, Y., Shibata, K., Inokuma, K., Zendo, T., and Sonomoto, K., *Continuous D-lactic acid production by a novelthermotolerant Lactobacillus delbrueckii subsp. lactis QU 41.* Applied Microbiology and Biotechnology, 2011. 89: p. 1741-1750.**
238. **Dong, Q., Li, Y., Han, C., Zhang, X., Xu, K., Zhang, H., and Dong, L., *Poly(l -lactide)/poly(d -lactide)/multiwalled carbon nanotubes nanocomposites: Enhanced dispersion, crystallization, mechanical properties, and hydrolytic degradation.* Journal of Applied Polymer Science, 2013. 130: p. 3919-3929.**
239. **Li, Y., Han, C., Zhang, X., Xu, K., Bian, J., and Dong, L., *Poly(L-lactide)/Poly(D-lactide)/clay nanocomposites: Enhanced dispersion, crystallization, mechanical properties, and hydrolytic degradation.* Polymer Engineering and Science, 2013. Article in Press.**
240. **Yuryev, Y. and Wood-Adams, P., *Rheological properties of crystallizing polylactide: Detection of induction time and modeling the evolving structure and properties.* Journal of Polymer Science, Part B: Polymer Physics, 2010. 48: p. 812-822.**
241. **Yuryev, Y. and Wood-Adams, P.M., *Crystallization of poly(L-/D-lactide) in the presence of electric fields.* Macromolecular Chemistry and Physics, 2012. 213: p. 635-642.**
242. **Fang, H., Zhang, Y., Bai, J., and Wang, Z., *Shear-induced nucleation and morphological evolution for bimodal long chain branched polylactide.* Macromolecules, 2013. 46: p. 6555-6565.**
243. **Saeidlou, S., Huneault, M.A., Li, H., and Park, C.B., *Effect of nucleation and plasticization on the stereocomplex formation between enantiomeric poly(lactic acid)s.* Polymer (United Kingdom), 2013. 54: p. 5762-5770.**

244. **Wu, D., Wu, L., Zhang, M., and Zhao, Y., *Viscoelasticity and thermal stability of polylactide composites with various functionalized carbon nanotubes.* Polymer Degradation and Stability, 2008. 93: p. 1577-1584.**

245. **Khanna, Y., *Rheological mechanism and overview of nucleated crystallization kinetics.* Macromolecules, 1993. 26: p. 3639-3643.**

246. **Li, Y., Han, C., Bian, J., Han, L., Dong, L., and Gao, G., *Rheology and biodegradation of polylactide/silica nanocomposites.* Polymer Composites, 2012. 33: p. 1719-1727.**

247. **Li, D.-C., Liu, T., Zhao, L., Lian, X.-S., and Yuan, W.-K., *Foaming of poly(lactic acid) based on its nonisothermal crystallization behavior under compressed carbon dioxide.* Industrial and Engineering Chemistry Research, 2011. 50: p. 1997-2007.**

248. **Taki, K., Kitano, D., and Ohshima, M., *Effect of growing crystalline phase on bubble nucleation in poly(L -lactide)/CO2 batch foaming.* Industrial and Engineering Chemistry Research, 2011. 50: p. 3247-3252.**

249. **Ji, G., Zhai, W., Lin, D., Ren, Q., Zheng, W., and Jung, D.W., *Microcellular foaming of poly(lactic acid)/silica nanocomposites in compressed CO2: Critical influence of crystallite size on cell morphology and foam expansion.* Industrial and Engineering Chemistry Research, 2013. 52: p. 6390-6398.**

250. **Ren, Q., Wang, J., Zhai, W., and Su, S., *Solid state foaming of poly(lactic acid) blown with compressed CO 2: Influences of long chain branching and induced crystallization on foam expansion and cell morphology.* Industrial and Engineering Chemistry Research, 2013. 52: p. 13411-13421.**

251. **Fujimoto, Y., Sinha Ray, S., Okamoto, M., Ogami, A., Yamada, K., and Ueda, K., *Well-controlled biodegradable nanocomposite foams: From microcellular to nanocellular.* Macromolecular Rapid Communications, 2003. 24: p. 457-461.**

252. **Guo, Q., Wang, J., Park, C.B., and Ohshima, M., *A microcellular foaming simulation system with a high pressure-drop rate.* Industrial and Engineering Chemistry Research, 2006. 45: p. 6153-6161.**

253. **Sane, A. and Thies, M.C., *Effect of material properties and processing conditions on RESS of poly(l-lactide).* Journal of Supercritical Fluids, 2007. 40: p. 134-143.**